

Hydrogen Production by Molecular Photocatalysis

Arthur J. Esswein and Daniel G. Nocera*

Department of Chemistry 6-335, Massachusetts Institute of Technology, 77 Massachusetts Avenue, Cambridge, Massachusetts 02139-4307

Received May 17, 2007

Contents

1. Introduction	4022
2. Hydrogen Production from RH Substrates	4024
2.1. Alkane Dehydrogenation	4024
2.1.1. Thermal Alkane Dehydrogenation Cycles	4024
2.1.2. Photochemical Alkane Dehydrogenation Cycles	4025
2.2. Mercury Photosensitization	4026
2.3. Alcohol Photo-dehydrogenations	4027
2.3.1. Rhodium Phosphine Complexes	4027
2.3.2. Binuclear Complexes	4028
2.3.3. M–Sn Complexes	4029
2.3.4. Rhodium Porphyrins	4029
2.3.5. Polyoxometalates	4029
2.4. Platinum Terpyridine Complexes	4030
3. Hydrogen Production from Acidic Solutions	4031
3.1. Mononuclear Catalysts	4031
3.2. Binuclear Catalysts	4032
3.2.1. Biradical Excited States	4032
3.2.2. Two-Electron Mixed Valency	4032
4. Photochemical Water–Gas Shift	4034
4.1. Homoleptic Metal Carbonyl Catalysts	4034
4.2. Ruthenium and Iridium Catalysts	4035
5. Three Component Systems	4036
5.1. Inorganic Sensitizers	4036
5.1.1. Metal Polypyridyl Photosensitizers	4036
5.1.2. Porphyrin Sensitizers	4038
5.2. Organic Sensitizers	4039
5.3. CO ₂ Reduction Systems	4039
6. Photobiological Approaches	4040
6.1. Hydrogenase	4040
6.2. Isolated Chloroplasts	4041
6.3. Other Photobiological Approaches	4041
7. Concluding Remarks and Future Directions	4041
8. Abbreviations	4043
9. Acknowledgments	4043
10. References	4043

1. Introduction

A great technological challenge facing our global future is the development of a secure, clean, and renewable energy source.^{1–4} Rising standards of living in a growing world population will cause global energy consumption to increase dramatically over the next half century. Energy consumption

is predicted to increase at least 2-fold, from our current burn rate of 12.8 TW to 28–35 TW by 2050.^{1,2,5,6} Proven reserves of coal, oil, and gas suggest that this energy need can be met with conventional sources;⁷ however, external factors of economy, environment, and security dictate that this energy need be supplemented by renewable and sustainable sources.^{8–11} If not, increases in energy intensity derived from economic and population growth will be inextricably linked to increased carbon emissions. While the precise response of the climate to continued runaway CO₂ emissions is not definitively known, it is abundantly clear that the current atmospheric CO₂ levels of 380 ppm are significantly higher than anything seen in the last 650 000 years.^{12,13} A “wait and see” policy toward the human impact on global climate change amounts, disconcertingly, to an experiment on a global scale with potentially profound consequences to life.

Hydrogen presents itself as a potential alternative to carboniferous fossil fuels but only with consideration of an appropriate source. A near-term H₂ source is methane and other petroleum-based fuels. However, in the absence of carbon capture and storage,¹⁴ the use of H₂ from methane results in only a marginal improvement in stemming carbon emissions. Conversely, carbon intensity will be decreased significantly if water, with solar light as an energy input, is the primary carbon-neutral H₂ source.

The benefit of solar energy conversion was recognized nearly a century ago as a means “to fix the solar energy through suitable photochemical reactions” by creating new compounds to master “the photochemical processes that hitherto have been the guarded secret of the plants”.¹⁵ As the phosphate bond in ATP is the basic unit of energy in biology, so can the H–H bond in H₂ become a basic unit of energy for a carbon-neutral society. For this to occur, H₂ must be freed from its stable carrier, water. The design premise is to use the energy of solar photons to drive the thermodynamically uphill splitting of water to produce H₂ with oxygen as a byproduct. The H₂ may be further “fixed” to a liquid fuel via hydrogenation of small molecules such as CO₂¹⁶ or used directly to power fuel cells.¹⁷ Significant technological challenges remain, however, before H₂ can be used routinely as a fuel source.^{18,19} Prominent among these is its storage and, of concern to this review, the development of new photochemical mechanisms that lead to the efficient production of H₂. For instance, H₂ may be produced along one-electron pathways to produce H•. However, this production of H• requires 1.8 V, which is recovered upon the second one-electron reduction. Thus, though 2H⁺ + 2e[−] → H₂ is thermoneutral, its production along the one-electron pathway minimally confronts a 1.8 V barrier. This overpotential may be obviated if efficient two-electron redox pathways are developed. Since an H[−] is formally produced by two-electron reduction, the coupling of a proton to the two-electron path-

* Corresponding author. E-mail: nocera@mit.edu.



Arthur J. Esswein was born on July 10, 1980, and grew up in Falmouth, Massachusetts. He received his B.A. in Chemistry and Mathematics from the Johns Hopkins University in Baltimore, Maryland, in 2002. At Hopkins, he worked in the laboratory of Prof. Gerald J. Meyer where his interests in solar energy conversion began. In the fall of 2002, he went to work in the laboratory of Daniel G. Nocera at the Massachusetts Institute of Technology. His Ph.D. work has involved the thermal and photochemical reactivity of late transition metal bimetallics, with a particular emphasis on the photocatalytic production of hydrogen. Arthur continues working in the field of solar energy conversion with a postdoctoral appointment at the University of California, Berkeley.

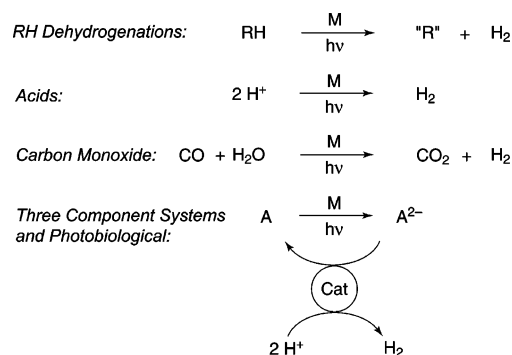


Daniel G. Nocera is the Henry Dreyfus Professor of Energy at the Massachusetts Institute of Technology. He received his early education at Rutgers University where he was a Henry Rutgers Scholar, obtaining a B.S. degree with Highest Honors in 1979, one year before Arthur Esswein was born. He moved to Pasadena, California, where he was mentored by Professor Harry Gray at the California Institute of Technology. Nocera studies the basic mechanisms of energy conversion in biology and chemistry with a primary focus in recent years on the photogeneration of hydrogen and oxygen from water. He also studies exotic states arising from highly correlated spin frustration and optical sensing, and his group developed at a mechanistic level the field of proton-coupled electron transfer, which is now used routinely to study radicals in biology. Afield from chemistry, Nocera invented the molecular tagging velocimetry (MTV) technique to make simultaneous, multipoint velocity measurements of highly turbulent three-dimensional flows. He has been awarded the Eni-Italgas Prize (2005), the IAPS Award (2006), and the Burghausen Prize (2007) for contributions to the development of renewable energy at the molecular level.

way is a necessity if the energy barrier is to be minimized. The creation of catalysts that perform multielectron photochemistry^{20–22} and proton-coupled electron transfer (PCET)^{23–36} are at the frontier of inorganic chemistry. Of equal challenge is that these catalysts ultimately be robust, cheap, and constructed from sustainable elemental components.

While the catalytic production of hydrogen and oxygen from water splitting has yet to be effectively achieved in homogeneous solution, some of the basic building blocks in

Scheme 1



the foundation of the science needed for this reaction have emerged over the past three decades. One of these important building blocks comes from knowledge accrued from studies concerning hydrogen production by photochemical means. This review serves to collect and distill research efforts in the area of molecular photocatalytic H₂ production so that a new generation of reaction chemists can make rapid progress in this time of renewed interest in hydrogen photoproduction from carbon neutral sources. In the interests of brevity, this review will not cover approaches to produce H₂ photoelectrochemically, by biomass conversion, or by enzymatic methods. Some discussion of photobiological mechanisms will be presented but only in cases where the molecular aspects of the pathway are known and for schemes in which the biological cofactor is isolated from its native environment. The review will also be confined to homogeneous systems; H₂ production at solid or semiconductor surfaces from direct band gap or sensitized photoexcitation will not be considered. For molecular systems, the focus will be on catalysis. Stoichiometric or thermal catalytic H₂ production schemes will not be specifically addressed unless the study of those systems underpins the development of photocatalytic cycles.

The treatment of molecular photocatalytic H₂ production will follow the outline shown in Scheme 1. The discussion is differentiated by the substrates from which the proton and electron equivalents originate.

(a) Direct RH Substrates. Hydrogen production from RH substrates derives electron and proton equivalents from either the homo- or heterolysis of C–H or O–H bonds and typically involves inner sphere mechanisms that invoke intermediates with substrate directly bound to the catalyst. Common substrates include alkanes and primary or secondary alcohols. The products of this photocatalysis are H₂ and the respective dehydrogenation product: alkenes, aldehydes, or ketones.

(b) Acids. Acids can be the direct substrate for H₂ production. The challenge to turnover is catalyst regeneration by oxidation of the conjugate base.

(c) Carbon Monoxide. The water–gas shift (WGS) reaction couples the oxidation of CO to CO₂ with the reduction of water to H₂.

(d) Indirect RH Substrates and Acids. The most prevalent approach to H₂-producing photocatalysis is the construction of three-component systems comprising a sensitizer to absorb light, a proton reduction catalyst, and an electron relay to shuttle reducing equivalents from the sensitizer to the catalyst. In these systems, the electron equivalents are derived from sacrificial reducing agents that involve either the homo- or heterolytic cleavage of C–H or O–H bonds of RH

Table 1. Representative Photocatalytic Alkane Dehydrogenation Catalysts

catalyst	substrate	product	<i>T</i> (°C)	λ_{exc} (nm)	time (h)	TON	TOF (h ⁻¹)	ref
Ir ^{III} H ₂ (CF ₃ CO ₂)(PCy ₃) ₂	cyclooctane	cyclooctene	25	254	168	7	<i>a</i>	53, 54
Rh ^I (PMe ₃) ₂ (CO)Cl	<i>n</i> -heptane	1 and 2-heptene	92	<300		<i>a</i>	795	72
Rh ^I (PEt ₃) ₂ (CO)Cl	<i>n</i> -heptane	1 and 2-heptene	92	<300			466	72
Rh ^I (PPh ₃) ₂ (CO)Cl	<i>n</i> -heptane	1 and 2-heptene	92	<300			136	72
Rh ^I (PMe ₃) ₂ (CO)Cl	<i>n</i> -nonane	1 and 2-nonene	132	<300			1404	78
Rh ^I (PMe ₃) ₂ (CO)Cl	cyclohexane	cyclohexene	25	<300	16.5	138		76
Rh ^I (PMe ₃) ₂ (CO)Cl	cyclooctane	cyclooctene	100	<300	1	72		77
Rh ^I (PMe ₃) ₂ (CO)Cl	benzene	biphenyl	15	<300	189	13		84
Rh ^I (PMe ₃) ₂ (CO)Cl	methyl propionate	4-propionyloxybutyrate	25	<300	6	20		85
Rh ₂ ^I (dppm) ₂ (CO) ₂ (μ -S)	cyclooctane	cyclooctene	151	<400	2	27		93
Ir ₂ ^{III} (dppm) ₂ (CO) ₂ (μ -S)	cyclooctane	cyclooctene	151	<300	2	16		94

^a Not applicable.

substrates and acids. Unlike direct RH dehydrogenations, substrate activation is coupled indirectly to H₂ production via the relay catalysts and cleavage of the substrate typically proceeds by an outer sphere mechanism.

We conclude by presenting new avenues for research in an attempt to stimulate researchers to explore new reactions for H₂ production that may ultimately be coupled to water oxidation. The latter reaction has been treated elsewhere.^{37–42}

2. Hydrogen Production from RH Substrates

Photocatalytic H₂ production from RH dehydrogenations refers to any system where the proton and electron equivalents for H₂ production originate from C–H or O–H bonds. The mechanism of action, whether by C–H activation, H atom abstraction, or sequential electron and proton transfers from the RH substrate, is not distinguished as they all fall into this general category and may include elements of each reaction type in the overall H₂ production mechanism.

2.1. Alkane Dehydrogenation

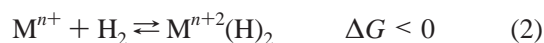
Alkane dehydrogenations are among the most well-defined schemes for photocatalytic H₂ production. The reaction type is characterized by the following:



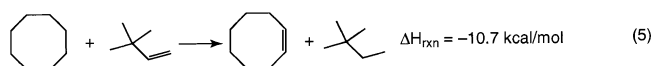
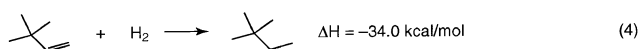
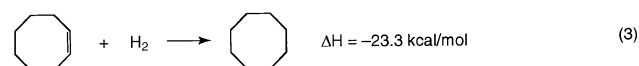
Hydrogen production occurs generally by classical organometallic mechanisms involving alkane C–H bond activation followed by β -hydride elimination. As a consequence many of these reactions are catalyzed by group 9 transition metal complexes (Table 1). The discovery and mechanistic understanding of photochemical alkane dehydrogenation reactions have been derived largely from cycles constructed for the thermal, as opposed to photochemical, dehydrogenation of alkanes. Accordingly, a presentation of thermal alkane dehydrogenation will precede a discussion of H₂ generation promoted along photochemical pathways.

2.1.1. Thermal Alkane Dehydrogenation Cycles

The discovery of the hydrogenation of alkenes using Wilkinson's celebrated catalyst, and the intensive study of group 9 complexes with alkenes and H₂, provided a backdrop for elucidating the reverse process, alkane dehydrogenation. Generally the reaction of H₂ with a coordinatively unsaturated metal complex is thermodynamically favorable,



and thus the dehydrogenation of alkanes typically requires an external thermodynamic driving force. Many thermal systems derive a thermodynamic advantage by coupling a H₂ donor such as cyclooctane to the high heat of hydrogenation of a sacrificial H₂ acceptor such as *tert*-butylethylene (TBE), eqs 3–5:



Early studies used iridium complexes to model and isolate intermediates in alkane hydrogenation cycles.⁴³ Following up on previous work involving dihydride olefin complexes of iridium,⁴⁴ Crabtree and co-workers noted that the *trans*-Ir^I(COE)₂L₂⁺ complex (COE = cyclooctene, L = PPh₃) converted to the cyclooctadiene (COD) complex, Ir^I(COD)-L₂⁺, and free cyclooctane when heated to 40 °C in CH₂Cl₂. The product distribution indicated that a transfer hydrogenation had occurred and suggested that iridium complexes could serve as alkane dehydrogenation catalysts under appropriate conditions. Several reports followed where the substrate scope was expanded to cyclohexene and cyclopentene to generate arenes and cyclopentadienyls, respectively.^{45–47} But these reactions were stoichiometric owing to the strength of the iridium arene and cyclopentadienyl interactions that resulted from dehydrogenation chemistry.

Concurrently, rhenium polyhydrides, ReL₂H₇ (L = PPh₃, PEt₂Ph), were observed to dehydrogenate cyclopentane to generate ReL₂(η^5 -C₅H₅)H₂ at 80 °C in the presence of excess TBE.⁴⁸ The dehydrogenation reaction was found to be catalytic when using alkane substrates that form weak interactions with the metal center upon dehydrogenation. As a consequence, the rhenium polyhydrides, Re(PR₃)₂H₇ (R = Ph, *p*-F-C₆H₄, *p*-CH₃-C₆H₄), were observed to dehydrogenate cyclohexane to cyclohexene with nine turnovers at 80 °C in the presence of excess TBE.⁴⁹ This catalysis was extended to include *n*-alkane substrates⁵⁰ and polyhydrides of ruthenium and iridium.^{51,52} Turnovers for the rhenium systems were typically low (<10), but turnovers as high as 70 were reported for cyclooctane dehydrogenation using Ir(PR₃)₂H₅ and TBE after 5 days at 150 °C.⁵¹

A host of Ir^{III} dihydrides were developed as catalytic dehydrogenation catalysts. They all are believed to operate by the general mechanism shown in Figure 1 (left) for the

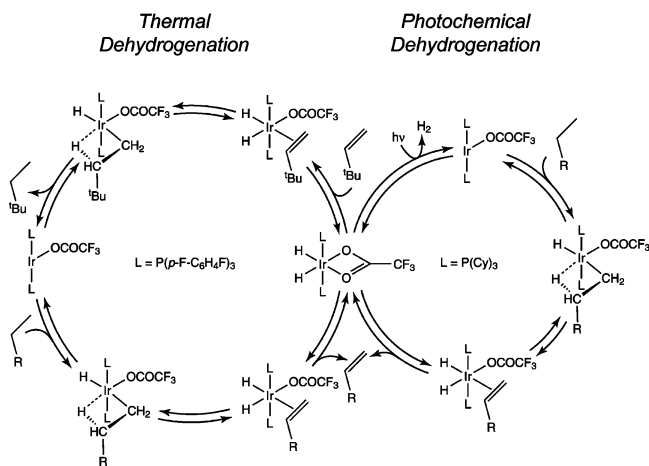


Figure 1. Proposed mechanism for alkane dehydrogenation catalyzed by $\text{Ir}^{\text{III}}\text{H}_2(\text{CF}_3\text{CO}_2)(\text{PR}_3)_2$ ($\text{R} = p\text{-F-C}_6\text{H}_4, \text{Cy}$) by photochemical (right) and thermal transfer hydrogenation (left) pathways.

dehydrogenation of cyclooctane by $\text{Ir}^{\text{III}}\text{H}_2(\text{CF}_3\text{CO}_2)(\text{PR}_3)_2$.^{53,54} For $\text{PR}_3 = \text{P}(p\text{-F-C}_6\text{H}_4)_3$, dehydrogenation proceeds from the dihydride $\text{Ir}^{\text{III}}\text{H}_2(\text{CF}_3\text{CO}_2)(\text{PR}_3)_2$ via a proposed initial conversion of the $\kappa^2\text{-CF}_3\text{CO}_2$ to a κ^1 binding mode to open a coordination site, followed by coordination of TBE. Presumably the ability of CF_3CO_2^- to interchange binding modes is important, because the use of CH_3CO_2^- in place of CF_3CO_2^- gave a catalytically inactive complex. The TBE is then hydrogenated to give 2,2-dimethylbutane, which binds weakly to the Ir^{I} center and upon dissociation generates a reactive three-coordinate, 14 electron Ir complex as a proposed intermediate. Alkane binding and C–H activation proceed to give a hydrido alkyl complex, which then β -hydride eliminates to give a dihydrido olefin species. Subsequent dissociation of alkene and conversion of the $\kappa^1\text{-CF}_3\text{CO}_2$ to a κ^2 -binding mode regenerates the starting $\text{Ir}^{\text{III}}\text{H}_2(\text{CF}_3\text{CO}_2)(\text{PR}_3)_2$ complex and closes the catalytic cycle. The overall determinant to the effectiveness of this catalysis appears to involve removal of the dihydride ligands from the coordination sphere of the metal center. With the $\text{P}(p\text{-F-C}_6\text{H}_4)_3$ ligand, this is accomplished by the transfer hydrogenation of TBE, which provides the thermodynamic driving force for the overall reaction. A maximum of 16 turnovers for cyclooctane dehydrogenation in the presence of excess TBE at 150 °C was observed. Since this initial work, thermal alkane dehydrogenation has progressed considerably with the application of Ir pincer complexes (pincer = 2,6-(R_2PCH_2)- C_6H_3 , $\text{R} = \text{tBu}, \text{iPr}$, for example).⁵⁵ A host of derivatives has been reported,^{56–67} all taking advantage of stability afforded by the pincer ligand, which allows catalysis to proceed at high temperatures without significant decomposition. Most schemes employ TBE or norbornene as sacrificial hydrogen acceptors in a similar fashion to that shown in Figure 1, but some acceptorless systems have been reported.^{62–66} Turnovers for cyclooctane dehydrogenation as high as 3300 have been observed when using a ferrocene-derived pincer ligand.⁶⁷ This strategy has been applied to tandem catalysis,⁶⁸ wherein lower alkanes are first dehydrogenated by an Ir pincer complex and then subsequently converted to higher olefins by in situ olefin metathesis. In this work, the alkenes generated by olefin metathesis serve as sacrificial hydrogen acceptors to regenerate the active dehydrogenation catalyst.

2.1.2. Photochemical Alkane Dehydrogenation Cycles

In principle, the driving force for alkane dehydrogenation can be supplied by a photon instead of hydrogenation of a sacrificial alkene such as TBE.^{69–71} This reactivity mode was first reported by Crabtree for $\text{Ir}^{\text{III}}\text{H}_2(\text{CF}_3\text{CO}_2)(\text{PR}_3)_2$ for $\text{R} = \text{Cy}$.^{53,54} The cyclohexyl derivative gave only 2 equiv of COE under thermal conditions, analogous to those used for $\text{R} = p\text{-F-C}_6\text{H}_4$ (150 °C, neat cyclooctane, 2 days). The activity of the system increases when room temperature solutions are subject to photolysis conditions. In the presence of TBE, 28 turnovers of COE were observed after prolonged photolysis with 254 nm light (25 °C, 7 days). Activity was maintained upon removal of TBE from the system, though at decreased turnover numbers. In the absence of the H_2 acceptor, 7 turnovers were obtained after 7 days, indicating that the dehydrogenation reaction can be driven by the energy derived from photon absorption. The photocatalysis was proposed to proceed by a C–H activation/ β -hydride elimination mechanism similar to that of the thermal dehydrogenation where photons were thought to generate the active $\text{Ir}^{\text{I}}(\text{CF}_3\text{CO}_2)(\text{PCy}_3)_2$ intermediate by expulsion of H_2 from $\text{Ir}^{\text{III}}\text{H}_2(\text{CF}_3\text{CO}_2)(\text{PCy}_3)_2$ (Figure 1, right).

Photocatalytic alkane dehydrogenations were also reported using monomeric Rh complexes of the Vaska type, $\text{Rh}^{\text{I}}(\text{PR}_3)_2(\text{CO})\text{Cl}$. Saito and co-workers were the first to report catalysis using $\text{Rh}^{\text{I}}(\text{PR}_3)_2(\text{CO})\text{Cl}$ ($\text{R} = \text{Me}, \text{Et}, \text{Ph}$) complexes in neat *n*-alkane solvent (heptane or octane) at elevated temperatures (60–92 °C) under constant irradiation.⁷² The activity of these catalysts is high compared with the dehydrogenation catalysts based on Ir or Re, with a maximum turnover frequency observed of 795 h^{-1} for $\text{PR}_3 = \text{PMe}_3$ at 92 °C. No appreciable rate differences were observed for the dehydrogenation of *n*-heptane vs *n*-octane, suggesting that the rate-determining step is not particularly sensitive to minor substrate modifications. Only moderate catalytic selectivity was observed as both a mixture of 1- and 2-heptene were obtained as the dehydrogenation products of *n*-heptane. Catalyst activity increased with increasing temperature and also increased with the donating ability of the phosphine along the series $\text{PMe}_3 > \text{PEt}_3 > \text{PPh}_3$. Catalyst initiation proceeded by CO photodissociation from $\text{Rh}^{\text{I}}(\text{PR}_3)_2(\text{CO})\text{Cl}$ ($\lambda_{\text{max}} > 340 \text{ nm}$), suggesting that the active intermediate is the 14 electron, three-coordinate fragment $\text{Rh}^{\text{I}}(\text{PR}_3)_2\text{Cl}$.^{73–75} The substrate scope was subsequently expanded to include cyclic alkanes such as cyclohexane and cyclooctane.^{76–82} $\text{Rh}^{\text{I}}(\text{PR}_3)_2(\text{CO})\text{Cl}$ complexes also catalyze dehydrogenative dimerization reactions under irradiation conditions of alkanes to dienes,⁸³ arenes to biaryls,⁸⁴ and methyl propionate to primarily 4-propionyloxybutyrate.⁸⁵ Thorough mechanistic studies were not undertaken, but the evidence suggesting initiation from the 14 electron Rh^{I} fragment led to the generally accepted proposition of an oxidative addition/ β -hydride elimination pathway, similar to that for the Ir complexes reported by Crabtree.

Detailed mechanistic studies for the $\text{Rh}^{\text{I}}(\text{PMe}_3)_2(\text{CO})\text{Cl}$ catalyzed photodehydrogenation of alkanes were carried out by Goldman and co-workers.^{86–88} In the proposed mechanism shown in Figure 2, photoinitiated dissociation of CO generates a reactive $\text{Rh}^{\text{I}}(\text{PMe}_3)_2\text{Cl}$ fragment as initially deduced by Saito. This fragment then oxidatively adds alkane C–H bonds (cyclooctane in Figure 2) to generate an alkyl hydride species, which β -hydride eliminates to generate the dihydrido alkene complex. Alkene dissociation followed by H_2 loss, induced by CO coordination, regenerates the starting complex

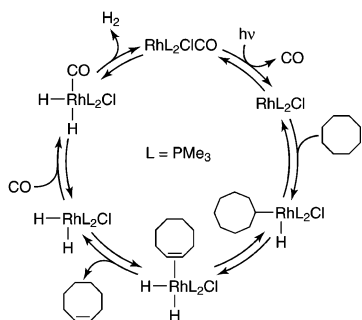
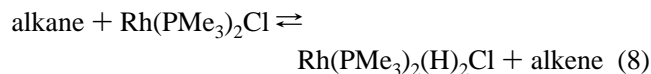
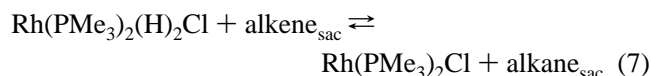
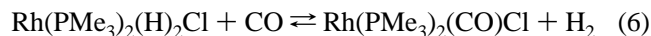


Figure 2. Proposed mechanism for the photocatalytic cyclooctane dehydrogenation at $\text{Rh}^{\text{I}}(\text{PMe}_3)_2(\text{CO})\text{Cl}$ as determined by Goldman and co-workers.

and closes the catalytic cycle. Notably the initial photodissociation of CO is the only photochemical step in the cycle, contrasting the mechanism proposed by Crabtree for $\text{Ir}^{\text{III}}\text{H}_2(\text{CF}_3\text{CO}_2)(\text{PCy}_3)_2$ where H_2 is eliminated from the dihydride in a photochemical step. Additionally, in neat cyclooctane and cyclohexane, dehydrogenation to give cyclooctene and cyclohexene proceeds with identical quantum yields, consistent with a rate-determining step that does not involve alkane. The observed CO inhibition of the reaction was not attributed to its reaction with the photogenerated $\text{Rh}^{\text{I}}(\text{PMe}_3)_2\text{Cl}$ fragment, but rather to CO coordination to the alkyl hydride intermediate, thereby preventing β -hydride elimination. Thus, even under the highest CO pressures employed in the study (800 Torr), the back reaction of CO with $\text{Rh}^{\text{I}}(\text{PMe}_3)_2\text{Cl}$ cannot compete kinetically with alkane C–H bond activation, which was found to be reversible.

As a result of the foregoing mechanistic work on $\text{Rh}^{\text{I}}(\text{PMe}_3)_2(\text{CO})\text{Cl}$, the following series of equilibrium reactions suggest that the photochemically generated fragment of Figure 2, $\text{Rh}^{\text{I}}(\text{PMe}_3)_2\text{Cl}$, can also be accessed via the thermal equilibrium described by eqs 7 and 8,^{89,90}



A moderate pressure of H_2 induces CO dissociation from $\text{Rh}^{\text{I}}(\text{PMe}_3)_2(\text{CO})\text{Cl}$ to generate the five-coordinate fragment $\text{Rh}^{\text{I}}(\text{PMe}_3)_2(\text{H})_2\text{Cl}$, by shifting the equilibrium of eq 6 to the left. Coordination of a sacrificial alkene to $\text{Rh}^{\text{I}}(\text{PMe}_3)_2(\text{H})_2\text{Cl}$ followed by hydrogenation generates alkane and the same catalytically active $\text{Rh}^{\text{I}}(\text{PMe}_3)_2\text{Cl}$ fragment from photochemical experiments, eq 7, where the thermodynamic driving force is provided by the exothermic hydrogenation of a sacrificial alkene. In this way, the photochemical alkane dehydrogenation catalyst, $\text{Rh}^{\text{I}}(\text{PMe}_3)_2(\text{CO})\text{Cl}$, may be changed to one that is a thermal-based transfer dehydrogenation by clever manipulation of the reaction equilibria.

In an attempt to shift the photon energy into the visible region, bimetallic analogs of $\text{Rh}^{\text{I}}(\text{PMe}_3)_2(\text{CO})\text{Cl}$ were examined. The bathochromic shift in the absorption bands of bimetallic square-planar Rh^{I} dimers arises from a $d\sigma^* \rightarrow p\sigma$ transition arising from the overlap of filled d_z^2 orbitals and

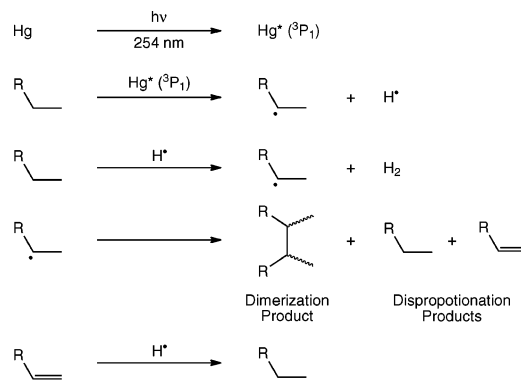


Figure 3. Generalized radical reactions of pertinence to the Hg photocatalyzed dehydrogenation of alkanes.

empty $p\sigma$ orbitals.^{91,92} The sulfide-bridged rhodium and iridium A-frames, $\text{M}_2^{\text{I}}(\text{dppm})_2(\mu\text{-S})(\text{CO})_2$, show mild activity (<30 turnovers for cyclooctane dehydrogenation to cyclooctene) when irradiating bands centered at 475 and 418 nm, respectively (dppm = bis(diphenylphosphino)methane, $\text{CH}_2[\text{P}(\text{C}_6\text{H}_5)_2]_2$).^{93,94} The initial turnover frequencies for $\text{M} = \text{Rh}$ were $\sim 32 \text{ h}^{-1}$, suggesting that the active catalyst is rapidly decomposed under the conditions employed. Conversely, the face-to-face Rh^{I} dimer, $\text{Rh}_2^{\text{I}}(\text{dppm})_2\text{Cl}_2(\text{CO})_2$, showed no alkane dehydrogenation activity.⁹⁵

2.2. Mercury Photosensitization

Mercury photosensitization of the dehydrodimerization of alkanes offers another photocatalytic route to the generation of H_2 . The method, which has been known since at least the 1920s, was developed, however, not for H_2 generation but rather for the synthesis of higher alkanes from low carbon feedstocks.^{96,97} A general reaction scheme for the overall process is shown in Figure 3.

Crabtree and co-workers revisited the method in attempts to make the technique synthetically viable for the formation of C–C bonds.^{98–100} The electronic structure of Hg atoms in the gas phase is well developed;¹⁰¹ the reaction proceeds by direct excitation (a $5d^{10}6s^2 \rightarrow 5d^{10}6s^16p^1$ transition) of gas-phase Hg atoms with 254 nm photons to generate the $^3\text{P}_1$ excited state. This triplet excited state abstracts a hydrogen atom (H atom) from the alkane substrate to generate a free H atom and an organic radical. The H atom can go on to produce H_2 by undergoing a bimolecular combination reaction with an H atom from another alkane. The alkyl radicals dimerize by the formation of a C–C bond or disproportionate to alkane and alkene products. Selectivity for dimerization over higher oligomerization was achieved by carefully controlling the temperature so that the vessel headspace was occupied by monomer precursors as opposed to C–C coupled products, which could effectively be removed from the headspace by condensation. The dimerization reaction proceeds with quantum yields at 254 nm as high as 0.8 for competent H atom donors such as triethylsilane, whereas cyclohexane is dimerized with a quantum yield of 0.42 with turnovers of $29 \times 10^{-4} \text{ mol}^{-1} \text{ h}^{-1}$ under reflux conditions.⁹⁹ The reaction may be extended to heterodimerizations in certain cases.¹⁰⁰ Recycling of the alkenes produced by radical disproportionation is achieved by H atom attack to regenerate alkyl radicals, which can then re-enter the catalytic cycle. Consistent with a radical mechanism, preferential attack of the more substituted C–H bonds, 3°

Table 2. Representative Photocatalysts for Alcohol Dehydrogenations

catalyst	substrate	product	<i>T</i> (°C)	λ_{exc} (nm)	time (h)	TON	TOF (h ⁻¹)	ref
Rh ^I (PPh ₃) ₃ Cl	isopropanol	acetone	21	<i>a</i>	1	670	<i>b</i>	102
Rh ^I (PPh ₃) ₃ Cl	isopropanol	acetone	21	<300		5370	<i>b</i>	103
Rh ^I (P(OPh) ₃) ₃ Cl	isopropanol	acetone	21	<300		6410	<i>b</i>	103
Rh ^I (PEt ₃) ₂ (CO)I	isopropanol	acetone	84	340 → 420	<i>b</i>	<i>b</i>	1110	105,106
Rh ^I (PEt ₃) ₂ (CO)Br	isopropanol	acetone	84	340 → 420	<i>b</i>	<i>b</i>	750	105,106
Rh ^I (PMe ₃) ₂ (CO)Br	isopropanol	acetone	84	340 → 420	<i>b</i>	<i>b</i>	810	105,106
<i>cis</i> -Rh ^I ₂ (dppm) ₂ (CO) ₂ Cl ₂	methanol	formaldehyde	64				130	111,112
Pd ₃ ^I (dppm) ₂ Cl ₂	methanol	formaldehyde	64				156	108,109
<i>cis</i> -Rh ^I ₂ (dppm) ₂ (CO) ₂ Cl ₂	isopropanol	acetone	20	312	6	15		108,109
Pt ₂ ^{II,II} (P ₂ O ₅ H ₂) ₄ ⁴⁻	isopropanol	acetone	<i>b</i>	<i>b</i>	<i>b</i>	>400	<i>b</i>	110
Ir ^{III} H(SnCl ₃) ₅ ³⁻	isopropanol	acetone	82	254			109	119
Rh ^{III} H(SnCl ₃) ₅ ³⁻	isopropanol	acetone	82	254			88	129–134
Ru ^{III} H(SnCl ₃) ₅ ³⁻	isopropanol	acetone	82	254			48	129–134
Rh ^{III} (TPP)Cl	isopropanol	acetone		>360				136–138
Rh ^{III} (TPP)Cl	cyclohexanol	cyclohexanone		>360	520	3430		136,139
H ₃ PW ₁₂ O ₄₀ ·6 H ₂ O	ethanol	<i>b</i>	27	>340	<i>b</i>	<i>b</i>	<i>b</i>	150

^a No filter. ^b Not described.

> 2° > 1°, was noted. The requirement of high-energy UV photons (254 nm) is a fundamental limitation of the mercury photosensitization scheme that prohibits the overall applicability of the system for H₂ generation.

2.3. Alcohol Photo-dehydrogenations

The dehydrogenation of alcohols to either ketones or aldehydes provides an avenue to photocatalytic H₂ production. In some cases, the same catalysts employed for the dehydrogenation of alkanes may also catalyze alcohol photo-dehydrogenations (Table 2). In addition to the typical oxidative addition/ β -hydride elimination pathways for alkane dehydrogenation, alcohol dehydrogenations can involve H atom transfers, fast stepwise electron transfer followed by proton transfer, or other radical pathways. As a result, unlike alkane dehydrogenation, these reactivity modes are not limited to late transition metal centers. A catalyst that can open a coordination site and support a two-electron oxidation state change can potentially generate H₂ by alcohol dehydrogenation.

2.3.1. Rhodium Phosphine Complexes

Several Rh^I phosphine complexes of the Wilkinson type have been used as photocatalysts for alcohol dehydrogenations. Some of these are listed in Table 2. For the case of Wilkinson's complex, Rh^I(PPh₃)₃Cl, Sugi and co-workers observed the photocatalytic production of H₂ from isopropanol solution with a maximum turnover of 670 h⁻¹.¹⁰² Interestingly, the catalysis was more efficient when exposed to air, although the role of oxygen in the reaction remains unclear. Irradiation with UV light ($\lambda_{\text{exc}} < 300$ nm) is required for catalysis, which nevertheless exhibits a significant induction period (1–1.5 h) before H₂ evolution is observed. Subsequent work by Smith and co-workers using Rh^I(PPh₃)₃-Cl, Rh^I(P(OPh)₃)₃Cl, and mixtures of [Rh^I(COD)Cl]₂ or [Rh^I(CO)₂Cl]₂ with PPh₃ or OPPh₃ reported increased turnover numbers for isopropanol dehydrogenation.¹⁰³ The most active catalyst was found to be Rh^I(P(OPh)₃)₃Cl, which exhibited a turnover number of ~6400 when irradiated with UV light ($\lambda_{\text{exc}} < 300$ nm) at 21 °C. While a complete mechanistic scheme remains undefined, it was suggested that the rate enhancement was attendant to oxygen exposure and the induction period is due to a slow oxidation of dissociated PR₃ to OPR₃. As opposed to PR₃, OPR₃ more weakly

coordinates the metal; the inability of the oxidized phosphine to fill a coordination site could allow for more facile binding of substrate to a putative 14 electron, three-coordinate fragment, followed by reductive elimination of H₂ from the Rh center. The role of the photon in this case remains undefined, but is likely involved in the photoextrusion of H₂ from an octahedral Rh^{III}(PPh₃)₂X(H)₂Cl intermediate (X = PPh₃, OPPh₃, or substrate) by analogy to the observations made by Ford et al. for Rh^{III}(PPh₃)₃(H)₂Cl.¹⁰⁴

Rhodium phosphine complexes of Vaska's type, Rh^I(PR₃)₂(CO)X, have also been employed as alcohol dehydrogenation photocatalysts. Saito and co-workers examined the reactivity of several derivatives as catalysts for the dehydrogenation of isopropanol, where PR₃ = PPh₃, PⁱPr₃, PEtPh₂, PEt₂Ph, PEt₃, and PMe₃ and X = Cl, Br, and I.^{105,106} The reactivity was found to increase in the order PR₃ = PPh₃ < PⁱPr₃ < PEtPh₂ < PEt₂Ph < PEt₃ < PMe₃ and also along the series X = Cl < Br < I, suggesting that an electron-rich catalyst is more active for dehydrogenation with Rh^I(PEt₃)₂(CO)I attaining turnover a frequency of 1110 h⁻¹ at 82 °C under irradiation. The corresponding activity of the Rh^I(PMe₃)₂(CO)I complex was not reported, although Rh^I(PMe₃)₂(CO)Br was found to be more active than Rh^I(PEt₃)₂(CO)Br with turnover frequencies of 810 and 750 h⁻¹, respectively. The role of the photon in the dehydrogenation cycle is revealed by the action spectrum, that is, wavelength dependence, of the photocatalysis. Significant H₂ photogeneration was observed when irradiation wavelengths were co-incident with that required for photoexpulsion of CO from the Rh^I(PR₃)₂(CO)X coordination sphere (340 nm < λ_{exc} < 420 nm). Additionally the turnover frequencies were observed to drop when conducted under a CO atmosphere. Based on these results, the active species is surmised to be a three-coordinate, 14 electron Rh^I(PR₃)₂X fragment, consistent with that postulated for alkane dehydrogenations from similar Vaska-type complexes.

Cole-Hamilton and co-workers proposed the mechanism shown in Figure 4 for the dehydrogenation of primary and secondary alcohols at related Rh^I(PⁱPr₃)₃H and Rh^I(PⁱPr₃)₂-HCO catalysts.^{107,108} In the case of the primary alcohol ethanol, irradiation in the presence of either Rh^I(PⁱPr₃)₃H and Rh^I(PⁱPr₃)₂(CO)H gives H₂, CO, and CH₄ as the primary products, though the turnover frequencies were low, with 6.2 h⁻¹ for H₂ and 0.48 h⁻¹ for CH₄ for photochemical dehydrogenation of ethanol using Rh^I(PⁱPr₃)₃H at 150 °C.¹⁰⁹

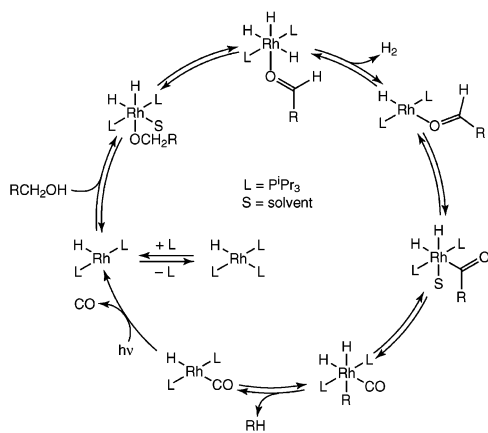


Figure 4. Proposed mechanism for the photocatalytic decomposition of methanol by $\text{Rh}^{\text{I}}(\text{PR}_3)_2(\text{CO})\text{H}$ ($\text{R} = \textit{i}\text{Pr}$) to give H_2 , CH_4 , and CO .

Though many mechanistic details remain unexplored, the observation by Otsuka and co-workers that $\text{Rh}^{\text{I}}(\text{P}^i\text{Pr}_3)_3\text{H}$ reacts with methanol to give $\text{Rh}^{\text{I}}(\text{P}^i\text{Pr}_3)_2(\text{CO})\text{H}$,¹¹⁰ together with the action spectrum for photocatalysis, form the basis for the photocycle of Figure 4. Initial photoexpulsion of CO from $\text{Rh}^{\text{I}}(\text{PR}_3)_2(\text{CO})\text{H}$ ($\text{R} = \text{P}^i\text{Pr}_3$) furnishes the reactive tri-coordinate intermediate, $\text{Rh}^{\text{I}}(\text{PR}_3)_2\text{H}$, which oxidatively adds across the $\text{O}-\text{H}$ bond of methanol; the coordination sphere is completed with a molecule of solvent to give $\text{Rh}^{\text{III}}(\text{PR}_3)_2(\text{H})_2(\text{OCH}_2\text{CH}_3)(\text{S})$. Dissociation of solvent followed by β -hydride elimination gives the trihydride, $\text{Rh}^{\text{III}}(\text{PR}_3)_2(\text{H})_3(\text{O}=\text{CHCH}_3)$. Elimination of H_2 followed by another β -hydride elimination and solvent coordination gives the acyl complex $\text{Rh}^{\text{III}}(\text{PR}_3)_2\text{H}(\text{C}=\text{OCH}_3)(\text{S})$. Methane may be generated by reductive elimination from $\text{Rh}^{\text{III}}(\text{PR}_3)_2(\text{H})_2(\text{CH}_3)\text{CO}$, which forms from the dissociation of the solvent followed by CO migration. The starting catalyst is regenerated with this reductive elimination. Based on this mechanism, H_2 and methane should be evolved in a 1:1 stoichiometry. It is perplexing then, that the reported turnover frequency for H_2 is a factor of ~ 13 greater than that for CH_4 . This discrepancy suggests that the mechanism is not fully understood and that other pathways for H_2 generation may be operative. One possibility is that the mechanism of Figure 4 represents a minor pathway for methanol dehydrogenation and that the major pathway proceeds via a mechanism similar to the Vaska-type $\text{Rh}^{\text{I}}(\text{PR}_3)_2(\text{CO})\text{Cl}$ complexes, that is, a pathway that converts methanol directly into formaldehyde and H_2 without invoking Rh acyl intermediates.

The photocatalyzed dehydrogenation of isopropanol by $\text{Rh}^{\text{I}}(\text{PR}_3)_2(\text{CO})\text{H}$ is also proposed to proceed by oxidative addition of the alcoholic $\text{O}-\text{H}$ bond followed by β -hydride elimination to generate a Rh^{III} dihydride and acetone.¹⁰⁹ In this case however the photochemical step was presumed to involve the reductive elimination of H_2 , because the system was catalytic under irradiation but also in the dark when in the presence of the transfer hydrogenation acceptor 1-hexene.

2.3.2. Binuclear Complexes

Alcohol dehydrogenation accompanied by H_2 evolution may also be accomplished by bimetallic late transition metal complexes. Methanol and isopropanol can be photocatalytically dehydrogenated upon irradiation of solutions of *cis*- $\text{Rh}_2^{\text{II}}(\text{dppm})_2\text{Cl}_2(\text{CO})_2$ and $\text{Pd}_2^{\text{II}}(\text{dppm})_2\text{Cl}_2$.^{111–113} For methanol dehydrogenation, the photoreactions were performed in

refluxing 9:1 methanol/acetone solutions. Turnovers of 130 and 156 h^{-1} were obtained for the Rh and Pd catalysts, respectively. Interestingly, the addition of acetone appears to be a requisite for catalytic activity. The photolysis was performed under full spectrum irradiation conditions, prompting the suggestion that direct excitation into the acetone $n \rightarrow \pi^*$ transition ($\lambda_{\text{exc}} < \sim 312 \text{ nm}$) photoinitiates the reaction. The $n\pi^*$ excited state was proposed to abstract a methyl H atom from methanol to generate the methoxy radical. The observed product distributions reflect this radical reactivity because ethylene glycol and formaldehyde dimethyl acetal are observed, in addition to formaldehyde, which is the product expected from simple dehydrogenation. Control experiments using only acetone and no transition metal catalyst showed low catalytic activity and a markedly different product ratio. The major products in the liquid phase were ethylene glycol and isopropanol; formaldehyde was obtained in only small quantities. The gaseous products were composed primarily of methane and only small quantities of H_2 (methane/hydrogen = $\sim 70:1$). These results establish that the bimetallic complex is needed to support high turnovers. Accordingly, it was proposed that the initial methanol activation occurs by H atom abstraction from a $\text{C}-\text{H}$ bond of methanol by the directly excited acetone to generate a ketyl radical and HOCH_2^{\cdot} . Hydrogen generation is then achieved in subsequent steps by reaction of the bimetallic transition metal catalysts with the organic radicals to give formaldehyde and acetone. This strategy was later applied to isopropanol dehydrogenation using *cis*- $\text{Rh}_2^{\text{II}}(\text{dppm})_2\text{Cl}_2(\text{CO})_2$.¹¹³ An induction period was ascribed to an initial slow dehydrogenation of isopropanol to generate acetone. As in the methanol dehydrogenation case, the acetone was proposed to act as a sensitizer once an appreciable concentration accumulated. Consistent with this contention, the induction period was eliminated when acetone was added to the solution.

Arguably, the most extensively examined system for the photocatalytic dehydrogenation of alcohols by a dinuclear complex is that of $\text{Pt}_2^{\text{II,II}}(\text{P}_2\text{O}_5\text{H}_2)_4^{4-}$, better known as PtPOP.¹¹⁴ First crystallized in 1990,¹¹⁵ PtPOP is a face-to-face dimer of two square-planar d^8 Pt^{II} metal centers. Penetrating spectroscopic studies^{116–119} reveal that the frontier metal centered molecular orbitals (MOs) arise from the overlap of the d_{z^2} orbitals in $d\sigma$ and $d\sigma^*$ linear combinations.¹¹⁴ In the 4-fold symmetry of the D_{4h} ligand environment, an allowed $d\sigma^* \rightarrow p\sigma$ electronic transition is assigned to an intense absorption feature at 367 nm ($\epsilon \approx 3 \times 10^4 \text{ M}^{-1} \text{ cm}^{-1}$).¹²⁰ Excitation into this band generates a long-lived phosphorescent $^3(d\sigma^*p\sigma)$ excited state with a nearly 10 μs lifetime and an emission maximum of 514 nm.¹²¹

The $^3(d\sigma^*p\sigma)$ excited state exhibits diradical character,¹¹⁴ from which the photoreactivity of PtPOP is derived. Roundhill irradiated the $d\sigma^* \rightarrow p\sigma$ absorption manifold in the presence of isopropanol to form H_2 with a turnover of > 400 after 3 h of irradiation at ambient temperature.¹²² The photoreaction mechanism shown in Figure 5 was deciphered by Gray and co-workers by undertaking a series of comprehensive studies. Initial photon absorption generates the $\text{Pt}_2^{\text{II,II}}$, $^3(d\sigma^*p\sigma)$ excited state, which abstracts a hydrogen atom from isopropanol and forms the mixed valence hydride complex, $\text{Pt}_2^{\text{II,III}}\text{H}$. The existence of this mixed valence complex was verified directly in pulse radiolysis spectra.¹²³ This mixed-valence intermediate abstracts a second H atom to form the valence symmetric dihydride, $\text{Pt}_2^{\text{III,III}}(\text{H})_2$ by analogy with

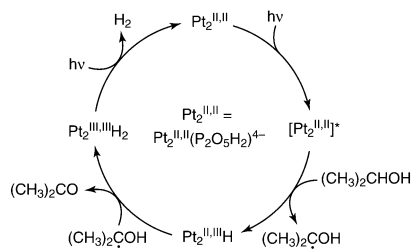


Figure 5. Proposed mechanism for the photocatalytic isopropanol dehydrogenation at PtPOP (POP = $\text{P}_2\text{O}_5\text{H}_2^{2-}$).

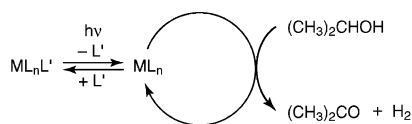


Figure 6. Proposed mechanism for isopropanol dehydrogenation by $\text{M}^{\text{III}}(\text{SnCl}_3)_x(\text{Y})_z^{3-}$ salts ($\text{Y} = \text{H}, \text{Cl}; x = 1 \text{ or } 2; z = 6 - x$).

previous work concerning the thermal oxidation chemistry of $\text{Pt}_2^{\text{II,II}}$ cores.¹²⁴ This intermediate was independently synthesized, and a binuclear axial dihydride formulation was confirmed.¹²⁵ Hydrogen release from the dihydride requires a photon, though the precise mechanism for this effective reductive elimination has eluded identification.¹²⁵ The photocycle of Figure 5 has been extended to numerous secondary alcohols and also to $d^8 \cdots d^8$ complexes of Ir.^{126–128}

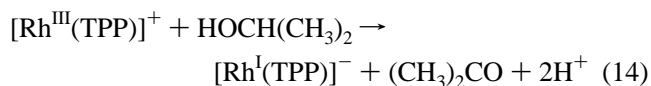
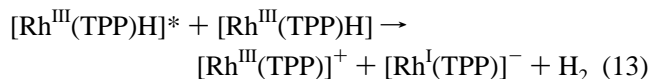
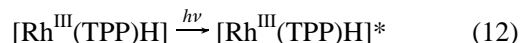
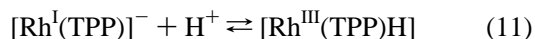
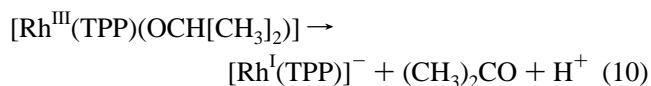
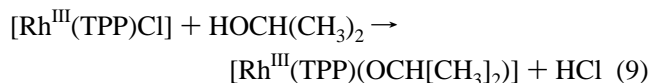
2.3.3. M–Sn Complexes

Transition metal complexes coordinated by tin-based ligands also exhibit alcohol dehydrogenation activity. Saito and co-workers initially reported that a mixture of $\text{Rh}^{\text{III}}\text{Cl}_3 \cdot (\text{H}_2\text{O})_3$, $\text{Sn}^{\text{II}}\text{Cl}_2(\text{H}_2\text{O})_2$, and LiCl in a 1:2:3 ratio dehydrogenated isopropanol with a quantum efficiency of 1.7 under UV irradiation ($\lambda_{\text{exc}} = 254 \text{ nm}$) at 82°C .^{129,130} The catalysis was later extended to $\text{M}^{\text{III}}\text{Cl}_3(\text{H}_2\text{O})_3$ complexes with $\text{M} = \text{Ir}^{131–133}$ and $\text{Ru}^{133,134}$. Quantum efficiencies as high as 12 were reported for $\text{M} = \text{Ir}$, where the active catalyst was suggested to be either *trans*- $\text{Ir}^{\text{III}}\text{Cl}_2(\text{SnCl}_3)_4^{3-}$ or $\text{Ir}^{\text{III}}\text{H}(\text{SnCl}_3)_5^{3-}$ on the basis of ^{119}Sn NMR spectra.¹³⁵ Mechanistic details are incomplete, but greater than unity quantum yields were rationalized by a general mechanism where irradiation into a $\text{M}(\text{d}\pi) \rightarrow \text{Sn}(\pi^*)$ transition induces dissociation of a SnCl_3^- ligand generating the active catalyst according to the steps shown in Figure 6. The coordinatively unsaturated species is proposed to dehydrogenate isopropanol for several turnovers thermally before being trapped by SnCl_3^- in a ligand recombination reaction. Although the participation of $n\pi^*$ excited states of acetone for H atom abstraction could also play a role in the observed isopropanol dehydrogenation catalysis.

2.3.4. Rhodium Porphyrins

Rhodium porphyrin complexes are active for the photochemical dehydrogenation of alcohols. A chloro rhodium tetraphenyl porphyrin complex $[\text{Rh}(\text{TPP})\text{Cl}]$ was found to dehydrogenate isopropanol^{136–138} and cyclohexanol^{136,139} to the corresponding ketones in neat alcohol at reflux temperatures under visible light irradiation ($\lambda_{\text{exc}} > 360 \text{ nm}$). Extended photolysis (520 h) gave 3430 turnovers with exclusive formation of H_2 and ketone products as determined by GC analysis.¹³⁸ The reaction was proposed to proceed

through the intermediacy of a $\text{Rh}^{\text{III}}(\text{TPP})\text{H}$ complex by the following reaction cascade (for the example of isopropanol):



No intermediates are observed along the pathway, but precedent for a bimolecular reactivity mode was found in the stoichiometric thermal generation of H_2 observed by Ogoshi et al from a reaction of a related $\text{Rh}^{\text{III}}(\text{OEP})\text{H}$ complex (OEP = octaethylporphyrin) with concomitant formation of $[\text{Rh}^{\text{II}}(\text{OEP})]_2$.¹⁴⁰ Wayland et al. later reported that the reaction is significantly enhanced under photolysis conditions indicating the involvement of $\text{Rh}^{\text{III}}(\text{OEP})\text{H}$ excited states along the reaction pathway.¹⁴¹ The authors suggest that the increased steric demands of TPP vs OEP prevent the formation of the metal–metal bonded d^7-d^7 $\text{Rh}^{\text{II}}(\text{TPP})$ dimer, and thus dimerization of a photoexcited $[\text{Rh}^{\text{III}}(\text{TPP})\text{H}]^*$ and a ground-state $\text{Rh}^{\text{III}}(\text{TPP})\text{H}$ are proposed to give H_2 and the valence disproportionated products $[\text{Rh}^{\text{III}}(\text{TPP})]^{2+}$ and $[\text{Rh}^{\text{I}}(\text{TPP})]^-$. The $[\text{Rh}^{\text{III}}(\text{TPP})]^{2+}$ is then suggested to oxidize isopropanol by two electrons to generate $[\text{Rh}^{\text{I}}(\text{TPP})]^-$, acetone, and two proton equivalents. The authors at this point chose to invoke successive proton and electron transfers, but the possibility of hydrogen atom transfers along the pathway, as seen for PtPOP, for example, cannot be ignored.

2.3.5. Polyoxometalates

Polyoxometalates (POMs) are typically composed of molybdates and tungstates of the Keggin, $[\text{XW}_{12}\text{O}_{40}]^{n-}$ ($\text{X} = \text{P}, \text{Si}, \text{Fe}, \text{H}_2$), or Dawson, $[\text{P}_2\text{W}_{18}\text{O}_{66}]^{6-}$, type. POMs have been widely studied, and the rich electrochemical and photochemical properties of these compounds have been reviewed elsewhere.^{142,143} POMs are excellent oxidation catalysts and have been reported to photooxidize alcohols in acidic solutions.^{144–146} Upon one-electron reduction, the initially colorless or pale yellow solutions of POMs acquire the bright blue hue ($\lambda_{\text{max}} = 500–800 \text{ nm}$) of the heteropolyblues (HPB). The low-energy electronic transitions are attributed to intervalence charge transfer (IVCT) bands within the lattice. The HPBs are ESR active and, at low temperatures, give signals with hyperfine couplings indicative of localization of the unpaired spin on a single metal center. Upon warming, the observed signal broadens, suggesting extensive electron delocalization over the POM. The two-electron reduction products are ESR silent, indicating strong antiferromagnetic coupling of the unpaired spins within the lattice, as is characteristic for species with oxo bridges.¹⁴⁷

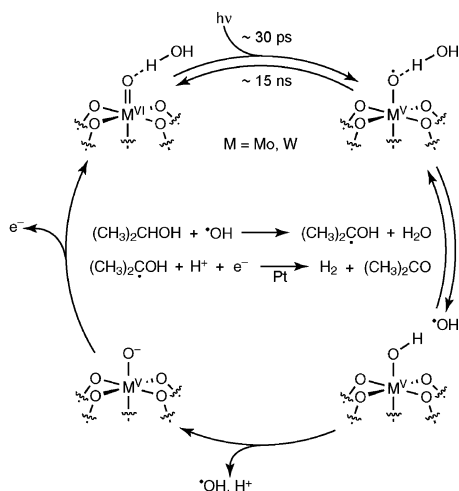


Figure 7. Proposed mechanism for the polyoxometalate-catalyzed anaerobic photocatalytic dehydrogenation of isopropanol to acetone. Hydrogen production is accelerated in the presence of colloidal Pt, but the Pt catalyst is not required.

In anaerobic solution, photoexcitation of POMs in the presence of oxidizable substrates such as alcohols gives the blue solution of HPB accompanied by H₂ production.^{148–157} The rate of H₂ production is faster in the presence of a colloidal Pt catalyst, but H₂ production is inhibited in the presence of oxygen, favoring the reduction of oxygen to water instead.¹⁵⁸ Wavelength selection of the excitation light shows that the irradiation into the blue absorption bands gives no H₂. Catalysis is induced when the excitation light is coincident with the higher energy oxo → metal, ligand to metal charge transfer (LMCT) transition. Transient spectroscopic studies indicate that the active oxidant of a related POM, [W₁₀O₃₂]⁴⁻, forms within 30 ps of excitation into the O → W LMCT absorption band. This excited state has a relatively long lifetime for a LMCT excited state of >15 ns, and it was found to possess significant radical character on oxygen.¹⁵⁹ In the presence of an oxidizable substrate, the oxygen radical abstracts an H atom, which then gives the one-electron-reduced HPB after the loss of a proton (Figure 7). The observation of H atom abstractions with rates above the diffusion limit suggest that the initial event proceeds through a preassociated complex.¹⁶⁰ The preassociation of substrate with the POM in ground state has been supported by X-ray structural evidence and shifted substrate NMR signals.^{161–163} In the absence of water, H atom abstraction from the alcohol occurs directly,^{164,165} but in aqueous solutions, water preferentially binds to the surface of the POM over alcohol, disposing the initial H atom abstraction process to proceed from water to yield hydroxyl radicals.¹⁶⁶ The hydroxyl radicals react with alcoholic substrates at a diffusion-controlled rate, eventually giving H₂ and acetone for the case of isopropanol dehydrogenations as shown in Figure 7.¹⁶⁷ The selectivity for acetone is under kinetic rather than thermodynamic control because POMs are known to fully degrade alcohols to H₂O and CO₂.^{168–171} The complete oxidation pathway is circumvented by much slower reaction kinetics (100 times slower) as compared with the kinetics for the oxidation of isopropanol to acetone. The generation of hydroxyl radicals is further supported by the observation of identical kinetics and product distributions for the dehydrogenation of isopropanol by *OH generated using ⁶⁰Co- γ -radiation.¹⁷²

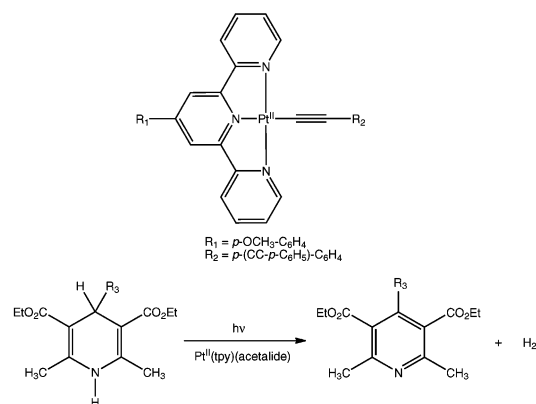


Figure 8. Structure of a Pt^{II} terpyridine photocatalyst for H₂ production (top) and an example of the Hantzsch 1,4-dihydropyridines used in that study as a dehydrogenation substrate (bottom).

2.4. Platinum Terpyridine Complexes

A Pt^{II}(tpy)(acetylide)⁺ (tpy = terpyridine) complex has recently been shown to catalytically dehydrogenate NADH analogs in anaerobic acetonitrile solution under irradiation.¹⁷³ The Pt^{II}(tpy)(acetylide)⁺ complex [(L)Pt^{II}(C≡C-*p*-C₆H₄-C≡C-C₆H₅)]ClO₄ (L = 4'-(4-methoxyphenyl)-2,2',6,2''-terpyridyl) was used as a photocatalyst, Figure 8 (top), and the substrate was diethyl-1,4-dihydro-2,6-dimethyl-3,5-pyridinecarboxylate (DHP), a member of the Hantzsch 1,4-dihydropyridines, which have been used as models for NADH.¹⁷⁴ Irradiation into the Pt(d π) → tpy(π^*) MLCT band generates the long-lived ³MLCT excited state, which possesses an emissive lifetime of 340 ns. In the presence of substrate, the emission is quenched with Stern–Volmer kinetics at a rate constant of 8.7 × 10⁹ M⁻¹. Upon continued irradiation, H₂ was produced photocatalytically according to the sequence shown in Figure 8 (bottom), DHP was completely converted to the corresponding substituted pyridine with a quantum yield of 0.38. No H₂ was produced when N-alkylated pyridines were used. Isotopic labeling studies showed that substitution of deuterium for hydrogen at the 4 position of the DHP gave no change in the observed quenching rate constant, but a decrease in the quantum yield for H₂ production from 0.38 to 0.32. Deuterium incorporation at the 1 position (pyridyl nitrogen) however gave a decreased quenching rate constant of 6.1 × 10⁹ M⁻¹ and also a decreased quantum yield of 0.31. With limited mechanistic details, the authors proposed a pathway where the excited ³MLCT state effects successive H atom abstractions from DHP to give the dehydrogenated DHP and H₂. No attempts were made to identify intermediates along the reaction pathway.

The Pt^{II}(tpy)(acetylide) congener [(mpt)Pt^{II}-(C≡C-*p*-C₆H₄Cl)]ClO₄ (mpt = 4'-(4-methylphenyl)-2,2',6,2''-terpyridyl) has been examined by transient absorption spectroscopy in an effort to further elucidate the operational mechanism.¹⁷⁵ Electron donors such as triethylamine and triphenylamine produce the same transient intermediates as observed when using the putative H atom donor, DHP. These results suggest that the ³MLCT excited state formed upon irradiation is quenched by electron transfer and not H atom abstraction. Accordingly, an electron-transfer mechanism may support H₂ generation where the primary photochemical process is one-electron reduction of the Pt^{II}(tpy^{•-}) ³MLCT state to generate [Pt^{II}(tpy^{•-})]⁻. Subsequent reaction steps are presumed to involve proton loss from the DHP^{•+}, followed

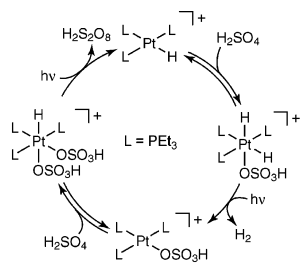


Figure 9. Proposed mechanism for platinum-catalyzed photocatalytic H_2 production from aqueous H_2SO_4 solutions.

by a net hydrogen atom loss from the 4 position of the substrate to aromatize the resulting pyridine. As of yet, no concrete evidence has been presented for the formation of an intermediate Pt hydride, but by analogy with other systems (*vide infra*) this type of electron transfer/proton-transfer pathway is plausible. The driving force for the reaction is likely to stem from the aromatization of the DHP upon removal of two hydrogen atoms.

3. Hydrogen Production from Acidic Solutions

Unlike the schemes of section 2, which rely on high-energy substrates, H_2 generation directly from low-energy substrates such as acids are relatively uncommon. Owing to the lower energy content of the substrate, H_2 photogeneration from inorganic acids heretofore generally requires high-energy photons to drive the reaction. Moreover, simple mineral acids like HCl and HBr have conjugate bases that form very strong M–X bonds ($\text{X} = \text{Cl}, \text{Br}$) with many transition metal centers. Hence if one is to achieve turnover, a potential catalyst must be able to activate the thermodynamically challenging M–X bond. Few systems have been able to achieve this type of reactivity to date.

3.1. Mononuclear Catalysts

Some of the earliest reports of H_2 photogeneration involve acidic solutions of simple metal salts. Whereas most reduced metal ions produce H_2 promptly upon their addition to mineral acids, some are thermally stable toward acid. In these cases, photoexcitation leads to the generation of H_2 stoichiometrically: Eu^{2+} ,¹⁷⁶ Cr^{2+} ,¹⁷⁷ Fe^{2+} ,¹⁷⁸ Ce^{3+} ,¹⁷⁹ and Cu^+ ¹⁸⁰ are all active under photolysis conditions.

Photocatalysis may be achieved upon complexation of metal ions with appropriate ligand sets. For instance, H_2 production from a mononuclear platinum phosphine complex in aqueous H_2SO_4 solutions was reported by Cole-Hamilton.¹⁸¹ In this scheme, a solution of $\text{Pt}^{\text{II}}(\text{PEt}_3)_2\text{Cl}_2$, PEt_3 , and Ag_2SO_4 in aqueous H_2SO_4 adjusted to pH 2.5 was irradiated with light from the full spectrum. Mechanistic details are not reported, but the authors propose that initial halide abstraction followed by phosphine coordination and two-electron reduction initially generates the reactive fragment $\text{Pt}^0(\text{PEt}_3)_3$, which is known to rapidly convert to $[\text{Pt}^{\text{II}}(\text{PEt}_3)_3\text{H}]^+$ in aqueous solution.¹⁸² The catalytically active $[\text{Pt}^{\text{II}}(\text{PEt}_3)_3\text{H}]^+$ species is proposed to enter the cycle shown in Figure 9. In brief, protonation of $[\text{Pt}^{\text{II}}(\text{PEt}_3)_3\text{H}]^+$ followed by coordination with HSO_4^- generates the $[\text{Pt}^{\text{IV}}(\text{PEt}_3)_3\text{H}_2(\text{HSO}_4)]^+$ cation. Photoinduced H_2 elimination is proposed to give the $[\text{Pt}^{\text{II}}(\text{PEt}_3)_3(\text{HSO}_4)]^+$ species, which activates another equivalent of H_2SO_4 to generate $[\text{Pt}^{\text{IV}}(\text{PEt}_3)_3\text{H}(\text{HSO}_4)_2]^+$. A second photoinduced step is proposed to effect

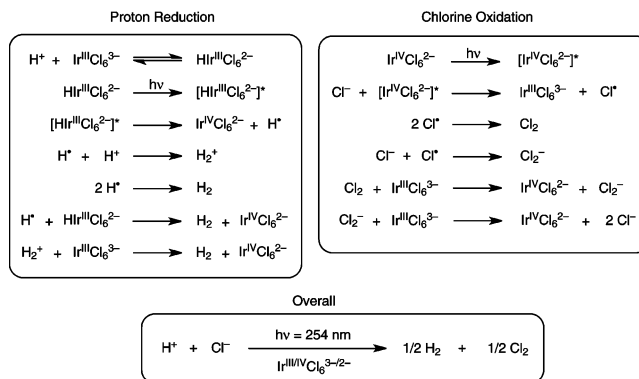


Figure 10. Proposed reactions involved in the photocatalytic production of H_2 from aqueous HCl solutions using an $\text{Ir}^{\text{III}}\text{Cl}_6^{3-}$ catalyst.

a reductive elimination of persulfuric acid, $\text{H}_2\text{S}_2\text{O}_8$, and regenerate the starting $[\text{Pt}^{\text{II}}(\text{PEt}_3)_3\text{H}]^+$ species. The authors report H_2 production and a 50% recovery of $[\text{Pt}^{\text{II}}(\text{PEt}_3)_3\text{H}]^+$ after 48 h of photolysis. The recovery of $[\text{Pt}^{\text{II}}(\text{PEt}_3)_3\text{H}]^+$ is given as evidence of catalysis, but no turnover data for H_2 generation is reported and the proposed Pt^{IV} intermediates as well as the persulfuric acid were not directly observed.

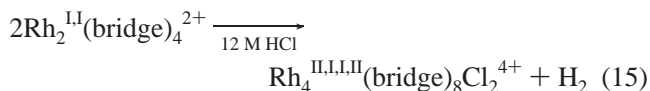
Photocatalytic H_2 production using a simple metal salt, $\text{Ir}^{\text{III}}\text{Cl}_6^{3-}$, from aqueous HCl has been proposed to proceed by the reaction sequence shown in Figure 10.^{183,184} Irradiation into the $\text{Cl}^- \rightarrow \text{Ir}^{\text{III}}$ LMCT bands with 254 nm light led to the disappearance of $\text{Ir}^{\text{III}}\text{Cl}_6^{3-}$ and produced the one-electron oxidized species $\text{Ir}^{\text{IV}}\text{Cl}_6^{2-}$ with the concomitant production of half an equivalent of molecular H_2 . The steps leading to this reactivity may involve a pre-equilibrium between $\text{Ir}^{\text{III}}\text{Cl}_6^{3-}$ and $\text{HIr}^{\text{III}}\text{Cl}_6^{2-}$ followed by photoexcitation of $\text{HIr}^{\text{III}}\text{Cl}_6^{2-}$ to generate the excited state $[\text{HIr}^{\text{III}}\text{Cl}_6^{2-}]^*$ (possessing significant $\text{Ir}^{\text{II}}-\text{Cl}^*$ character), which is then proposed to decompose to a H atom and $\text{Ir}^{\text{IV}}\text{Cl}_6^{2-}$. Possible reactions for the resulting H atoms include dimerization to generate H_2 , reaction with another equivalent of $\text{HIr}^{\text{III}}\text{Cl}_6^{2-}$ to generate H_2 and $\text{Ir}^{\text{IV}}\text{Cl}_6^{2-}$, and the more unlikely reaction of the H atom with a proton to generate H_2^+ , which is subsequently reduced to H_2 by another equivalent of $\text{Ir}^{\text{III}}\text{Cl}_6^{3-}$. Catalysis is accomplished by secondary photolysis of the $\text{Ir}^{\text{IV}}\text{Cl}_6^{2-}$ generated during the course of hydrogen production. In a similar fashion to proton reduction, $\text{Cl}^- \rightarrow \text{Ir}^{\text{IV}}$ LMCT excitation generates a charge-transfer complex with $\text{Ir}^{\text{III}}-\text{Cl}^*$ character, and this intermediate is capable of oxidizing a free Cl^- ion from the aqueous mineral acid solution to furnish unbound chlorine radicals and $\text{Ir}^{\text{III}}\text{Cl}_6^{3-}$. The chlorine radicals are then proposed to undergo radical-based reactivity similar to that of the hydrogen atoms to eventually generate chlorine and the starting $\text{Ir}^{\text{IV}}\text{Cl}_6^{2-}$ photoreactant. The catalytic cycle is closed with the recovery of $\text{Ir}^{\text{III}}\text{Cl}_6^{3-}$ by the secondary photolysis reaction of $\text{Ir}^{\text{IV}}\text{Cl}_6^{2-}$ and provides the net conversion of HCl to $\frac{1}{2}\text{H}_2$ and $\frac{1}{2}\text{Cl}_2$. The quantum efficiency of the overall conversion is 0.28 in 12 M HCl using 254 nm irradiation. This quantum efficiency is observed to drop off sharply with decreasing photon energy and turns off completely when using wavelengths longer than 366 nm, consistent with photoreactivity derived from high-energy $\text{Cl}^- \rightarrow \text{Ir}$ charge-transfer excited states. Although the system carries out the photocatalytic splitting of HCl to $\frac{1}{2}\text{H}_2$ and $\frac{1}{2}\text{Cl}_2$ while under constant irradiation, the produced Cl_2 is observed to reoxidize the $\text{Ir}^{\text{III}}\text{Cl}_6^{3-}$ to $\text{Ir}^{\text{IV}}\text{Cl}_6^{2-}$ when the photolysis is ceased.

3.2. Binuclear Catalysts

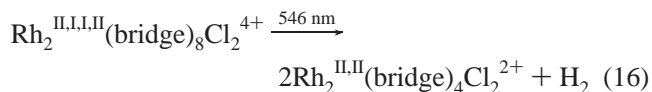
The mononuclear systems outlined above suffer either from single-electron steps or the need for high-energy irradiation for catalytic reactivity or both. More ideal catalysts would absorb visible photons and have the ability to participate in the two-electron reactivity needed for H₂ generation. To this end, bimetallic complexes with strongly interacting metal centers possess a number of attractive features for the development of photocatalysts. Low-lying, allowed transitions with parentage from the bimetallic core can give rise to reactive electronic excited states accessed with visible photons. Additionally bimetallic reactivity^{185,186} is based on the tenet that two metals combined might enable transformations inaccessible to single metal ions.^{187,188} One commonly encounters dinuclear and higher nuclearity metal sites in Nature: in the diiron enzymes¹⁸⁹ soluble methane monooxygenase^{190,191} and class I ribonucleotide reductase,^{32,192} in the dicopper and iron–copper sites of cytochrome *c* oxidase,^{193,194} in the dinickel center of urease,¹⁹⁵ in the O₂-transport proteins hemerythrin^{189,196} and hemocyanin,¹⁹⁷ in the photosystem II oxygen-evolving complex,¹⁹⁸ in the enzymes nitrogenase^{199–201} and nickel–carbon monoxide dehydrogenase/acetyl coenzyme A synthase,^{202–205} in at least a dozen zinc enzymes,^{206,207} in certain iron–sulfur clusters,^{208,209} *inter alia*,^{210,211} and of course the iron-only and Ni–Fe active sites of hydrogenase.^{212–217} Most of these enzymes activate small molecules by multielectron transformations. Though the precise mechanistic details of substrate activation in many such systems await elucidation, reactivity and spectroscopic studies indicate that the metals of the bioactive site may work cooperatively to activate substrates one electron at a time.²¹⁸ The protein environment, among other functions, ensures that one-electron intermediates are channeled along the desired multielectron reaction course and not diverted to nonproductive and uncontrollable one-electron/radical side-reaction channels. Such is not the case for a coordination compound. When removed from the protected environment of the protein, an exposed polynuclear metal core is subject to a variety of one-electron redox pathways that can subvert multielectron reactivity; however intermetal redox cooperation in polynuclear metal coordination compounds can potentially be achieved by judicious ligand design.

3.2.1. Biradical Excited States

Ligation of binuclear Rh₂^{I,I} centers by 1,3-diisocyanopropane (bridge) gives rise to a dσ* → pσ transition that falls in the visible spectral region (λ_{max} = 546 nm). Irradiation into this absorption manifold of the d⁸...d⁸ Rh₂^{I,I}(bridge)₄²⁺ complex in hydrochloric acid causes the generation of one equivalent of hydrogen and the metal–metal bonded d⁷–d⁷ dimer, Rh₂^{II,II}(bridge)₄X₂²⁺,^{219–221} A dimer of dimers, Rh₄^{II,I,I,II}(bridge)₈Cl₂⁴⁺, results from a thermal reaction of the Rh₂^{I,I} core with HCl as depicted in eq 15. The photon is



needed to cleave the putative Rh^I–Rh^I bond in the Rh₂^{II,I,I,II}(bridge)₈Cl₂⁴⁺ tetranuclear complex followed by the reaction of the resultant dimers with HCl, eq 16,



to generate 2 equiv of Rh₂^{II,II}(bridge)₄Cl₂²⁺ and H₂ in an undefined manner.^{222,223} The visible-light-promoted H₂ production is stoichiometric and not catalytic. The strong Rh^{II}–Cl bonds of the oxidized Rh₂^{II,II}(bridge)₄Cl₂²⁺ cannot be activated to regenerate the active Rh₂^{I,I}(bridge)₄²⁺ for reentry into a catalytic cycle.

The two-electron photoreactivity of the Rh₂^{I,I}(bridge)₄²⁺ system is derived from coupling the one-electron reactivity of the individual Rh^I centers of the bimetallic core. Spectroscopic studies show that the dσ* → pσ excited state of the d⁸...d⁸ excited state is metal-based with two electrons in a triplet configuration,^{224,225} each localized on a metal center of a singly bonded binuclear core. The excited states of binuclear d⁸...d⁸ complexes, and d¹⁰...d¹⁰ complexes as well, may therefore be described chemically as a diradical tethered by a metal–metal bond ([d⁸...d⁸]^{*} = [^{*}M–M]^{*}).²²⁶ Not surprisingly, these types of excited states drive primary one-electron photoevents, as observed in the hydrogen atom chemistry of PtPOP (section 2.3.2) and the Rh bridge chemistry of eqs 15 and 16.

3.2.2. Two-Electron Mixed Valency

Using the connection between one-electron chemistry and biradical excited states, Nocera and co-workers sought to emphasize the multielectron chemistry of binuclear complexes by singlet coupling of two electrons on one metal of the binuclear core, as opposed to the triplet coupling of biradical states. The design is predicated on electrons that are weakly coupled such that the multielectron excited state may be prepared by exciting a metal-to-metal charge transfer (MMCT). Here, electrons originally localized on the individual metal centers of a bimetallic core in the ground state are paired upon the absorption of a photon to produce an excited state that is zwitterionic, M⁺–M:[−], in nature. Two-electron reductions of substrate may be promoted at the M:[−] site, whereas substrates susceptible to two-electron oxidation may react at the M⁺ site.

The electronic configuration formalism for a zwitterionic excited state was established with a detailed laser-induced two-photon spectroscopic investigation of the δ bonding manifold of quadruple metal–metal bond complexes. The two electrons residing in the d_{xy} orbitals of the δ bond are weakly coupled owing to the parallel disposition of the orbitals on each metal center to one another. By spectroscopically determining the energies of the four states of the δ/δ* manifold bond, the ionic and covalent natures of the excited state can be determined. The challenge confronting this longstanding identification of the two-electron bond has been the identification of the two-electron state; in the case of the quadruple-bonded complexes, this state arises from the ¹δ*δ* configuration. Laser-induced two-photon spectroscopy allowed this elusive excited state to be identified.^{227,228} The discovery of the ¹δ*δ* excited state was important on several fronts: (1) Though discussed since the inception of valence²²⁹ and molecular orbital²³⁰ bonding theories, this was the first time that the four states of a two-electron bond had been spectroscopically characterized in a discrete molecular species.²³¹ (2) The ionic contribution of the wavefunction to the δδ* excited state was ascertained from the state energies of the δ-manifold and found to be

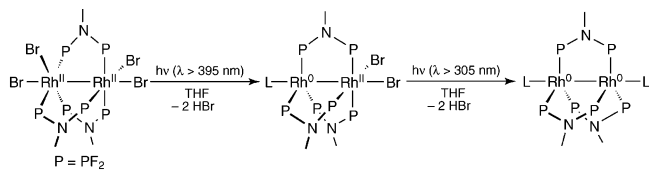


Figure 11. Stepwise two-electron halogen elimination photochemistry of binuclear rhodium cores ligated by dfpma initiated by the population of a $d\sigma^*$ excited state.

80%. Indeed, the M^+-M^- zwitterion mediates both two-electron photochemical oxidative addition^{232–234} and reductive elimination reactions.²³⁵ However, it has not been observed to drive hydrogen production directly. Quadruple bonds can photogenerate hydrogen but by a one-electron reaction in the case of $\text{Mo}_2(\text{SO}_4)_4^{4-}$ ^{236,237} or by coupling two one-electron reactions in the case of $\text{Mo}_2(\text{HPO}_4)_4^{4-}$.²³⁸ The two-electron chemistry of the zwitterionic state is prevented by the rigid tetrakis ligation geometry of the D_{4h} complexes. Terminal ligands are needed to allow the excited-state complex to relax into a bioctahedral geometry, which has been shown to trap the zwitterionic nature of the $\delta\delta^*$ excited state.²³⁹ The inability of the zwitterionic M^+-M^- excited state of quadruple bond complexes to drive hydrogen production called for consideration of a re-engineered binuclear core. Unfortunately, preparation of zwitterionic excited states by pairing two electrons within the binuclear core is largely unique to quadruple bond metal compounds, with some notable exceptions.²⁴⁰ Most excited states are derived from the population of molecular orbitals that are delocalized over the entire bimetallic core, and consequently, in such cases it is not appropriate to think about electron pair localization. For this reason, multielectron schemes based on zwitterionic excited states are difficult to generalize to most other classes of binuclear complexes, and new approaches must be developed.

The challenge presented by orbital delocalization may be overcome, however, if one realizes that the zwitterionic excited state, at a more general level, is a two-electron mixed valence, M^n-M^{n-2} , complex. Under this formalism, a promising line of research is the synthesis of complexes with the two-electron mixed valency already present in the ground state. This two-electron mixed valency may be ligand-based^{241–244} or metal-based.^{20,21} With regard to the latter, Rh bimetallics, when ligated by three dfpma ligands (dfpma = bis(difluorophosphino)methylamine, $\text{CH}_3\text{N}[\text{PF}_2]_2$), evidence an unusual two-electron mixed-valence ground state: $\text{Rh}_2^{0,\text{II}}(\text{dfpma})_3\text{X}_2\text{L}$ ($\text{X} = \text{Cl}, \text{Br}$; $\text{L} = \text{PR}_3, \text{CN}^t\text{Bu}, \text{CO}$) containing a formal Rh–Rh bond.²⁴⁵ The metal–metal single bond can be envisioned as arising from the pairing of odd electrons in the out of plane d_z^2 orbitals on the d^7-d^9 (or $[d^6]d^1-d^1-[d^8]$) bimetallic core.^{20,246} The two-electron mixed-valence ground state is thought to be stabilized relative to a valence-symmetric redox congener by asymmetric π -donation of the bridgehead amine lone pair allowing the ligand to concomitantly accommodate metals both in low and in moderate oxidation states.

These cores are capable of facilitating four-electron redox chemistry in discrete two-electron steps along the series $\text{Rh}_2^{0,0}(\text{dfpma})_3\text{L}_2$, $\text{Rh}_2^{0,\text{II}}(\text{dfpma})_3\text{X}_2\text{L}$, and $\text{Rh}_2^{\text{II},\text{II}}(\text{dfpma})_3\text{X}_4$ (Figure 11).²⁴⁷ Moreover the oxidized cores are capable of $\text{Rh}^{\text{II}}-\text{X}$ bond photoactivations with the expulsion of halogen radicals by excitation into a Rh–Rh $d_z^2-d_z^2$ $d\sigma^*$ combination. Population of this excited state formally nullifies the metal–metal bond and is simultaneously σ^* with respect to the axial

halogen ligands. Excitation into this absorption manifold leads to $\text{Rh}-\text{X}$ bond homolysis and eventually the generation of the reduced complexes in discrete two-electron steps. The related ligand tfepma can also achieve this $\text{Rh}-\text{X}$ bond photoactivation chemistry (tfepma = $\text{CH}_3\text{N}[\text{P}(\text{OCH}_2\text{CF}_3)_2]_2$).²⁴⁸ When a photolabile ligand such as CO is coordinated to the Rh^0 center, proton reduction is observed upon excitation. The ambidextrous ability of these compounds to not only reduce protons but also photochemically regenerate reduced metal centers suggested that a photocatalytic H_2 production cycle can be closed. In keeping with this, solutions of the reduced complex, $\text{Rh}_2^{0,0}(\text{dfpma})_3(\text{PPh}_3)(\text{CO})$, in THF were observed to photocatalytically reduce HCl to H_2 upon light excitation ($\lambda_{\text{exc}} > 338 \text{ nm}$).²⁴⁹ In this case, the Cl radicals generated in the photochemical $\text{M}-\text{X}$ bond activation were trapped by hydrogen atom abstraction from THF. At 20 °C in 0.1 M HCl in THF, the catalyst $\text{Rh}_2^{0,0}(\text{dfpma})_3(\text{PPh}_3)(\text{CO})$ was able to achieve ~ 80 turnovers of H_2 with ($\lambda_{\text{exc}} > 338 \text{ nm}$). Monitoring the solution during the course of the photocatalysis by UV–vis spectroscopy showed a new band at 580 nm that quickly converted into the isolable two-electron mixed-valence $\text{Rh}_2^{0,\text{II}}(\text{dfpma})_3\text{X}_2\text{L}$ complex.

The pathway for the observed photocatalysis was probed by modifying the phosphorus ligands bridging the bimetallic core in order to directly identify the pertinent intermediates involved in the H_2 photocatalysis. Hydride or hydrido halide intermediates were not observed for Rh dimers ligated with the dfpma ligand used in the authentic photocatalytic system but could be isolated when using the more sterically demanding and less electron-withdrawing ligand tfepma.²⁵⁰ In this case, addition of H_2 to the coordinatively unsaturated species $\text{Rh}_2^{0,\text{II}}(\text{tfepma})_3\text{Cl}_2$ gave three isomeric hydrido halide products, from which the *syn*- $\text{Rh}_2^{\text{II},\text{II}}(\text{tfepma})_3(\text{H})_2(\text{Cl})_2$ could be separated. Photolysis of this isomer in THF gave prompt expulsion of 1 equiv of H_2 and regenerated the starting $\text{Rh}_2^{0,\text{II}}(\text{tfepma})_3\text{Cl}_2$ complex. Additional photolysis reactions in THF-*d*₈ and with 1:1 mixtures of *syn*- $\text{Rh}_2^{\text{II},\text{II}}(\text{tfepma})_3(\text{H})_2(\text{Cl})_2$ and *syn*- $\text{Rh}_2^{\text{II},\text{II}}(\text{tfepma})_3(\text{D})_2(\text{Cl})_2$ gave H_2 and H_2 and D_2 , respectively, indicating that H_2 elimination proceeds by an intramolecular mechanism. Exposure of *syn*- $\text{Rh}_2^{\text{II},\text{II}}(\text{tfepma})_3(\text{H})_2(\text{Cl})_2$ to excess HCl gave no reaction suggesting that H_2 production does not proceed by the protonation of a hydride. Monitoring the photolysis reaction by UV–vis showed the growth of a short-lived intermediate with a blue absorption feature centered at 600 nm, analogous to that observed in the dfpma photocatalysis, and suggested that the blue intermediate results from a reductive elimination of H_2 from the bimetallic core. Replacement of the bridgehead amine of the diphosphazane ligand backbone with a methylene unit gave the ligand tfepm (tfepm = $\text{H}_2\text{C}[\text{P}(\text{OCH}_2\text{CF}_3)_2]_2$ (bis[bis(trifluoroethoxyphosphino)]methane)) and allowed for the stabilization of valence-symmetric products by eliminating the asymmetric π -donation that engenders two-electron mixed valency. Rh complexes ligated by tfepm exhibit a face-to-face $d^8 \cdots d^8$ geometry and display a pronounced low-energy absorption feature consistent with a $d\sigma^* \rightarrow p\sigma$ electronic transition analogous to PtPOP and $\text{Rh}_2^{\text{II},\text{II}}(\text{bridge})_4^{2+}$. The stabilization of such species allowed for the assignment of the blue intermediate observed in the H_2 photocatalysis as a valence-symmetric $\text{Rh}_2^{\text{II},\text{II}}$ dimer that results from the intramolecular elimination of H_2 from two Rh hydrides. Although the tfepm complexes exhibit a valence-symmetric ground state, upon addition of $^t\text{BuNC}$ the $\text{Rh}_2^{\text{II},\text{II}}(\text{tfepm})_3\text{Cl}_2$ valence disproportionation proceeds quan-

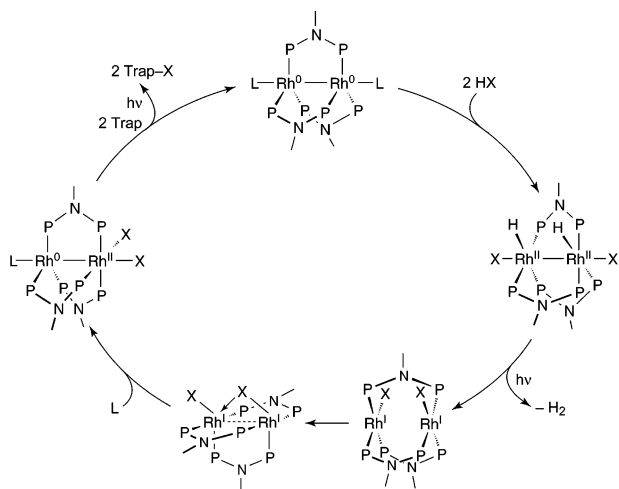


Figure 12. Proposed photocycle for H₂ production from HCl solutions in THF as determined from the thermal and photochemical chemistry of model complexes.

tatively to give a two-electron mixed-valent complex, Rh₂^{0,II}(tfepm)₃Cl₂(CN^tBu).

Taken together the reaction chemistry of the tfepma and tfepm complexes allows for the proposal of a photocycle for H₂ production from homogeneous acidic solutions, Figure 12. In brief, from a reduced Rh₂^{0,0} complex an equivalent of HX can oxidatively add at each metal center to generate a hydrido halide complex analogous to the isolated *syn*-Rh₂^{II,II}-(tfepma)₃(H)₂(Cl)₂. Hydrogen elimination is achieved from this species by a photoinduced process giving the blue intermediate with a valence-symmetric Rh₂^{I,I} core. Subsequent coordination of a two-electron ligand gives the two-electron mixed-valent Rh₂^{0,II} core by analogy with the Rh tfepm complexes. Once formed, the mixed-valent Rh₂^{0,II} core undergoes photoinduced Rh–X bond activation with the assistance of a halogen radical trap to regenerate the reduced Rh₂^{0,0} core, closing the catalytic cycle. The overall reaction converts HX to 1/2 H₂ and X[•]; however the requirement of a halogen radical trapping reagent (in most cases THF) precludes solar energy storage that would accompany the splitting of HCl into its constituent elemental forms and introduces ambiguity into the nature of the organic products.

Although considerable mechanistic insight has been gleaned from the model studies, many details require further clarification before a complete picture can be presented. Of these unknowns, perhaps the greatest is the nature of the photo-initiated Rh^{II}–X bond activation that regenerates the reduced Rh₂^{0,0} cores from the Rh₂^{0,II}X₂. In the cycle presented in Figure 12, this reduction is presumed to occur by the initial formation of Rh₂^{0,II} followed by a net two-electron reduction accompanied by two Rh^{II}–X bond activations to give a d⁹–d⁹ Rh₂^{0,0} core. Elucidation of short-lived intermediates by transient absorption spectroscopy has been hampered by low quantum yields for the primary photoproducts. Efforts to enhance these quantum yields have centered around the incorporation of electronegative metals into a heterobimetallic construct. In this way, the redox and photochemistry of Rh^I...Au^I and Pt^{II}...Au^I heterobimetallics have been explored, wherein two-electron oxidation of [Rh^IAu^I(tfepma)₂(CN^tBu)₂]²⁺ and [Pt^{II}Au^I(dppm)₂PhCl]⁺ gives the singly bonded d⁹–d⁷ Rh^{II}–Au^{II} and Pt^{III}–Au^{II} complexes, [Rh^{II}Au^{II}-(tfepma)₂(CN^tBu)₂Cl₂]²⁺ and [Pt^{III}Au^{II}(dppm)₂PhCl]⁺. Whereas the bimetallic Rh^{II}–Au^{II} core is thermally unstable

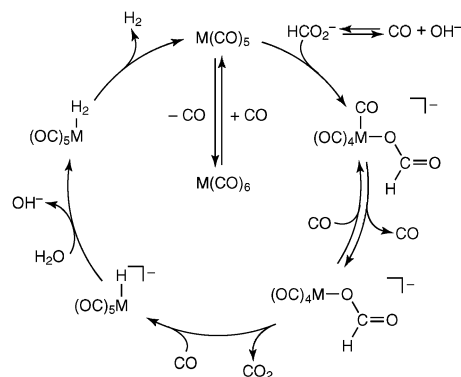
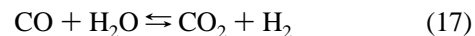


Figure 13. Proposed mechanism for the thermal water–gas shift reaction catalyzed by homoleptic group 6 carbonyls.

and disproportionates to form Rh^{III} and Au₂^{I,I} products,²⁵¹ the Pt^{III}–Au^{II} core is robust. Steady-state photolysis of [Pt^{III}Au^{II}(dppm)₂PhCl₃]⁺ in the presence of 1,3-dimethyl-2,3-butadiene as a radical trap evidences a linear increase in quantum yield with trap concentration, with a maximum of 5.7% with visible light excitation ($\lambda_{\text{ex}} = 405 \text{ nm}$), representative of a nearly 10-fold increase over Rh₂ homobimetallic complexes.²⁵² The high quantum yields and well-defined photoreactivity of the Pt^{III}–Au^{II} core should provide an excellent platform from which to examine M–X bond photoactivation by transient absorption in penetrating detail.

4. Photochemical Water–Gas Shift

The water–gas shift reaction (WGS),



is widely employed in industry to enrich the hydrogen content in water gas (synthesis gas) after the steam reforming of methane. The WGS reaction is typically performed at high temperatures over heterogeneous iron oxide or copper oxide catalysts. Interest in the WGS shift reaction under mild, homogeneous conditions has been long-standing.^{253,254} Many soluble transition metal carbonyl complexes show activity for thermal WGS catalysis,²⁵⁵ usually in basic media and rarely in acidic media.²⁵⁶ In some cases, WGS activity is promoted photocatalytically, where the photons are typically used to open coordination sites by the expulsion of CO or photoextrusion of H₂ from the transition metal center.

4.1. Homoleptic Metal Carbonyl Catalysts

King and Ford employed M(CO)₆ complexes (M = Cr, Mo, W) for homogeneous WGS catalysis initially under thermal conditions^{257,258} according to the cycle shown in Figure 13. Thermal expulsion of a CO ligand from M(CO)₆ generates an open coordination site at the metal center, which is rapidly coordinated by a formate ion that is produced in situ by the reaction of OH[−] and CO. Dissociation of an additional CO opens a coordination site for β -hydride elimination from the formate²⁵⁹ accompanied by CO₂ elimination. Uptake of an equivalent of CO generates the M(CO)₅H[−] complex, which is proposed to abstract a proton from H₂O to regenerate OH[−] and the M(CO)₅(H₂) dihydrogen complex. Thermal dissociation of H₂ regenerates the active M(CO)₅ species for catalytic turnover.^{260,261} This catalytic cycle involving homogeneous reagents operates at significantly reduced temperatures (100–170 °C) as com-

pared with the heterogeneous systems using iron or copper oxide catalysts (200 and 300+ °C). The highest turnover frequencies were observed for $W(CO)_6$, with 900 molecules of H_2 produced per day.

The initiation step of the WGS cycle in Figure 13 is the thermal dissociation of CO from $M(CO)_6$ to generate the active $M(CO)_5$ for reaction with formate ion ($M = Cr, Mo, W$). In principle, the active WGS catalyst may be accessed by the photochemical elimination of CO at even milder temperatures. Indeed, the benefit of the photon for WGS was recognized shortly after reports of $M(CO)_6$ catalyzed WGS appeared. Using $W(CO)_6$, King reported sluggish thermal WGS chemistry at 75 °C with a turnover frequency for H_2 of $\sim 5 \text{ day}^{-1}$; exposure to sunlight enhanced this turnover frequency to 83 day^{-1} .²⁶² The mechanism was proposed to largely follow that outlined in Figure 13 with the notable distinction of the introduction of the photon to remove CO from the hexacarbonyl starting complex. King reports that irradiated solutions retain catalytic activity for hours after the cessation of illumination. This observation is entirely consistent with the mechanism of Figure 13 since the photon is needed only once to extrude CO.

Detailed kinetic analysis of the photochemical WGS reaction using H_2O /methanol solvent mixtures under pseudo-first-order conditions with respect to substrate allowed for an analysis of the post-formate binding steps.^{263,264} Dissociation of an additional CO and replacement by solvent gives active intermediates of the general formula $M(CO)_{4-x}(S)_xCOOH^-$ ($S = H_2O$ or methanol). Additionally, in the absence of a rate-determining CO dissociation from $M(CO)_6$ to activate the catalyst, a second rate-determining step was reported to result from decarboxylation of $M(CO)_{4-x}(S)_xCOOH^-$ to give $M(CO)_{4-x}(S)_xH^-$ and CO_2 . This was determined on the basis of the observed normal kinetic isotope effect of 3.4 ± 0.9 for Cr and 4.4 ± 0.2 for W upon deuterium substitution. An enhanced rate of this secondary reaction with photolysis was attributed to photoinduced dissociation of another CO ligand to open a coordination site for the β -hydride elimination. Hydrogen production was postulated to proceed by subsequent protonation of the $M(CO)_{4-x}(S)_xH^-$ by H_2O in a thermal step.²⁶⁵

Iron pentacarbonyl can also support WGS upon the in situ treatment of the complex with three equivalents of NaOH to furnish $Fe(CO)_4H^-$.²⁶⁶ Photolysis of 9:1 THF/ H_2O solutions of $Fe(CO)_4H^-$ furnishes a 1:1 ratio of H_2/CO_2 at ~ 6 turnovers after ~ 60 h of irradiation. Interestingly, the H_2 production step was not proposed to stem from deprotonation of water by the hydride, as is the case for $M(CO)_5H^-$ ($M = Cr, Mo, \text{ or } W$), but rather from reaction of $Fe(CO)_4H^-$ with photochemically generated $Fe(CO)_3H^-$ via the dinuclear elimination mechanism.²⁶⁷ In this mechanism, H_2 evolution proceeds from a bridging hydride intermediate formed by the association of $Fe(CO)_4H^-$ and $Fe(CO)_3H^-$.

4.2. Ruthenium and Iridium Catalysts

The $M(CO)_6$ precatalysts ($M = Cr, Mo, \text{ or } W$) perform WGS by acting on HCO_2^- that results from the reaction of free CO with hydroxide in solution as opposed to a direct reaction with coordinated CO. In the case of *cis*- $Ru^{II}(bpy)_2Cl_2$ ($bpy = 2,2'$ -bipyridine), CO is proposed to trap the metal center upon dissociation of Cl^- and a metalcarboxylic acid is formed by attack of OH^- on the coordinated CO. The WGS with these systems operates at 100–140 °C in water under 1–3 atm of CO and under white light irradiation.²⁶⁸

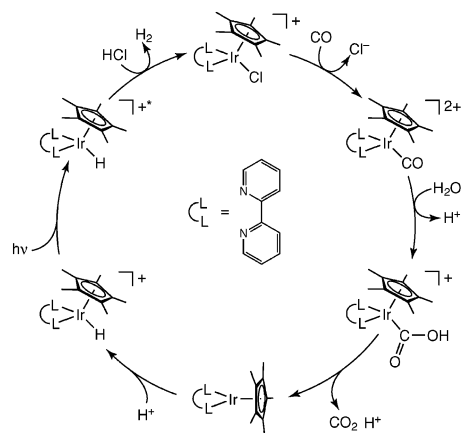


Figure 14. Proposed mechanism for photocatalytic water gas shift chemistry using an $Ir^{III}(\eta^5-C_5Me_5)(bpy)Cl^+$ complex.

Decarboxylation of the metalcarboxylic acid complex generates $Ru^{II}(bpy)_2HCl$ followed by its protonation to yield $Ru^{II}(bpy)_2(H_2)Cl^+$. Hydrogen elimination is rate-determining and proposed to be photoinduced. The product of this photoreaction is $Ru^{II}(bpy)_2Cl^+$, which is available to re-enter the catalytic cycle. Turnover frequencies as high as 20 h^{-1} were reported, and the catalysis was observed to proceed at relatively low pressures of CO and in moderately acidic solutions. These experimental conditions disfavor production of formate from free CO. As expected for reactivity derived from both H^+ and OH^- induced transformations, a complicated dependence of the H_2 production rate on pH was observed, with significant rate enhancement observed at both slightly basic (pH 8.9) and slightly acidic (pH 6.88) conditions. The role of photons in the catalysis is unclear, however, because subsequent reports indicated that the catalysis proceeds at nearly the same efficiency without irradiation.^{269,270}

Ziessel reported that $Ir^{III}(\eta^5-C_5Me_5)(bpy)Cl^+$ catalyzes WGS at room temperature, 1 atm CO, and neutral pH with a high quantum yield using visible light irradiation.^{271–273} The $bpy = 4,4'$ -COOH-2,2'-bipyridine catalyst was especially active, proceeding with a 12.7% photoreaction quantum yield (37 turnovers after 2 h) at 410 nm. The proposed photoinduced mechanism for WGS catalysis is outlined in Figure 14. The chloride ligand of the starting complex is liberated by CO coordination to give a dicationic $Ir^{III}(\eta^5-C_5Me_5)(bpy)CO^{2+}$ species. Attack of CO by water generates the $Ir^{III}(\eta^5-C_5Me_5)(bpy)(COOH)^+$ cation, which is proposed to undergo a rate-determining decarboxylation accompanied by proton loss. The overall transformation, $Ir^{III}(\eta^5-C_5Me_5)(bpy)(COOH)^+ \rightarrow Ir^{III}(\eta^5-C_5Me_5)(bpy)H^+$, amounts to a two-electron reduction of the Ir center. Subsequent protonation to generate the hydride, $Ir^{III}(\eta^5-C_5Me_5)(bpy)H^+$, offers the intermediate needed for H_2 production. The electronic excited state of the hydride, $[Ir^{III}(\eta^5-C_5Me_5)(bpy)H^+]^*$, is proposed to be protonated by HCl to give H_2 and return the starting complex, $Ir^{III}(\eta^5-C_5Me_5)(bpy)Cl^+$.

It is interesting to note that Ziessel chooses a stepwise path for the decarboxylation and protonation steps as opposed to the concerted β -hydride elimination as proposed in other WGS systems. This appears to be based on the fact that $Ir^I(\eta^5-C_5Me_5)(bpy)$ is an isolable compound and not a high-energy intermediate. Hydride protonation of the excited state is also unusual. This reactivity mode is supported by 1H NMR studies where the $Ir^{III}(\eta^5-C_5Me_5)(bpy)H^+$ hydride signal at -11.45 ppm is stable in the dark but rapidly

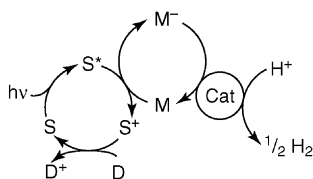


Figure 15. A generalized three component photocatalytic system for H_2 production where S = sensitizer, D = sacrificial electron donor, M = electron mediator or relay, and Cat = proton reduction catalyst.

vanishes upon exposure of the solution to visible light. This suggests that visible light irradiation of $\text{Ir}^{\text{III}}(\eta^5\text{-C}_5\text{Me}_5)(\text{bpy})\text{-H}^+$ complex pumps a transition that engenders significant hydridic character.

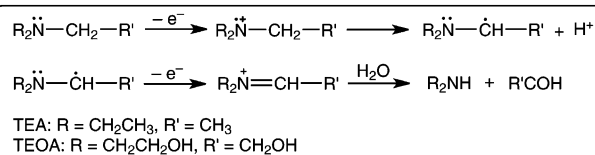
5. Three Component Systems

Oxidation–reduction reactions of electronically excited transition metal complexes customarily proceed by single-electron mechanisms. The molecule in its excited state is simultaneously a more potent oxidant and reductant than in its ground state. By itself, single-electron transfer is confining inasmuch as the reduction of protons to evolve molecular H_2 is a two-electron process. It follows that in order to employ a traditional one-electron excited state, the primary photoredox event must be coupled to H_2 reduction, remote to the excited state. Current strategies for proton reduction emphasize the development of systems that directly engage in a multielectron redox event such as that described in section 3.2.2. In the absence of such novel excited states, the one-electron excited state must be conveyed to a homogeneous or heterogeneous site capable of storing multiple redox equivalents. Such constructs are achieved with the so-called “three component system”.

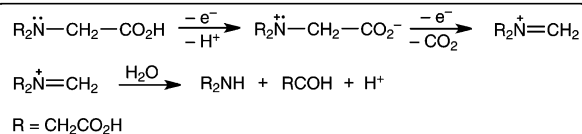
The most prevalent design of three component schemes is shown in Figure 15. The scheme comprises a one-electron photosensitizer, a redox mediator, and the redox-storing catalyst. The sensitizer, S, functions as both a light-harvesting complex for photon absorption and the primary photoreductant and may be a metal complex or an organic compound. Most metal-based sensitizers are metal polypyridyl complexes or metalloporphyrins. Organic photosensitizers are typically conjugated organic molecules with accessible π^* excited states. The mediator, M, is any molecule that can be reversibly reduced by one or two electrons. In most cases, the mediator serves as a bimolecular quencher of the photosensitizer by outer sphere electron transfer. Diffusion of the reduced mediator from the oxidized sensitizer aids in the prevention of energy-wasting back electron transfer. The catalyst is any species that carries out the reduction of protons to H_2 . These are typically chosen for low proton reduction overpotentials and most commonly are colloidal noble metals such as Pt, biological constructs such as hydrogenase, or small-molecule catalysts. The photooxidized sensitizer, S^+ , must be re-reduced to effect catalysis. The reducing equivalents for this process are typically derived from a sacrificial donor, D, such as triethylamine (TEA),²⁷⁴ triethanolamine (TEOA),²⁷⁵ ascorbic acid (H_2A), NADH, EDTA,²⁷⁶ or cysteine, which decompose upon oxidation. The decomposition pathways for some of the more common sacrificial electron donors are outlined in Figure 16.

Alternative three component systems are designed to reduce the system complexity by eliminating or combining the roles of one or more components, wherein chemistry

TEA|TEOA Oxidation



EDTA Oxidation



Thiol Oxidation

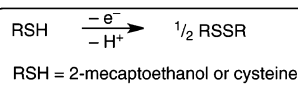


Figure 16. Decomposition pathways for TEA, TEOA, EDTA, and thiol-derived sacrificial electron donors.

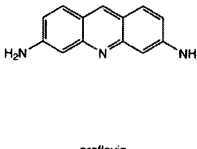
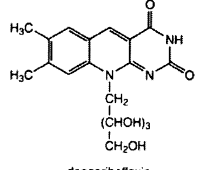
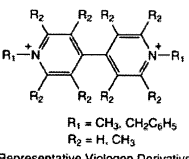
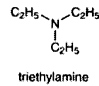
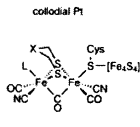
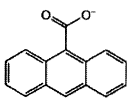
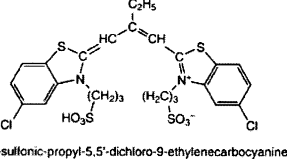
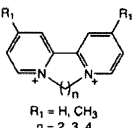
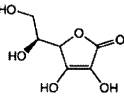
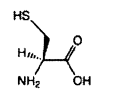
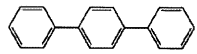
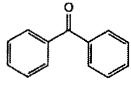

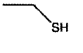
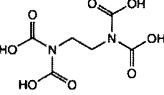
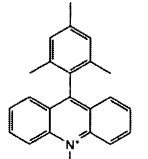
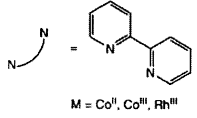
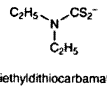
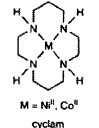
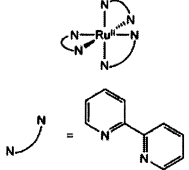
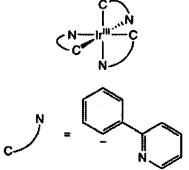
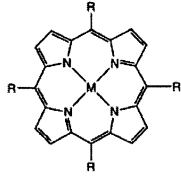
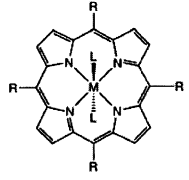
beyond simple proton reduction has been investigated including the simultaneous photocatalytic reduction of CO_2 to CO and H^+ to H_2 . These schemes employ photosensitizers for light harvesting and sacrificial electron donors for reducing equivalents but differ from the three component system of Figure 15 inasmuch as no redox mediator or colloidal catalyst is employed. Table 3 compiles the sensitizers, redox shuttles, and catalysts discussed below.

5.1. Inorganic Sensitizers

5.1.1. Metal Polypyridyl Photosensitizers

Classical three component systems commonly employ $\text{Ru}^{\text{II}}(\text{bpy})_3^{2+}$ as a light-harvesting complex. $\text{Ru}^{\text{II}}(\text{bpy})_3^{2+}$ and derivatives thereof have a long and rich history in inorganic chemistry and photochemistry. The parent compound, first prepared in 1936,²⁷⁷ was later obtained by a more practical synthesis,²⁷⁸ thus opening the way for Adamson's first use of the $\text{Ru}^{\text{II}}(\text{bpy})_3^{2+*}$ excited state as a photochemical reductant in 1972.²⁷⁹ The potential of this excited state for water splitting was quickly noted by other authors,^{280,281} and the numerous attempts to realize this reactivity directly grew into the field of three component catalysis. The first reports using $\text{Ru}^{\text{II}}(\text{bpy})_3^{2+}$ for “water splitting” focused on the hydrogen half-reaction, using a modified photosensitizer that can be cast into films.^{282–285} Though the H_2 -generating properties of the systems were ill-defined, this work was the predecessor of three component systems composed of a $\text{Ru}^{\text{II}}(\text{bpy})_3^{2+}$ sensitizer, colloidal Pt as a H_2 production catalyst, and methylviologen (MV^{2+}) as a mediator.²⁸⁶ The primary photoprocess occurs by fast oxidative quenching of the $\text{Ru}^{\text{II}}(\text{bpy})_3^{2+*}$ excited state by electron transfer to MV^{2+} to generate $\text{Ru}^{\text{III}}(\text{bpy})_3^{3+}$ and the cation radical $\text{MV}^{\bullet+}$. Hydrogen production is catalyzed at the surface of colloidal Pt, which efficiently couples the one-electron $\text{MV}^{\bullet+}$ oxidation to two-electron proton reduction.^{274,275,286–288} The photoreactant is returned to its resting state by reduction of $\text{Ru}^{\text{III}}(\text{bpy})_3^{3+}$ with a sacrificial donor. Although MV^{2+} serves as a paradigm, other alkylated bipyridine derivatives have been employed as redox shuttles including tetramethyl- or hexamethylviologen and diquats of various substitution patterns (Table 3). Functionally these derivatives are largely the same, and in all cases, the efficiency of the MV^{2+} - or diquat-based systems are gradually attenuated by the irreversible hydro-

Table 3. Representative Constituents of Three Component Photocatalytic Hydrogen Production Systems

Photosensitizer		Redox Shuttle	Sacrificial Donor	Catalyst
 proflavin	 deazariboflavin	 Representative Viologen Derivatives $R_1 = \text{CH}_3, \text{CH}_2\text{C}_6\text{H}_5$ $R_2 = \text{H}, \text{CH}_3$	 triethylamine	 colloidal Pt
 9-anthracenecarboxylate	 3,3'-sulfonic-propyl-5,5'-dichloro-9-ethylenecarboxyanine	 Representative Diquat Derivatives $R_1 = \text{H}, \text{CH}_3$ $n = 2, 3, 4$	 ascorbic acid	 cysteine
 <i>p</i> -terphenyl	 benzophenone	 NADH	 2-mercaptoethanol	 EDTA
 9-mesityl-10-methylacridinium		 $M = \text{Co}^{\text{II}}, \text{Co}^{\text{III}}, \text{Rh}^{\text{III}}$	 diethyldithiocarbamate	 cyclam
 $\text{Ru}^{\text{II}}(\text{bpy})_3^{2+}$	 $\text{Ir}^{\text{III}}(\text{ppy})_3$			
 $M = \text{Zn}, \text{Sn} \text{ R} = \textit{p}\text{-tolyl}$ $\text{R} = \text{C}_6\text{H}_4\text{N}^+\text{CH}_3$ $\text{R} = \text{C}_6\text{H}_4\text{SO}_3^-$	 $M = \text{Sn} \text{ R} = \text{N}^+(\text{C}_2\text{H}_5)(\text{CH}_3)_2 \text{ L} = \text{OH}^-$ $M = \text{Ru} \text{ R} = \text{N}^+(\text{C}_2\text{H}_5)(\text{CH}_3)_2 \text{ L} = \text{pyridine}$			
$M = \text{Zn}, \text{Sn} \text{ R} = \text{C}_6\text{H}_5$				

generation of the redox shuttle catalyzed by the Pt surface.^{289,290} The protonated cation radical is proposed to be an active intermediate for the direct production of H_2 at low pH. At higher pH, H_2 production is believed to be dominated by electron transfer from reduced $\text{MV}^{+\cdot}$ to the Pt surface.^{276,291,292} The efficiency of the system is observed to increase with more reducing viologen or diquat derivatives and is typically attributed to the increased driving force for electron transfer from the cation radicals of more reducing shuttles to the Pt surface.^{293–295}

Sauvage and co-workers^{296,297} modified the three component approach by using a Rh polypyridyl complex as the redox mediator. The advantage of this approach is that the mediator is both a proton carrier and a two-electron shuttle. Initial mechanistic proposals invoked a dihydride of the formula $\text{Rh}^{\text{III}}(\text{bpy})_2(\text{H})_2^+$ as the critical shuttle.^{296,297} This

proposal was subsequently modified by Cruetz and Sutin^{298,299} using a $\text{Ru}^{\text{II}}(\text{bpy})_3^{2+}/\text{Rh}^{\text{III}}(\text{bpy})_3^{3+}/\text{TEOA}$ system at neutral pH (7–8) in the absence of Pt. The one-electron reduction product $\text{Rh}^{\text{II}}(\text{bpy})_3^{2+}$ was found to be unstable with respect to disproportionation driven by the loss of bpy to yield $\text{Rh}^{\text{III}}(\text{bpy})_3^{3+}$ and $\text{Rh}^{\text{I}}(\text{bpy})_2^+$, which reacts with a proton to yield the hydride $\text{Rh}^{\text{III}}(\text{bpy})_2(\text{H}_2\text{O})\text{H}^+$ at low pH. $\text{Rh}^{\text{II}}(\text{bpy})_3^{2+}$ may serve as a one-electron reductant to generate $\text{Rh}^{\text{II}}(\text{bpy})_2(\text{H}_2\text{O})\text{H}^+$, which was thought to produce H_2 either by protonation of the hydride or by the bimolecular reaction of two hydride species. The same mechanism is believed to be operative if $\text{Rh}^{\text{III}}(\text{bpy})_3^{3+}$ is replaced by $\text{Co}^{\text{III}}(\text{bpy})_3^{3+}$.^{300–304} The foregoing mechanism does not require Pt as a catalyst for H_2 generation. Indeed, the systems are operative in the absence of the noble metal. If present, the Rh bpy complex functions simply as a redox reservoir, similar to MV^{2+} ,

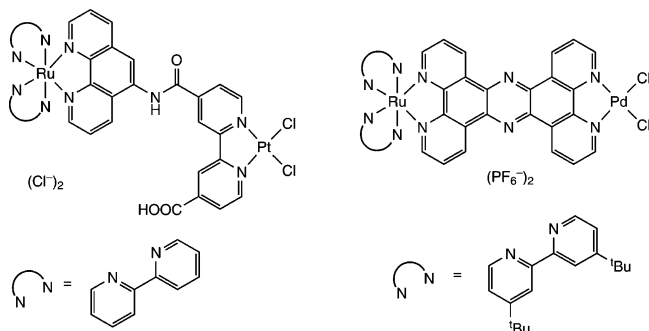


Figure 17. Heterobimetallic constructs of Sakai (left) and Rau (right) for photocatalytic H₂ production.

because the electron transfer from Rh^{II}(bpy)₃²⁺ to the Pt surface is faster than disproportionation and bpy loss that gives Rh^I(bpy)₂⁺.²⁹⁹

Iridium coordination complexes have also been employed as sensitizers for H₂ production in three component systems.^{305,306} Anionic donors derived from 2-phenylpyridine (ppy) replace the ubiquitous bpy ligands of Ru-based photosensitizers. The electronic properties of the Ir excited state may be modulated by the functionalization of ppy, as has routinely been performed for the development of OLED devices.³⁰⁷ With use of high-throughput techniques to screen a library of ppy-modified complexes, it was found that the heteroleptic [Ir^{III}(dF[DF₃]ppy)₂(dtbbpy)]PF₆ (where dF[DF₃]ppy = 2-(2,4-difluoromethyl)-5-trifluoromethyl-pyridine and dtbbpy = 4,4'-di-*tert*-butyl-2,2'-bipyridine) was the most active photocatalyst (Co^{II}(bpy)₃Cl₂ = electron relay and TEOA = sacrificial electron donor), achieving 430 equiv of H₂ with quantum yields ~37 times greater than that of Ru^{II}(bpy)₃²⁺-sensitized systems. The authors suggest that the enhanced efficiencies are a result of the long lifetime and increased reducing strength of the Ir^{III} excited state.

The MLCT excited states of group 10 coordination complexes can also be exploited for charge transfer leading to their use as photosensitizers. Photocatalytic hydrogen generation has been observed recently using terpyridine arylacetelide complexes of Pt^{II}, similar to those of section 2.4, in a three component system composed a Pt(terpyridine)-(arylacetalide) photosensitizer, TEOA as a sacrificial reductant, MV²⁺ as a redox shuttle, and colloidal Pt as the catalyst.³⁰⁸ The most successful system for hydrogen production uses a Pt(4'-*p*-tolylterpyridine)(C≡CC₆H₅)⁺ photosensitizer, 4,4'-dimethyl-1,1'-trimethylene-2,2'-bipyridinium as a redox shuttle, TEOA as a sacrificial electron donor, and a Pt colloid as a hydrogen evolution catalyst achieving 800 turnovers for H₂ after 20 h of photolysis with λ > 410 nm excitation light.³⁰⁹

Recent efforts have sought to eliminate the electron relay and colloidal Pt catalyst by appending Pt^{II}(bpy)Cl₂ to Ru^{II}(bpy)₂(phen) (phen = 1,10-phenanthroline), Figure 17 (left).^{310,311} This complex was active for photocatalytic H₂ production in the presence of EDTA, however at low turnover and quantum yield (~5 and 0.01). At about the same time, Rau and co-workers presented a similar construct linking a Ru^{II} polypyridyl complex to a Pd^{II} center via a tetrapyrrophenazine unit as a conjugated and reducible bridge, Figure 17 (right).³¹² Hydrogen production proceeded with TEA as a sacrificial electron donor giving 56 turnovers after ~30 h of irradiation. This assembly was also active for the hydrogenation of toluene to *cis*-stilbene without added hydrogen, leading the authors to suggest that H₂ production

proceeds through a palladium hydride species. Another strategy to eliminate bimolecular electron relays such as MV²⁺ is to adsorb the photosensitizer and proton reduction catalyst directly to the surface of a semiconductor particle.³¹³ In this way, a Pt^{II}(4,4'-dicarboxyl-2,2'-bipyridine)(SS) complex (SS = *cis*-1,2-dicarbomethoxyethylene-1,2-dithiolate or 1,2-benzenedithiolate) chromophore adsorbed on a TiO₂ nanoparticle catalyzes the generation of hydrogen using TEOA as a sacrificial donor. In this case, MV²⁺ is not required because the Pt^{II} excited state injects an electron into the conduction band of the TiO₂ nanoparticle. The conduction band electrons initially reduce K₂Pt^{IV}Cl₆ in solution to form a Pt colloid on the nanoparticle surface that subsequently serves as a catalyst for proton reduction.

5.1.2. Porphyrin Sensitizers

Porphyrins are widely employed for their light-harvesting properties. Natural photosynthetic systems contain rings of porphyrin macrocycles to collect the light and funnel that energy to the reaction centers from which the photochemical energy conversion pathway originates.³¹⁴ The attractive light-harvesting properties have not been overlooked for schemes aimed at driving photocatalytic H₂ production³¹⁵ and a large body of work has centered about porphyrin photosensitizers.

5.1.2.1. Zinc Porphyrins. Zinc porphyrins (PZn) may be used in place of Ru polypyridyl complexes as light harvesters in a three component system. In a parallel function to Ru^{II}(bpy)₃²⁺, photon absorption initially forms a PZn singlet excited state that relaxes to the long-lived triplet from which electron transfer to MV²⁺ occurs. As is generally the case for a three component system, a sacrificial electron donor reduces the oxidized porphyrin macrocycle and MV^{•+} oxidation is attendant to H₂ generation at a Pt surface. McClendon et al. were the first to report such a strategy using both Zn(II) tetra(*N*-methylpyridyl)porphyrin (Zn^{II}TMPP) and Zn(II) tetra(sulfonato-phenyl)porphyrin (Zn^{II}TPPS₄) with EDTA and a Pt catalyst in aqueous solutions.³¹⁶ Using Zn^{II}-TMPP, a maximum rate of 175 equiv of H₂ per hour was attained. The H₂ was derived from the protons of water as evidenced by the production of >95% D₂ when the photolysis was conducted in D₂O. Similar results are obtained for other PZn photosensitizers.^{317–321}

Zn^{II}TMPP can also function as a photosensitizer when adsorbed onto the exterior of a zeolite.³²² Photocatalytic H₂ was produced from acidic aqueous solutions (pH = 4) when the zeolite channel was platinized and the sodium cations were replaced with MV²⁺. Interestingly, electron transfer from the Zn^{II}TMPP sensitizer originates from the singlet excited state as the normally facile intersystem crossing to the triplet is circumvented by an adsorption-induced 200 mV shift of the Zn^{II}TMPP redox potential.

5.1.2.2. Tin, Ruthenium, and Free-Base Porphyrins. Tetraphenylporphyrin (TPP) complexes of Sn^{II} photocatalytically generate H₂ in micellar and PVC films using 2-mecaptoethanol in the presence of colloidal Pt.^{323–325} The mechanism for H₂ generation is initiated from the [TPPSn^{II}]⁻ anion, which is formed by reductive quenching of the triplet excited state of TPPSn^{II} by mercaptoethanol. Subsequent electron transfer to the surface of Pt and proton reduction closes the cycle. Catalytic turnover in this system is low, with a maximum of 30 turnovers observed after 30 h of photolysis. A water-soluble tetra-*p*-(*N*-ethyl-*N,N*-dimethyl)-ammoniumporphyrin of Sn^{IV} (TEAPSn^{IV}(OH)₂) has also been reported to photocatalytically generate H₂. The H₂ reduction

cycle is distinguished by the sequential two-electron reduction of the porphyrin macrocycle followed by the uptake of two protons to generate first the chlorin congener, TEACSn^{IV}(OH)₂, and finally the bacteriochlorin, TEABSn^{IV}(OH)₂.³²⁶ Hydrogen photogeneration is believed to occur from the bacteriochlorin excited state via a two-electron two-proton process to give the chlorin and H₂ at the colloidal Pt surface. The chlorins and bacteriochlorins, though difficult to observe under photocatalytic conditions, are spectroscopically characterized upon photolysis of TEAPSn^{IV}(OH)₂ in the absence of electron shuttle and colloidal Pt. The identical porphyrin macrocycle metalated with Ru, TEAPRu^{II}(pyridine)₂, does not form the corresponding chlorins and bacteriochlorins, though H₂ photogeneration is observed. Instead a mechanism similar to that of PZn^{II} photosensitizers is proposed, involving oxidative quenching of the TEAPRu^{II}(pyridine)₂ excited state by a redox shuttle, which produces H₂ at the Pt surface.³²⁶ The photocycle is closed by re-reduction of the photooxidized porphyrin sensitizer by EDTA.

Platinized Langmuir–Blodgett (LB) films containing free-base porphyrins produce H₂ under continuous irradiation in aqueous solutions of EDTA.³²⁷ Hydrogen production is stable and lasts over extended reaction times (350 h). The long-term stability is postulated to stem from the inability of the colloidal Pt catalyst to coagulate owing to immobilization in the LB film. Increased efficiencies for H₂ production were observed upon covalently linking a MV²⁺ electron carrier to the porphyrin macrocycle.^{328–330}

5.2. Organic Sensitizers

Photosensitization is not a prerequisite of metal polypyridyls and porphyrins: organic excited states may function as sensitizers of H₂ production as well. Benzophenone has seen some use for photocatalytic H₂ production in a role that is similar to the metal complexes of section 2.3 for alcohol dehydrogenation cycles. UV excitation of the $n \rightarrow \pi^*$ transition of benzophenone generates the reactive diradical, which has long been known to rapidly abstract H atoms to form a stable ketyl radical.^{331,332} The reaction can be diverted toward photocatalytic H₂ production under certain conditions. For instance, irradiation of isopropanol solutions of benzophenone in the presence of colloidal Pt under anaerobic conditions favors photocatalytic H₂ production over the formation of pinacols.^{333,334} The mechanism is proposed to proceed by direct $n \rightarrow \pi^*$ excitation of benzophenone to generate a ketyl radical after H atom abstraction from isopropanol. A second H atom abstraction from the organic radical intermediate by another benzophenone excited state generates acetone. Colloidal Pt reoxidizes the ketyl radicals to regenerate benzophenone, and H₂ is evolved by the coupling of two hydrogen atoms at the heterogeneous surface. The isopropanol dehydrogenation is similar to those reported using late metal phosphine complexes of section 2.3.1, excepting the requirement of the heterogeneous noble metal catalyst. The benzophenone excited state is also capable of dehydrogenating cyclohexane to cyclohexene.³³⁵ However in this case the cyclohexane dehydrogenation is performed aerobically so H₂O is obtained as the terminal reduction product as opposed to H₂.

Hydrogen generation may be promoted by a host of other organic photosensitizers. 9-Anthracenecarboxylate, in the presence of MV²⁺ and Pt, produces H₂ according to the scheme shown in Figure 15. The triplet form of 9-anthracenecarboxylate can either be formed by direct excitation³³⁶ or

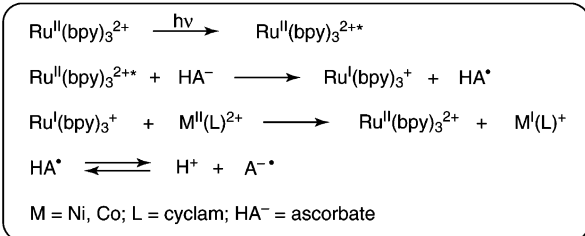
by energy transfer from photoexcited Ru^{II}(bpy)₃^{2+*} or Cu^I(dpp)₂^{+*} (dpp = 2,9-diphenylphenanthroline).^{337,338} Krasna first reported the use of proflavin to photocatalytically generate H₂ from a variety of sacrificial electron donors, using MV²⁺ and either platinum or isolated hydrogenase (*vide infra*) as a catalyst.³³⁹ The triplet excited state of proflavin is reduced by EDTA (for example), and in turn, the reduced proflavin reduces MV²⁺ followed by electron transfer from MV⁺ to the colloidal Pt or hydrogenase that effects H₂ production.³⁴⁰ The efficiencies for MV²⁺ reduction using proflavin sensitizers were approximately twice as high as those using Ru^{II}(bpy)₃²⁺. The maximum quantum yields for MV⁺ generation were observed at pH 6–8. Although the reductive quenching reaction is more efficient at higher pH, the H₂ production reactions were slow, presumably due to the low concentrations of protons. The rate of MV²⁺ reduction may be accelerated if the proflavin sensitizer is substituted with deazariboflavin; a fivefold increase in the rate of MV⁺ formation was observed in some cases.³⁴¹ In these systems, the scope of the sacrificial reagent was expanded to include amino acids and also simple sugars such as glucose and fructose. In an interesting application, flavin-sensitized H₂ production has been elaborated in a photogalvanic cell. Excitation of the flavin followed by one-electron reduction by EDTA furnishes the reduced flavin, which is rapidly oxidized at a Pt disk anode. The circuit may be completed by proton reduction at the cathode in a separate compartment linked via a salt bridge.³⁴²

Recently 9-mesityl-10-methylacridium (Acr⁺–Mes) has been employed as an organic photosensitizer in a three component system.³⁴³ In this case, the MV²⁺-based electron acceptor is directly attached to a Pt nanocluster via a thiol-terminated alkyl chain, and NADH is used as a sacrificial electron donor. The mechanism proceeds by reductive quenching of the initially formed Acr⁺–Mes excited state by NADH to give Acr[•]–Mes, which then reduces the MV²⁺-modified Pt cluster where H₂ evolution occurs. The authors report an order of magnitude improvement in H₂ evolution efficiency over traditional systems using unbound MV²⁺. The system was later modified by eliminating the MV²⁺ electron shuttle and using alcohol dehydrogenase to regenerate the NADH used as a sacrificial donor by the enzymatic decomposition of ethanol.³⁴⁴

5.3. CO₂ Reduction Systems

Sacrificial electron donors may be employed to simultaneously reduce protons to H₂ and CO₂ to CO. Photocatalytic H₂ production linked to carbon dioxide reduction has been observed using Co(II) and Ni(II) complexes of macrocyclic tetradentate nitrogen donors ligands for which cyclam (L) is the prototype.^{345–348} The [LM^{II}]²⁺ (M = Co, Ni) complex serves as both the redox shuttle and catalyst in the presence of a Ru^{II}(bpy)₃²⁺ photosensitizer and an ascorbate sacrificial electron donor. Figure 18 shows the reaction sequence that leads to H₂ and CO production. The reaction cascade is initiated by reductive quenching of the Ru^{II}(bpy)₃^{2+*} excited state by ascorbate to generate Ru^I(bpy)₃⁺, which goes on to reduce [LM^{II}]²⁺ to [LM^I]⁺. The reduced macrocyclic complex is proposed to either react with either CO₂ or H⁺ to generate [LM(CO₂)]⁺ or [LM^{III}H]²⁺. Hydrogen may then evolve from the hydride directly by net H atom transfer to regenerate [LM^{II}]²⁺, or [LM^{III}H]²⁺ can insert CO₂ to generate a metal formate complex (a metal carboxylic acid complex however cannot be ruled out because the precise nature of the CO₂

Initiation



Hydrogen Production

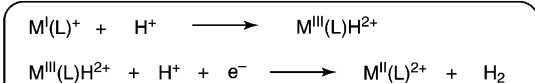
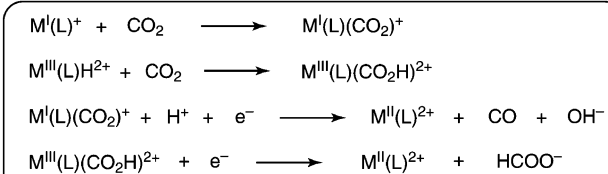
CO₂ Reduction

Figure 18. Reactions of nickel or cobalt cyclams (or cyclam derivatives) leading to the simultaneous photocatalytic reduction of protons to H₂ and CO₂ to CO.

insertion product is not known). The formate species can react either by H atom transfer to generate the [LM^{II}]²⁺ complex along with hydroxide and carbon monoxide or by a one-electron reduction to generate [LM^{II}]²⁺ and free formate ion. A critical feature of this catalytic scheme is that the [LM^I]⁺ intermediate is reactive toward both protons and CO₂. As a result of the catalyst's promiscuity, the CO and H₂ yields are not stoichiometrically defined as in the photochemical WGS chemistry of section 4. Additionally, the CO/H₂ ratios appear to be very sensitive to the experimental conditions because differing ratios are reported by different investigators, even when the same catalyst (e.g., Ni^{II}cyclam) is employed. For the case where the reducing equivalents are provided electrochemically rather than in homogeneous solution, H₂ production is completely shut down.^{349,350} Strategies for enhancing selectivity for H₂ over CO include the use of *p*-terphenyl as a sensitizer and TEA as a sacrificial electron donor, although the reasons for this enhancement in selectivity are not clear.^{351,352} Attempts to increase the efficiency of the process has led to the covalent tethering of the nickel macrocycle to the Ru polypyridyl sensitizer.^{353,354} Nonetheless, no significant gains in efficiency or selectivity were observed over bimolecular constructs.

In a somewhat remarkable reaction, the reduction of CO₂ to H₂ and CH₄ in aqueous solution is reported to be promoted by a Ru^{II}(bpy)₃²⁺ sensitizer, TEOA as a sacrificial electron donor, a series of alkylated bipyridines as electron relays, and Ru or Os colloids as catalysts.³⁵⁵ The observed quantum yields are low (ca 10⁻⁴–10⁻⁵), and the complex mechanism is not understood.

6. Photobiological Approaches

Photobiological approaches to H₂ production are almost exclusively based on the activity of photosynthetic organisms or the enzymatic activity of hydrogenase. While this review does not venture into the domain of biological or photobiological H₂ production per se,³⁵⁶ studies that utilize biological

constructs outside of the natural systems will be discussed here.

6.1. Hydrogenase

The active site of hydrogenase is composed of either a diiron or nickel–iron core that is capable of proton reduction to generate molecular H₂ at low overpotentials. Consensus structures^{212–214} for the primary coordination sphere of the iron only and Ni–Fe hydrogenase active sites are shown in Table 3. An unusual characteristic of these cofactors is that the metal centers are ligated with strong π-acceptor ligands such as CO and CN⁻, consistent with the low formal oxidation states of the cofactor. The mechanism for H₂ production occurs by transporting protons into the active site along pathways distinct from those traversed by the electron equivalents. Electrons are putatively injected into the active site via a chain of [FeS] clusters, while proton channels and acidic/basic residues at the active site manage the substrate inventory,^{215–217} though the details of the mechanism remain to be deciphered.

Outside of the biological milieu, the isolated hydrogenase enzyme may be incorporated into three component systems. In this context, the enzyme serves to replace colloidal Pt in the microheterogeneous systems of section 5. The Ni–Fe enzyme isolated from *Desulfovibrio vulgaris* (Miyazaki type) by the method of Yagi³⁵⁷ is a prevalent hydrogenase cofactor employed with a TPPZn^{II} photosensitizer, MV²⁺ as the electron relay and a variety of sacrificial electron donors including TEOA,^{358,359} NADH,³⁶⁰ 2-mercaptoethanol,^{321,361–364} Na₂S,³⁶⁵ and lysine.³⁶⁶ These systems share significant mechanistic commonalities with the PZn/MV²⁺/Pt systems of section 5.1.2.1. Activities for H₂ evolution for PZn/MV²⁺/Pt and PZn/MV²⁺/hydrogenase systems are generally in accord, excepting the system employing the Na₂S sacrificial reagent, which showed minimal hydrogen evolution for the colloidal Pt catalyst owing most likely to fouling of Pt by the sulfur-containing reaction products. A second pathway for suppressed H₂ generation activity for Pt-catalyzed systems was uncovered with a side by side comparison between water-soluble ZnTPPS₄, MV²⁺, and 2-mercaptoethanol systems. Whereas H₂ evolution from hydrogenase catalysis was linear with irradiation time, a marked reduction in the H₂ evolution rate was observed when using a Pt colloid. This was attributed to coagulation of the colloidal Pt and the Pt-assisted hydrogenation of MV²⁺ under the reaction conditions.^{321,367}

Hydrogenase has been employed in micellar systems of varying compositions in attempts to increase cage escape yields of the primary charge-transfer products as had been observed for the photoreaction of Ru^{II}(bpy)₃²⁺ and MV²⁺ in micelles.^{368,369} The observation of little to no H₂ production from mixtures of ZnTPPS₄, TEOA, MV²⁺, and hydrogenase in the presence of anionic surfactants such as sodium dodecyl sulfate (SDS) was attributed to denaturation of hydrogenase by the surfactant.^{370,371} Neutral surfactants appear to induce a 4-fold increase in the rate of MV²⁺ formation,³⁷² which translates directly into an increased rate of H₂ production from 0.17 × 10⁻⁷ mol h⁻¹ to 0.78 × 10⁻⁷ mol h⁻¹. In a system of analogous compositions, Okura and co-workers investigated the affect of the cationic surfactant cetyltrimethylammonium bromide (CTAB) on the rate of H₂ evolution.³⁷³ A 50-fold increase in the rate of H₂ was observed for “optimized” systems composed of 15 μM ZnTPPS, 0.1 mM MV²⁺, 0.5 M TEOA, and 25 mM CTAB over a

“conventional” solution (0.15 μM ZnTPPS, 0.22 mM MV^{2+} , 0.25 M TEOA). Langmuir–Blodgett films³⁷⁴ also show effects on H_2 production rates.

In parallel approaches to those of section 5.1 with Pt colloid catalyst, the MV^{2+} redox shuttle has been covalently linked to a variety of PZn photosensitizers.^{375–386} A distinct dependence of the alkyl chain length was observed on the formation of MV^{+} as compared with the free components at similar concentrations. In particular, methylene linkers of 4–5 carbons in length gave the most favorable yield of MV^{+} . When NADH was used as the sacrificial electron donor, a reductive quenching mechanism was proposed, where the triplet porphyrin excited state is initially reduced by NADH prior to charge transfer to the tethered MV^{2+} . Hydrogen was produced photocatalytically when hydrogenase was added to the solutions. Electron relays can potentially be eliminated if the photosensitizer is directly attached to the proton reduction catalyst. Some inroads into this chemistry have been made by tethering Ru-^{387–392} or porphyrin-based^{393,394} photosensitizers to diiron cores of synthetic hydrogenase mimics. These supramolecular constructs, however, fail to generate H_2 via photochemical mechanisms. The excited-state dynamics of the system engender reductive quenching of the MLCT excited state by the diiron core, instead of the desired photoreduction of the diiron core by the Ru excited state, precluding hydrogen production catalysis. Despite this limitation, some constructs serve as functional proton reduction catalysts under electrochemical conditions.³⁸⁸ Recently diethyldithiocarbamate has been employed as a sacrificial electron donor to reductively quench the Ru MLCT state and thereby engender electron transfer to proceed to the diiron core as necessary for proton reduction,³⁹² although the H_2 production activity has not been presented using this system as of yet.

Hydrogen production mediated by hydrogenase may also be effected from organic photosensitizers. The alcohol photodehydrogenation induced by benzophenone utilizes hydrogenase as a catalyst.³⁹⁵ Also, hydrogenase evolves H_2 at the terminus of a system comprising the carbocyanine derivative (3,3'-sulfonic-propyl-5,5'-dichloro-9-ethylene-carbocyanine) shown in Table 3, as an organic light-harvesting complex along with MV^{2+} as an electron relay and 2-mercaptoethanol as a sacrificial electron donor.³⁹⁶ Turnovers as high as 70 h^{-1} were reported though we note that analysis of the data provided seems to suggest turnovers frequencies for H_2 of 6 h^{-1} .

6.2. Isolated Chloroplasts

The complex biological machinery of photosystems I and II (PSI and PSII) work in concert within the thylakoid membranes of chloroplasts to carry out the four-electron oxidation of water to generate oxygen. The reducing equivalents are utilized to generate NADPH, which is subsequently used as a reductant to fix CO_2 for carbohydrate synthesis. A goal has been to divert the transmembrane potential of the protons directly into H_2 production by isolating PSI from chloroplasts. Some of the earliest reports of such systems used sodium ascorbate as a sacrificial electron donor, and Pt was precipitated on the reducing end of PSI.^{397,398} Spinach plastocyanin was used as an electron relay to shuttle reducing equivalents derived from sodium ascorbate to the oxidized PSI. The system retained activity when immobilized in a borosilicate glass.³⁹⁹ Cross-linking the spinach plastocyanin to the PSI gave a 3-fold increase

in the initial rate of H_2 evolution and also a 3-fold increase in the total yield of H_2 where peak H_2 evolution rates of $\sim 90 \text{ nmol h}^{-1}$ were achieved.⁴⁰⁰ Photocatalytic H_2 production has also been reported using hydrogenase in conjunction with PSI in both untethered⁴⁰¹ and tethered constructs.⁴⁰²

6.3. Other Photobiological Approaches

A complex of human serum albumin and Zn protoporphyrin IX has been reported to give 57 turnovers for H_2 under photolysis conditions in the presence of EDTA as a sacrificial electron donor, MV^{2+} as a relay, and colloidal platinum as a catalyst.⁴⁰³ The Zn protoporphyrin ligated to albumin sensitizer was $\sim 25\%$ more efficient than ZnTMPP as a traditional sensitizer under similar conditions, although the reasons for this are unclear.

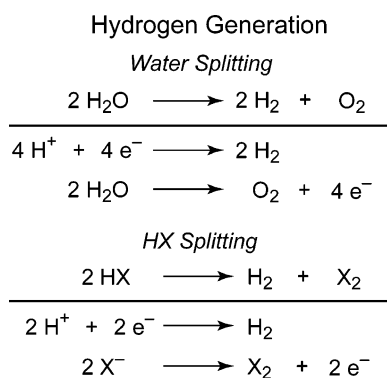
Efforts have been directed to replace irreversible sacrificial electron donors with reducing equivalents reversibly generated via biocatalysis. Amao and co-workers employed this strategy in systems composed of a PZn sensitizer, MV^{2+} electron carrier, NADH as an electron donor, and colloidal Pt as a catalyst.^{404,405} In this case, the NADH that typically is used as a sacrificial electron donor was regenerated in situ from sucrose. The transformation was achieved via an enzymatic pathway using invertase to convert sucrose to glucose followed by gluconic acid formation by glucose dehydrogenase coupled to NADH formation.

7. Concluding Remarks and Future Directions

The formation of H–H bonds is not expressly targeted in many of the H_2 photogeneration cycles presented in section 2. Rather H_2 is generated as a side product. Accordingly, the proton and electron equivalents for H_2 production are often derived from high-energy substrates such as alkanes and alcohols. In systems in which H_2 is the object of the photochemistry, like the three component systems of sections 5 and 6, H_2 generation is driven by a sacrificial donor. Because the photoevent leading to H_2 generation is not predicated on excited states capable of participating directly in the two-electron chemistry required for H_2 production, redox shuttles are needed that can couple the one-electron reactions of the photosensitizer to a H_2 -generating catalyst, usually Pt or hydrogenase. The challenge confronting this approach is that the relay catalyst, upon its one-electron reduction by the photosensitizer, often participates in an energy-wasting recombination reaction. This back reaction can be circumvented by appropriate photocatalyst design as demonstrated by the systems of section 3.

The limitations of photocatalytic H_2 -producing schemes sends a clear message. In order for significant progress to be made for the solar production of H_2 on a globally significant scale, new systems and design strategies must be pursued that allow H_2 to be photogenerated at low electrochemical overpotentials using photons that match the solar spectrum. But this is not enough. If the tie of H_2 generation to a carbon-based fuel supply is to be severed, then the oxidative half of the H_2 generating cycle must also be solved, preferably using sunlight to drive the reaction. In response to this challenge, two logical sources for H_2 emerge, H_2O and HX. If $\text{X} = \text{Cl}$, both HX and H_2O splitting store approximately the same amount of energy, which may be released by an appropriately designed fuel cell. Regardless of the source, significant fundamental challenges confront such H_2 generation schemes that become immediately

Scheme 2



apparent when parsed into their constituent redox half-reactions, Scheme 2. Not only is the reductive generation of H_2 from HX and H_2O splitting a multielectron event, but so is the oxidative half reaction. In this regard, HX is more attractive than H_2O splitting because it only requires the coupling of a two-electron oxidation to H_2 generation. The water oxidation half-reaction requires four electrons and necessarily involves the intimate coupling of electrons to proton transfer. Nonetheless, from an environmental and sustainability viewpoint, H_2O splitting, though more challenging, is the most desirable.

In driving any closed H_2 photogeneration cycle, new approaches should be considered that diverge from the typical photochemical strategy of the last 30 years, namely, the design of an excited state that efficiently performs both solar capture and catalysis. Not only are the issues of multielectron redox chemistry coupled to proton transport daunting catalyst design problems in their own right, but this chemistry must simultaneously be performed within an absorption manifold that matches the solar spectrum. Dyad and triad strategies seek to address this challenge by coupling a light-harvesting center to donors, acceptors, or both.⁴⁰⁶ In this way, solar capture and conversion might be more easily realized, since the additional requirement of catalysis is not an element of the design. Yet, only the separation of a single electron has been achieved with a dyad or triad to date, and in no case has the donor or acceptor been interfaced to a multielectron catalytic site. An alternative strategy is to borrow the design of nature in an artificial photosynthetic process. In natural photosynthesis, the anodic charge of the wireless current from the solar capture and conversion apparatus is used at the oxygen-evolving complex (OEC) to oxidize water to oxygen, with the concomitant release of four protons. The cathodic charge of the wireless current is captured by photosystem I to reduce the protons to “hydrogen”; the reduced hydrogen equivalents are stored through the conversion of NADP to NADPH. Outside the leaf, an artificial photosynthetic system may be realized by spatially separating independent solid-state or molecular reduction and oxidation catalysts connected via a photon capture and charge separation apparatus in an arrangement reminiscent of an electrochemical cell. In one such construct, the spatially separated electron–hole pairs provided by a photovoltaic cell are efficiently utilized by the tailored catalysts, and the energy is stored in the bond rearrangement of water (or HX) to H_2 and O_2 (or X_2). From this standpoint, the challenge for molecule makers centered on H_2 generation now begins to take shape. When catalysis is isolated from solar capture and conversion, the basic tools common to the expansive organometallic precedence of the past three decades come into play with the caveat that O (or

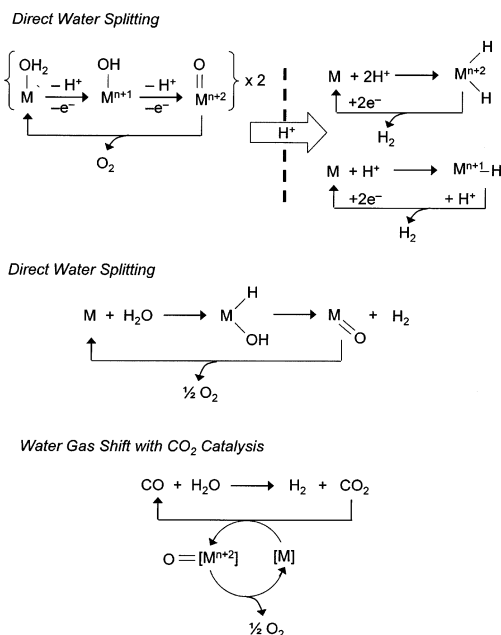


Figure 19. Three potential mechanisms for H_2 generation by water splitting.

X), as opposed to C or N, need to be managed. To highlight this contention, consider the H_2 generation schemes of Figure 19. The most straightforward scheme employs catalysts that directly act on the half-reactions of water splitting (Figure 19, top). The spatial separation of the catalysts requires that the charge-separation function be imbedded in some type of membrane, so that the protons generated on the anodic side of the cell are transported to the cathodic side of the cell for reduction. In effect, the system must be run in the opposite direction of a fuel cell, with sunlight providing the thermodynamic impetus to drive the cell in the desired fuel-forming direction. But other H_2 generation approaches may also be constructed: two of several possibilities that can be envisioned are shown in Figure 19. Oxidative cleavage of X–H (X = C, N) bonds is a basic reaction of organometallic chemistry but is not yet well-established for water.^{407–412} If this reaction can be achieved cleanly, hydrogen may be generated by α -H abstraction (Figure 19, middle), which is a common reaction in organometallic chemistry and is used to generate metal–ligand multiple bonds. For instance, α -H abstraction of metal–alkylidenes produces alkylidynes.⁴¹³ But α -H abstraction to produce metal–oxo species and H_2 is uncommon for well-defined hydroxo–hydrido complexes. Alternatively, the WGS reaction (Figure 19, bottom) may be augmented with a catalyst capable of the conversion of CO_2 to CO. On this front, little is known. Some inroads to CO_2 reduction have been achieved by (or via) photo-^{414,415} and electrocatalysis,^{416–418} but generally the precise CO_2 reduction mechanism is ill-defined, making it difficult to improve these systems by design. A recent report of CO_2 reduction by a well-defined homogeneous metal complex operating at high turnover number and frequency⁴¹⁹ is a harbinger of the promise that basic science holds for the design of efficient CO_2 reduction catalysts. Of course, for all schemes, the cycle must be finally closed with an oxygen-generating catalyst. The point here is that the approach of Figure 19 opens the field of H_2 photogeneration to the entire community; it is not necessarily the exclusive domain of the photochemist. In elucidating new reaction chemistries such as those shown in Figure 19, the chemical community as a

whole can contribute to the scientific toolbox necessary for society to utilize H₂ directly or indirectly as the primary energy carrier of the future.

8. Abbreviations

bpy	2,2'-bipyridine
COD	1,5-cyclooctadiene
COE	cyclooctene
CTAB	cetyltrimethylammonium bromide
DHP	diethyl-1,4-dihydro-2,6-dimethyl-3,5-pyridinecarboxylate
EDTA	ethylenediaminetetracetic acid or the sodium salt thereof
ESR	electron spin resonance
H atom	hydrogen atom
H ₂ A	ascorbic acid
HPB	heteropolyblue
IVCT	intervalence charge transfer
LB	Langmuir–Blodgett
LMCT	ligand to metal charge transfer
mpt	4'(-4-methylphenyl)-2,2',6,2''-terpyridyl
MV ²⁺	1,1'-dimethyl-4,4'-bipyridinium dication
NADH	nicotinamide adenine dinucleotide
NADPH	nicotinamide adenine dinucleotide phosphate
OEP	octaethylporphyrin
OLED	organic light-emitting device
phen	1,10-phenanthroline
POM	polyoxometalate
ppy	2-phenylpyridine
PSI	photosystem I
PSII	photosystem II
PV	photovoltaic
PVC	polyvinylcarbonate
SDS	sodium dodecyl sulfate
TBE	<i>tert</i> -butylethylene
TEA	triethylamine
TEAB	tetra- <i>p</i> -(<i>N</i> -ethyl- <i>N,N</i> -dimethyl)ammoniumbacteriochlorin
TEAC	tetra- <i>p</i> -(<i>N</i> -ethyl- <i>N,N</i> -dimethyl)ammoniumchlorin
TEAP	tetra- <i>p</i> -(<i>N</i> -ethyl- <i>N,N</i> -dimethyl)ammoniumporphyrin
TEOA	triethanolamine
TPP	tetraphenylporphyrin
tpy	terpyridine
WGS	water–gas shift
TMPP	tetra(<i>N</i> -methyl-pyridyl)porphyrin
TPPS ₄	tetra(sulfonatophenyl)porphyrin

9. Acknowledgments

We acknowledge sustained support from the National Science Foundation (Grant CHE-0132680 and a Chemical Bonding Center Grant CP-CP0533150) for basic research in renewable energy and photocatalytic hydrogen production. D.G.N. would also like to especially thank all the students past and present who contributed to the work presented herein. A.J.E. would like to thank Dilek Barlow for insightful discussions.

10. References

- Lewis, N. S.; Nocera, D. G. *Proc. Nat. Acad. Sci. U.S.A.* **2006**, *103*, 15729.
- Nocera, D. G. *Dædulus* **2006**, *135*, 112.
- Eisenberg, R.; Nocera, D. G. *Inorg. Chem.* **2005**, *44*, 6799.
- Nocera, D. G. *Chem. Eng. News* **2001**, *79*, 250.
- Hoffert, M. I.; Caldeira, K.; Jain, A. K.; Haites, E. F.; Harvey, L. D. D.; Potter, S. D.; Schlesinger, M. E.; Schneider, S. H.; Watts, R. G.; Wigley, T. M. L.; Wuebbles, D. J. *Nature* **1998**, *395*, 881.
- Lewis, N. S. In *Energy and Transportation*; The National Academies Press: Washington, DC, 2003; pp 33.
- World Energy Assessment Report: Energy and the Challenge of Sustainability*; United Nations Development Program, United Nations: New York, 2003.
- Basic Research Needs to Assure a Secure Energy Future*; A Report from the Basic Energy Sciences Advisory Committee; U.S. Department of Energy: Washington, DC, 2003.
- Karas, T. H. *Energy and National Security*; Sandia Report SAND2003-3287; Sandia National Laboratory: Albuquerque, NM, 2003.
- Address to the National Hydrogen Association, Secretary of Energy Spencer Abraham, 5 March 2003; available at http://www.energy.gov/engine/content.do?PUBLIC_ID=13384 & BT_CODE=PR_SPEECHES&TT_CODE=PRESSRELEASE.
- The Effect on the National Security of Imports of Crude Oil and Refined Petroleum Products*; U.S. Department of Commerce, An Investigation Conducted Under Section 232 of the Trade Expansion Act of 1962, as Amended, November 1999, p. ES-9.
- Petit, J. R.; Jouzel, J.; Raynaud, D.; Barkov, N. I.; Barnola, J.-M.; Basile, I.; Bender, M.; Chappellaz, J.; Davis, M.; Delaygue, G.; Delmotte, M.; Kotlyakov, V. M.; Legrand, M.; Lipenkov, V. Y.; Lorius, C.; Pépin, L.; Ritz, C.; Saltzman, E.; Stievenard, M. *Nature* **1999**, *399*, 429.
- Siegenthaler, U.; Stocker, T. F.; Monnin, E.; Lüthi, D.; Schwander, J.; Stauffer, B.; Raynaud, D.; Barnola, J.-M.; Fischer, H.; Masson-Delmotte, V.; Jouzel, J. *Science* **2005**, *310*, 1313.
- The Future of Coal: An MIT Interdisciplinary Study*; Deutch, J., Moniz, E. J., Eds.; Massachusetts Institute of Technology: Cambridge, MA, 2007; ISBN 978-0-615-14092-6.
- Ciamician, G. *Science* **1912**, *36*, 642.
- See, for example: Jessop, P. G.; Ikariya, T.; Noyori, R. *Chem. Rev.* **1995**, *95*, 259.
- Winter, M.; Brodd, R. J. *Chem. Rev.* **2004**, *104*, 4245.
- Crabtree, G. W.; Dresselhaus, M. S.; Buchanan, M. V. *Phys. Today* **2004**, *57*, 39.
- Basic Research Needs for the Hydrogen Economy*; A Report from the Basic Energy Sciences Workshop on Hydrogen Production, Storage, and Use; U.S. Department of Energy: Washington, DC, 2003.
- Dempsey, J. L.; Esswein, A. J.; Manke, D. R.; Rosenthal, J.; Soper, J. D.; Nocera, D. G. *Inorg. Chem.* **2005**, *44*, 6879.
- Rosenthal, J.; Bachman, J.; Dempsey, J. L.; Esswein, A. J.; Gray, T. G.; Hodgkiss, J. M.; Manke, D. R.; Luckett, T. D.; Pistorio, B. J.; Veige, A. S.; Nocera, D. G. *Coord. Chem. Rev.* **2005**, *249*, 1316.
- Nocera, D. G. *Acc. Chem. Res.* **1995**, *28*, 209.
- Soper, J. D.; Kryatov, S. V.; Rybak-Akimova, E. V.; Nocera, D. G. *J. Am. Chem. Soc.* **2007**, *129*, 5069.
- Yang, J. Y.; Nocera, D. G. *J. Am. Chem. Soc.* **2007**, *129*, 8192.
- Reece, S. Y.; Hodgkiss, J. M.; Stubbe, J.; Nocera, D. G. *Philos. Trans. R. Soc. B* **2006**, *361*, 1351.
- Hodgkiss, J. M.; Rosenthal, J.; Nocera, D. G. In *Handbook of Hydrogen Transfer. Physical and Chemical Aspects of Hydrogen Transfer*; Hynes, J. T., Schowen, R. L., Limbach, H. H., Eds.; Wiley VCH: Germany, 2006; Vol. 1.
- Liu, S.-Y.; Soper, J. D.; Yang, J. Y.; Rybak-Akimova, E. V.; Nocera, D. G. *Inorg. Chem.* **2006**, *45*, 7572.
- Yang, J. Y.; Bachmann, J.; Nocera, D. G. *J. Org. Chem.* **2006**, *71*, 8706.
- Liu, S.-Y.; Nocera, D. G. *J. Am. Chem. Soc.* **2005**, *127*, 5278.
- Chang, C. J.; Chang, M. C. Y.; Damrauer, N. H.; Nocera, D. G. *Biochim. Biophys. Acta* **2004**, *1655*, 13.
- Chang, C. J.; Loh, Z.-H.; Shi, C.; Anson, F. C.; Nocera, D. G. *J. Am. Chem. Soc.* **2004**, *126*, 10013.
- Stubbe, J.; Nocera, D. G.; Yee, C. S.; Chang, M. C. Y. *Chem. Rev.* **2003**, *103*, 2167.
- Chang, C. J.; Chng, L. L.; Nocera, D. G. *J. Am. Chem. Soc.* **2003**, *125*, 1866.
- Chng, L. L.; Chang, C. J.; Nocera, D. G. *Org. Lett.* **2003**, *5*, 2421.
- Yeh, C.-Y.; Chang, C. J.; Nocera, D. G. *J. Am. Chem. Soc.* **2001**, *123*, 1513.
- Chang, C. J.; Deng, Y.; Shi, C.; Chang, C.-K.; Anson, F. C.; Nocera, D. G. *Chem. Commun.* **2000**, 1355.
- Rappaport, F.; Joliot, P. In *Encyclopedia of Biological Chemistry*; Lennarz, W. J., Lane, M. D., Eds.; Elsevier: Oxford, U.K., 2004; Vol. 3, pp 375.
- Barber, J. *Curr. Opin. Struct. Biol.* **2002**, *12*, 523.
- Ruttinger, W.; Dismukes, G. C. *Chem. Rev.* **1997**, *97*, 1.
- Yagi, M.; Kaneko, M. *Chem. Rev.* **2001**, *101*, 21.
- McEvoy, J. P.; Brudvig, G. W. *Chem. Rev.* **2006**, *106*, 4455.
- For the most recent treatments on oxygen production from water, see upcoming issues of *Philos. Trans. R. Soc., B* entitled "Revealing How Nature uses Sunlight to Split Water" and a Forum issue of *Inorg. Chem.* entitled "Making Oxygen".
- Crabtree, R. H.; Miheleic, J. M.; Quirk, J. M. *J. Am. Chem. Soc.* **1979**, *101*, 7738.

- (44) Crabtree, R. H. *Acc. Chem. Res.* **1979**, *12*, 331.
- (45) Crabtree, R. H.; Mellea, M. F.; Mihelcic, J. M.; Quirk, J. M. *J. Am. Chem. Soc.* **1982**, *104*, 107.
- (46) Crabtree, R. H.; Parnell, C. P.; Uriarte, R. *J. Organometallics* **1987**, *6*, 696.
- (47) Crabtree, R. H.; Demou, P. C.; Eden, D.; Mihelcic, J. M.; Parnell, C. P.; Quirk, J. M.; Morris, G. E. *J. Am. Chem. Soc.* **1982**, *104*, 6994.
- (48) Baudry, D. E.; Ephritikhine, M.; Felkin, H. *J. Chem. Soc., Chem. Commun.* **1980**, 1243.
- (49) Baudry, D. E.; Ephritikhine, M.; Felkin, H.; Holmes-Smith, R. *J. Chem. Soc., Chem. Commun.* **1983**, 788.
- (50) Baudry, D. E.; Ephritikhine, M.; Felkin, H.; Zakrzewski, J. *Tetrahedron Lett.* **1984**, *25*, 1283.
- (51) Felkin, H.; Khan-Fillebeen, T.; Gault, Y. *Tetrahedron Lett.* **1984**, *25*, 1279.
- (52) Felkin, H.; Khan-Fillebeen, T.; Holmes-Smith, R.; Yingrui, L. *Tetrahedron Lett.* **1985**, *26*, 1999.
- (53) Burk, M. J.; Crabtree, R. H.; McGrath, D. M. *J. Chem. Soc., Chem. Commun.* **1985**, 1829.
- (54) Burk, M. J.; Crabtree, R. H. *J. Am. Chem. Soc.* **1987**, *109*, 8025.
- (55) For a review of recent progress in this area, see: Jensen, C. M. *Chem. Commun.* **1999**, 2443.
- (56) Gupta, M.; Hagen, C.; Flesher, R. J.; Kaska, W. C.; Jensen, C. M. *Chem. Commun.* **1996**, 2083.
- (57) Gupta, M.; Hagen, C.; Kaska, W. C.; Cramer, R. E.; Jensen, C. M. *J. Am. Chem. Soc.* **1997**, *119*, 840.
- (58) Liu, F.; Pak, E. B.; Singh, B.; Jensen, C. M.; Goldman, A. S. *J. Am. Chem. Soc.* **1999**, *121*, 4086.
- (59) Göttker-Schnetmann, I.; White, P.; Brookhart, M. *J. Am. Chem. Soc.* **2004**, *126*, 1804.
- (60) Göttker-Schnetmann, I.; White, P.; Brookhart, M. *Organometallics* **2004**, *23*, 1766.
- (61) Göttker-Schnetmann, I.; Brookhart, M. *J. Am. Chem. Soc.* **2004**, *126*, 9330.
- (62) Morales-Morales, D.; Redon, R.; Yung, C.; Jensen, C. M. *Inorg. Chim. Acta* **2004**, *357*, 2953.
- (63) Zhu, K.; Achord, P. D.; Zhang, X.; Krogh-Jespersen, K.; Goldman, A. S. *J. Am. Chem. Soc.* **2004**, *126*, 13044.
- (64) Xu, W.-W.; Rosini, G. P.; Gupta, M.; Jensen, C. M.; Kaska, W. C.; Krogh-Jespersen, K.; Goldman, A. S. *Chem. Commun.* **1997**, 2273.
- (65) Liu, F.; Goldman, A. S. *Chem. Commun.* **1999**, 655.
- (66) Haebel, M.; Oevers, S.; Angermund, K.; Kaska, W. C.; Fan, H.-J.; Hall, M. B. *Angew. Chem., Int. Ed.* **2001**, *40*, 3596.
- (67) Kuklin, S. A.; Sheloumov, A. M.; Dolgushin, F. M.; Ezernitskaya, M. G.; Peregodov, A. S.; Petrovskii, P. V.; Koridze, A. A. *Organometallics* **2006**, *25*, 5466.
- (68) Goldman, A. S.; Roy, A. H.; Huang, Z.; Ahuja, R.; Schinski, W.; Brookhart, M. *Science* **2006**, *312*, 257.
- (69) See, for example: Geoffroy, G. L.; Wrighton, M. S. *Organometallic Photochemistry*; Academic Press: New York, 1979.
- (70) Bitterwolf, T. E. *J. Organomet. Chem.* **2004**, *689*, 3939.
- (71) Vlček, A., Jr. *Coord. Chem. Rev.* **1998**, *177*, 219.
- (72) Nomura, K.; Saito, Y. *J. Chem. Soc., Chem. Commun.* **1988**, 161.
- (73) Brady, R.; Flynn, B. R.; Geoffroy, G. L.; Gray, H. B.; Peone, J., Jr.; Vaska, L. *Inorg. Chem.* **1976**, *15*, 1485.
- (74) Wink, D.; Ford, P. C. *J. Am. Chem. Soc.* **1985**, *107*, 1794.
- (75) Wink, D.; Ford, P. C. *J. Am. Chem. Soc.* **1987**, *109*, 436.
- (76) Sakakura, T.; Sodeyama, T.; Tokunaga, Y.; Tanaka, M. *Chem. Lett.* **1988**, 263.
- (77) Sakakura, T.; Ishida, K.; Tanaka, M. *Chem. Lett.* **1990**, 585.
- (78) Nomura, K.; Saito, Y. *J. Mol. Catal.* **1989**, *54*, 57.
- (79) Sakakura, T.; Sodeyama, T.; Tanaka, M. *New J. Chem.* **1989**, *13*, 737.
- (80) Tanaka, M.; Sakakura, T. *Pure Appl. Chem.* **1990**, *62*, 1147.
- (81) Iwamoto, A.; Itagaki, H.; Saito, Y. *J. Chem. Soc., Dalton Trans.* **1991**, 1093.
- (82) Moriyama, H.; Sakakura, T.; Yabe, A.; Tanaka, M. *J. Mol. Catal.* **1990**, *60*, L9.
- (83) Sakakura, T.; Tokunaga, Y.; Sodeyama, T.; Tanaka, M. *Chem. Lett.* **1988**, 885.
- (84) Sakakura, T.; Sodeyama, T.; Tokunaga, Y.; Tanaka, M. *Chem. Lett.* **1987**, 2211.
- (85) Sakakura, T.; Sodeyama, T.; Tanaka, M. *Chem. Lett.* **1988**, 683.
- (86) Maguire, J. A.; Boese, W. T.; Goldman, A. S. *J. Am. Chem. Soc.* **1989**, *111*, 7088.
- (87) Maguire, J. A.; Boese, W. T.; Goldman, M. E.; Goldman, A. S. *Coord. Chem. Rev.* **1990**, *97*, 179.
- (88) Rosini, G. P.; Soubra, S.; Vixamar, M.; Wang, S.; Goldman, A. S. *J. Organomet. Chem.* **1998**, *554*, 41.
- (89) Maguire, J. A.; Goldman, A. S. *J. Am. Chem. Soc.* **1991**, *113*, 6706.
- (90) Maguire, J. A.; Petrillo, A.; Goldman, A. S. *J. Am. Chem. Soc.* **1992**, *114*, 9492.
- (91) Mann, K. R.; Gordon, J. G., II; Gray, H. B. *J. Am. Chem. Soc.* **1975**, *97*, 3553.
- (92) Fordyce, W. A.; Brummer, J. G.; Crosby, G. A. *J. Am. Chem. Soc.* **1981**, *103*, 7061.
- (93) Itagaki, H.; Einaga, H.; Saito, Y. *J. Chem. Soc., Dalton Trans.* **1993**, 1689.
- (94) Itagaki, H.; Einaga, H.; Saito, Y. *Chem. Lett.* **1993**, 2097.
- (95) Sakakura, T.; Abe, F.; Tanaka, M. *Chem. Lett.* **1991**, 297.
- (96) Taylor, H. S.; Hill, D. G. *J. Am. Chem. Soc.* **1929**, *51*, 2922.
- (97) Steacie, E. W. R.; Phillips, N. W. F. *J. Chem. Phys.* **1938**, *6*, 179.
- (98) Brown, S. H.; Crabtree, R. H. *Tetrahedron Lett.* **1987**, *28*, 5599.
- (99) Brown, S. H.; Crabtree, R. H. *J. Am. Chem. Soc.* **1989**, *111*, 2935.
- (100) Brown, S. H.; Crabtree, R. H. *J. Am. Chem. Soc.* **1989**, *111*, 2946.
- (101) Gunning, H. E.; Strausz, O. P. *Adv. Photochem.* **1963**, *1*, 209.
- (102) Arakawa, H.; Sugi, Y. *Chem. Lett.* **1981**, 1323.
- (103) Griggs, C. G.; Smith, D. J. H. *J. Organomet. Chem.* **1984**, *273*, 105.
- (104) Wink, D.; Ford, P. C. *J. Am. Chem. Soc.* **1986**, *108*, 4838.
- (105) Yamakawa, T.; Katsurao, T.; Shinoda, S.; Saito, Y. *J. Mol. Catal.* **1987**, *42*, 183.
- (106) Nomura, K.; Saito, Y.; Shinoda, S. *J. Mol. Catal.* **1989**, *52*, 99.
- (107) Delgado-Lieta, E.; Luke, M. A.; Jones, F. A.; Cole-Hamilton, D. J. *Polyhedron* **1982**, *1*, 839.
- (108) Simpson, M. C.; Cole-Hamilton, D. J. *Coord. Chem. Rev.* **1996**, *155*, 163.
- (109) Morton, D.; Cole-Hamilton, D. J.; Utuk, I. D.; Paneque-Sosa, M.; Lopez-Poveda, M. *J. Chem. Soc., Dalton Trans.* **1989**, 489.
- (110) Yoshida, T.; Okano, T.; Otsuka, S. *J. Am. Chem. Soc.* **1980**, *102*, 5966.
- (111) Takahashi, T.; Shinoda, S.; Saito, Y. *J. Mol. Catal.* **1985**, *31*, 301.
- (112) Yamamoto, H.; Shinoda, S.; Saito, Y. *J. Mol. Catal.* **1985**, *30*, 259.
- (113) Shinoda, S.; Kobayashi, A.; Aoki, T.; Saito, Y. *J. Mol. Catal.* **1986**, *38*, 279.
- (114) Roundhill, D. M.; Gray, H. B.; Che, C.-M. *Acc. Chem. Res.* **1989**, *22*, 55.
- (115) Pinto, F. D. R.; Sadler, P. J.; Neidle, S.; Sanderson, M. R.; Subbiah, A.; Kuroda, R. *J. Chem. Soc., Chem. Commun.* **1980**, 13.
- (116) Roundhill, D. M.; Gray, H. B.; Che, C.-M. *Acc. Chem. Res.* **1989**, *22*, 55.
- (117) Fordyce, W. A.; Brummer, J. G.; Crosby, G. A. *J. Am. Chem. Soc.* **1981**, *103*, 7061.
- (118) Parker, W. L.; Crosby, G. A. *Chem. Phys. Lett.* **1984**, *105*, 544.
- (119) Rice, S. F.; Gray, H. B. *J. Am. Chem. Soc.* **1983**, *105*, 4571.
- (120) Sperline, R. P.; Dickson, M. K.; Roundhill, D. M. *J. Chem. Soc., Chem. Commun.* **1977**, 62.
- (121) Che, C.-M.; Butler, L. G.; Gray, H. B. *J. Am. Chem. Soc.* **1981**, *103*, 7796.
- (122) Roundhill, D. M. *J. Am. Chem. Soc.* **1985**, *107*, 4354.
- (123) Roundhill, D. M.; Atherton, S. J.; Shen, Z.-P. *J. Am. Chem. Soc.* **1987**, *109*, 6076.
- (124) Che, C.-M.; Schaefer, W. P.; Gray, H. B.; Dickson, M. K.; Stein, P.; Roundhill, D. M. *J. Am. Chem. Soc.* **1982**, *104*, 4253.
- (125) Harvey, E. L.; Stiegman, A. E.; Vlček, A., Jr.; Gray, H. B. *J. Am. Chem. Soc.* **1987**, *109*, 5233.
- (126) Che, C.-M.; Lee, W. M.; Cho, K. C.; Harvey, P. D.; Gray, H. B. *J. Phys. Chem.* **1989**, *93*, 3095.
- (127) Smith, D. C.; Gray, H. B. *Coord. Chem. Rev.* **1990**, *100*, 169.
- (128) Sweeney, R. J.; Harvey, E. L.; Gray, H. B. *Coord. Chem. Rev.* **1990**, *105*, 23.
- (129) Shinoda, S.; Moriyama, H.; Kise, Y.; Saito, Y. *J. Chem. Soc., Chem. Commun.* **1978**, 348.
- (130) Moriyama, H.; Aoki, T.; Shinoda, S.; Saito, Y. *J. Chem. Soc., Perkin II* **1982**, 369.
- (131) Matsubara, T.; Saito, Y.; Yamakawa, T.; Shinoda, S. *J. Mol. Catal.* **1991**, *67*, 175.
- (132) Makita, K.; Nomura, K.; Saito, Y. *J. Mol. Catal.* **1994**, *89*, 143.
- (133) Yamakawa, T.; Miyake, H.; Moriyama, H.; Shinoda, S.; Saito, Y. *J. Chem. Soc., Chem. Commun.* **1986**, 326.
- (134) Matsubara, T.; Saito, Y.; Yamakawa, T.; Shinoda, S. *J. Mol. Catal.* **1993**, *79*, 29.
- (135) Moriyama, H.; Pregosin, P. S.; Saito, Y.; Yamakawa, T. *J. Chem. Soc., Dalton Trans.* **1984**, 2329.
- (136) Irie, R.; Li, X.; Saito, Y. *J. Mol. Catal.* **1983**, *18*, 263.
- (137) Irie, R.; Li, X.; Saito, Y. *J. Mol. Catal.* **1984**, *23*, 17.
- (138) Irie, R.; Li, X.; Saito, Y. *J. Mol. Catal.* **1984**, *23*, 23.
- (139) Shinoda, S.; Li, X.; Saito, Y. *J. Mol. Catal.* **1989**, *49*, 113.
- (140) Ogoishi, H.; Setsune, J.; Yoshida, Z. *J. Am. Chem. Soc.* **1977**, *99*, 3869.
- (141) Wayland, B. B.; Newman, A. R. *J. Am. Chem. Soc.* **1979**, *101*, 6472.
- (142) Pope, M. T. In *Inorganic Chemistry Concepts*; Jorgensen, C. K., Ed.; Springer-Verlag: Berlin, 1983.
- (143) Papaconstantinou, E. *Chem. Soc. Rev.* **1989**, *18*, 1.
- (144) Papaconstantinou, E. *J. Chem. Soc., Chem. Commun.* **1982**, 12.
- (145) Papaconstantinou, E.; Ioannidis, A. *Inorg. Chim. Acta* **1983**, *75*, 235.

- (146) Papaconstantinou, E.; Dimotikali, D.; Politou, A. *Inorg. Chim. Acta* **1980**, *46*, 155.
- (147) Kahn, O. *Molecular Magnetism*; VCH Publishing: New York, 1993.
- (148) Darwent, J. R. *J. Chem. Soc., Chem. Commun.* **1982**, 798.
- (149) Yamase, T. *Inorg. Chim. Acta* **1982**, *64*, L155.
- (150) Savinov, E. N.; Saidkhanov, S. S.; Parman, V. N.; Zamaraev, K. I. *Dolk. Phys. Chem. SSSR* **1983**, *272*, 916.
- (151) Yamase, T.; Takabayashi, N.; Kaji, M. *J. Chem. Soc., Dalton Trans.* **1984**, 793.
- (152) Argitis, P.; Papaconstantinou, E. *J. Photochem.* **1985**, *30*, 445.
- (153) Hill, C. L.; Bouchard, D. A. *J. Am. Chem. Soc.* **1985**, *107*, 5148.
- (154) Akid, R.; Darwent, J. R. *J. Chem. Soc., Dalton Trans.* **1985**, 395.
- (155) Renneke, R. F.; Hill, C. L. *J. Am. Chem. Soc.* **1986**, *108*, 3528.
- (156) Hiskia, A.; Papaconstantinou, E. *Polyhedron* **1988**, *7*, 477.
- (157) Muradov, N.; Raissi, A. T. *J. Sol. Energy Eng.* **2006**, *128*, 326.
- (158) Ward, M. D.; Brazdil, J. F.; Grasselli, R. K. *J. Phys. Chem.* **1984**, *88*, 4210.
- (159) Duncan, D. C.; Netsel, T. L.; Hill, C. L. *Inorg. Chem.* **1995**, *34*, 4640.
- (160) Fox, M. A.; Cardona, R.; Gailard, E. *J. Am. Chem. Soc.* **1987**, *109*, 6347.
- (161) Williamson, M. M.; Bouchard, D. A.; Hill, C. L. *Inorg. Chem.* **1987**, *26*, 1436.
- (162) Hill, C. L.; Bouchard, D. A.; Kadkhodayan, M. M.; Schmidt, J. A.; Hilinski, E. F. *J. Am. Chem. Soc.* **1988**, *110*, 5471.
- (163) Gomez-Garcia, C. J.; Gimenez-Saiz, C.; Triki, S.; Coronado, E.; Le Magueres, P.; Quahab, L.; Ducasse, L.; Sourisseau, C.; Delhaes, P. *Inorg. Chem.* **1995**, *34*, 4139.
- (164) Kraut, B.; Ferraudi, G. *Inorg. Chem.* **1990**, *29*, 4834.
- (165) Tanielian, C.; Duffy, K.; Jones, A. *J. Phys. Chem. B* **1997**, *101*, 4276.
- (166) Swallow, A. J. *Prog. React. Kinet.* **1978**, *9*, 195 and references therein.
- (167) Mylonas, A.; Hiskia, A.; Androulaki, E.; Dimotikali, D.; Papaconstantinou, E. *Phys. Chem. Chem. Phys.* **1999**, *1*, 437.
- (168) Mylonas, A.; Papaconstantinou, E. *J. Mol. Catal.* **1994**, *92*, 261.
- (169) Mylonas, A.; Papaconstantinou, E. *J. Photochem. Photobiol. A* **1996**, *94*, 77.
- (170) Mylonas, A.; Roussis, V.; Papaconstantinou, E. *Polyhedron* **1996**, *15*, 3211.
- (171) Mylonas, A.; Hishkia, A.; Papaconstantinou, E. *J. Mol. Catal.* **1996**, *114*, 191.
- (172) Anbar, M.; Neta, P. *Int. J. Appl. Radiat. Isotopes* **1967**, *18*, 493.
- (173) Zhang, D.; Wu, L.-Z.; Zhou, L.; Han, X.; Yang, Q.-Z.; Zhang, L.-P.; Tung, C.-H. *J. Am. Chem. Soc.* **2004**, *126*, 3440.
- (174) Sambongi, Y.; Nitta, H.; Ichihashi, K.; Futai, M.; Ueda, I. *J. Org. Chem.* **2002**, *67*, 3499.
- (175) Prabhu-Narayana, R.; Schmehl, R. H. *Inorg. Chem.* **2006**, *45*, 4319.
- (176) Ryason, P. R. *Sol. Energy* **1977**, *19*, 445.
- (177) Collinson, E.; Dainton, F. S.; Malati, M. A. *Trans. Faraday Soc.* **1959**, *55*, 2096.
- (178) Heidt, L. J.; Mullin, M. G.; Martin, W. B., Jr.; Beatty, M. J. *J. Phys. Chem.* **1962**, *66*, 336.
- (179) Heidt, L. J.; McMillan, A. F. *J. Am. Chem. Soc.* **1954**, *76*, 2135.
- (180) Stevenson, K. L.; Kaehr, D. M.; Davis, D. D.; Davis, C. R. *Inorg. Chem.* **1980**, *19*, 781.
- (181) Jones, R. F.; Cole-Hamilton, D. J. *J. Chem. Soc., Chem. Commun.* **1981**, 1245.
- (182) Yoshida, T.; Matsuda, T.; Okano, T.; Kitani, T.; Otsuka, S. *J. Am. Chem. Soc.* **1979**, *101*, 2027.
- (183) Eidem, P. K.; Maverick, A. W.; Gray, H. B. *Inorg. Chim. Acta* **1981**, *50*, 59.
- (184) Gray, H. B.; Maverick, A. W. *Science* **1981**, *214*, 1201.
- (185) Bosnich, B. *Inorg. Chem.* **1999**, *38*, 2554.
- (186) McCollum, D. G.; Bosnich, B. *Inorg. Chim. Acta* **1998**, *270*, 13.
- (187) Fackler, J. P., Jr. *Inorg. Chem.* **2002**, *41*, 6959.
- (188) Halpern, J. *Inorg. Chim. Acta* **1982**, *62*, 31.
- (189) Solomon, E. I.; Brunold, T. C.; Davis, M. I.; Kemsley, J. N.; Lee, S.-K.; Lehnert, N.; Neese, F.; Skulan, A. J.; Yang, Y.-S.; Zhou, J. *Chem. Rev.* **2000**, *100*, 235.
- (190) Baik, M.-H.; Newcomb, M.; Friesner, R. A.; Lippard, S. J. *Chem. Rev.* **2003**, *103*, 2385.
- (191) Wallar, B. J.; Lipscomb, J. D. *Chem. Rev.* **1996**, *96*, 2625.
- (192) Stubbe, J.; van der Donk, W. *Chem. Rev.* **1998**, *98*, 705.
- (193) Ferguson-Miller, S.; Babcock, G. T. *Chem. Rev.* **1996**, *96*, 2889.
- (194) Einarsdóttir, O. *Biochim. Biophys. Acta* **1995**, *1229*, 129.
- (195) Mobley, H. L. T.; Island, M. D.; Hausinger, R. P. *Microbiol. Rev.* **1995**, *59*, 451.
- (196) Stenkamp, R. E. *Chem. Rev.* **1994**, *94*, 715.
- (197) Magnus, K. A.; Ton-That, H.; Carpenter, J. E. *Chem. Rev.* **1994**, *94*, 727.
- (198) Diner, B. A.; Rappaport, F. *Annu. Rev. Plant Biol.* **2002**, *53*, 551.
- (199) Howard, J. B.; Rees, D. C. *Chem. Rev.* **1996**, *96*, 2965.
- (200) Burgess, B. K.; Lowe, D. J. *Chem. Rev.* **1996**, *96*, 2983.
- (201) Rees, D. C. *Annu. Rev. Biochem.* **2002**, *71*, 221.
- (202) Dobbek, H.; Svetlitchnyi, V.; Gremer, L.; Huber, R.; Meyer, O. *Science* **2001**, *293*, 1281.
- (203) Drennan, C. L.; Heo, J.; Sintchak, M. D.; Schreiter, E.; Ludden, P. W. *Proc. Natl. Acad. Sci. U.S.A.* **2001**, *98*, 11973.
- (204) Doukov, T.; Iverson, T. M.; Seravalli, J.; Ragsdale, S. W.; Drennan, C. L. *Science* **2002**, *298*, 567.
- (205) Darnault, C.; Volbeda, A.; Kim, E. J.; Vernède, X.; Lindahl, P. A.; Fonticella-Camps, J. C. *Nat. Struct. Biol.* **2003**, *10*, 271.
- (206) Lowther, W. T.; Matthews, B. W. *Chem. Rev.* **2002**, *102*, 4851.
- (207) Lipscomb, W. N.; Sträter, N. *Chem. Rev.* **1996**, *96*, 2375.
- (208) Beinert, H.; Holm, R. H.; Münck, E. *Science* **1997**, *277*, 653.
- (209) Holm, R. H.; Ciurli, S.; Weigel, J. A. *Prog. Inorg. Chem.* **1990**, *39*, 1.
- (210) Wilcox, D. E. *Chem. Rev.* **1996**, *96*, 2435.
- (211) Solomon, E. I.; Chen, P.; Metz, M.; Lee, S.-K.; Palmer, A. E. *Angew. Chem., Int. Ed.* **2001**, *40*, 4570.
- (212) Peters, J. W. *Curr. Opin. Struct. Biol.* **1999**, *9*, 670.
- (213) Nicolet, Y.; Piras, C.; Legrand, P.; Hatchikian, C. E.; Fonticella-Camps, J. C. *Structure* **1999**, *7*, 13.
- (214) Volbeda, A.; Fonticella-Camps, J. C. *Coord. Chem. Rev.* **2005**, *249*, 1609.
- (215) For a recent review on Ni-Fe and Fe only hydrogenase, see: Evans, D. J.; Pickett, C. J. *Chem. Soc. Rev.* **2003**, *32*, 268.
- (216) Rauchfuss, T. B. *Inorg. Chem.* **2004**, *43*, 14.
- (217) Marr, A. C.; Spencer, D. J. E.; Schröder, M. *Coord. Chem. Rev.* **2001**, *219*, 1055.
- (218) Holm, R. H.; Kennepohl, P.; Solomon, E. I. *Chem. Rev.* **1996**, *96*, 2239.
- (219) Lewis, N. S.; Mann, K. R.; Gordon, J. G., II; Gray, H. B. *J. Am. Chem. Soc.* **1976**, *98*, 7461.
- (220) Mann, K. R.; Lewis, N. S.; Miskowski, V. M.; Erwin, D. K.; Hammond, G. S.; Gray, H. B. *J. Am. Chem. Soc.* **1977**, *99*, 5525.
- (221) Mann, K. R.; Bell, R. A.; Gray, H. B. *Inorg. Chem.* **1979**, *18*, 2671.
- (222) Miskowski, V. M.; Sigal, I. S.; Mann, K. R.; Gray, H. B.; Milder, S. J.; Hammond, G. S.; Ryason, P. R. *J. Am. Chem. Soc.* **1979**, *101*, 4383.
- (223) Sigal, I. S.; Mann, K. R.; Gray, H. B. *J. Am. Chem. Soc.* **1980**, *102*, 7252.
- (224) Rice, S. F.; Gray, H. B. *J. Am. Chem. Soc.* **1983**, *105*, 4571.
- (225) Rice, S. F.; Miskowski, V. M.; Gray, H. B. *Inorg. Chem.* **1988**, *27*, 4704.
- (226) Roundhill, D. M.; Gray, H. B.; Che, C.-M. *Acc. Chem. Res.* **1989**, *22*, 55.
- (227) Engebretson, D. S.; Zaleski, J. M.; Leroi, G. E.; Nocera, D. G. *Science* **1994**, *265*, 759.
- (228) Engebretson, D. S.; Graj, E. M.; Leroi, G. E.; Nocera, D. G. *J. Am. Chem. Soc.* **1999**, *121*, 868.
- (229) Heitler, W.; London, F. Z. *Phys.* **1927**, *44*, 455.
- (230) Coulson, C. A.; Fischer, I. *Philos. Mag.* **1949**, *40*, 386.
- (231) Cotton, F. A.; Nocera, D. G. *Acc. Chem. Res.* **2000**, *33*, 483.
- (232) Partigianoni, C. M.; Turró, C.; Hsu, T. L. C.; Chang, I.-J.; Nocera, D. G. In *Photosensitive Metal-Organic Systems; Mechanistic Principles and Applications*; Kutal, C., Serpone, N., Eds.; Advances in Chemistry Series 238, American Chemical Society: Washington, DC, 1993; p 147.
- (233) Partigianoni, C. M.; Nocera, D. G. *Inorg. Chem.* **1990**, *29*, 2033.
- (234) Hsu, T. L. C.; Helvoigt, S. A.; Partigianoni, C. M.; Turró, C.; Nocera, D. G. *Inorg. Chem.* **1995**, *34*, 6186.
- (235) Pistorio, B. J.; Nocera, D. G. *Chem. Commun.* **1999**, 1831.
- (236) Erwin, D. K.; Geoffroy, G. L.; Gray, H. B.; Hammond, G. S.; Solomon, E. I.; Troglor, W. C.; Zagars, A. A. *J. Am. Chem. Soc.* **1977**, *99*, 3620.
- (237) Troglor, W. C.; Erwin, D. K.; Geoffroy, G. L.; Gray, H. B. *J. Am. Chem. Soc.* **1978**, *100*, 1160.
- (238) Chang, I.-J.; Nocera, D. G. *J. Am. Chem. Soc.* **1987**, *109*, 4901.
- (239) Partigianoni, C. M.; Chang, I.-J.; Nocera, D. G. *Coord. Chem. Rev.* **1990**, *97*, 105.
- (240) Rosenfeld, D. C.; Wolczanski, P. T.; Barakat, K. A.; Buda, C.; Cundari, T. R. *J. Am. Chem. Soc.* **2005**, *127*, 8262.
- (241) Bachmann, J.; Nocera, D. G. *J. Am. Chem. Soc.* **2004**, *126*, 2829.
- (242) Bachmann, J.; Nocera, D. G. *J. Am. Chem. Soc.* **2005**, *127*, 4730.
- (243) Bachmann, J.; Nocera, D. G. *Inorg. Chem.* **2005**, *44*, 6930.
- (244) Bachmann, J.; Hodgkiss, J. M.; Young, E. R.; Nocera, D. G. *Inorg. Chem.* **2007**, *46*, 607.
- (245) Dulebohn, J. I.; Ward, D. L.; Nocera, D. G. *J. Am. Chem. Soc.* **1990**, *112*, 2969.
- (246) Kadis, J.; Shin, Y. K.; Dulebohn, J. I.; Ward, D. L.; Nocera, D. G. *Inorg. Chem.* **1996**, *35*, 811.
- (247) Heyduk, A. F.; Macintosh, A. M.; Nocera, D. G. *J. Am. Chem. Soc.* **1999**, *121*, 5023.
- (248) Odom, A. L.; Heyduk, A. F.; Nocera, D. G. *Inorg. Chim. Acta* **2000**, *297*, 330.
- (249) Heyduk, A. F.; Nocera, D. G. *Science* **2001**, *293*, 1639.

- (250) Esswein, A. J.; Veige, A. S.; Nocera, D. G. *J. Am. Chem. Soc.* **2005**, *127*, 16641.
- (251) Esswein, A. J.; Dempsey, J. L.; Nocera, D. G. *Inorg. Chem.* **2007**, *46*, 2362.
- (252) Cook, T. R.; Esswein, A. J.; Nocera, D. G. *J. Am. Chem. Soc.* **2007**, *129*, 10094.
- (253) Ford, P. C. *Acc. Chem. Res.* **1981**, *14*, 31.
- (254) King, R. B. *J. Organomet. Chem.* **1999**, *586*, 2.
- (255) For a general review, see: Laine, R. M.; Crawford, E. J. *J. Mol. Catal.* **1988**, *44*, 357.
- (256) For an early example, see: Cheng, C. H.; Hendriksen, D. E.; Eisenberg, R. *J. Am. Chem. Soc.* **1977**, *99*, 2791.
- (257) King, R. B.; Frazier, C. C.; Hanes, R. M.; King, A. D. *J. Am. Chem. Soc.* **1978**, *100*, 2925.
- (258) Laine, R. M.; Rinker, R. G.; Ford, P. C. *J. Am. Chem. Soc.* **1977**, *99*, 252.
- (259) Darensbourg, D. J.; Rokicki, A. *Organometallics* **1982**, *1*, 1685.
- (260) Church, S. P.; Grevels, F.-W.; Hermann, H.; Schnaffner, K. *J. Chem. Soc., Chem. Commun.* **1985**, 30.
- (261) Upmacis, R. T.; Poliakov, M.; Turner, J. T. *J. Am. Chem. Soc.* **1986**, *108*, 3645.
- (262) King, A. D., Jr.; King, R. B.; Sailors, E. L., III *J. Am. Chem. Soc.* **1981**, *103*, 1867.
- (263) Nagorski, H.; Mirbach, M. J.; Mirbach, M. J. *J. Organomet. Chem.* **1985**, *297*, 171.
- (264) Linn, D. E.; King, R. B.; King, A. D., Jr. *J. Mol. Catal.* **1993**, *80*, 151.
- (265) Weiller, B. H.; Liu, J.-P.; Grant, E. R. *J. Am. Chem. Soc.* **1985**, *107*, 1595.
- (266) Pac, C.; Miyaka, K.; Matsuo, T.; Yanagida, S.; Sakurai, H. *J. Chem. Soc., Chem. Commun.* **1986**, 1115.
- (267) For a full explanation of this phenomenon, see: Norton, J. R. *Acc. Chem. Res.* **1979**, *12*, 139.
- (268) Choudary, D.; Cole-Hamilton, D. J. *J. Chem. Soc., Dalton Trans.* **1982**, 1885.
- (269) Tanaka, K.; Morimoto, M.; Tanaka, T. *Chem. Lett.* **1983**, 901.
- (270) Ishida, H.; Tanaka, K.; Morimoto, M.; Tanaka, T. *Organometallics* **1986**, *5*, 724.
- (271) Ziessel, R. *J. Chem. Soc., Chem. Commun.* **1988**, 16.
- (272) Ziessel, R. *Angew. Chem., Int. Ed. Engl.* **1991**, *30*, 844.
- (273) Ziessel, R. *J. Am. Chem. Soc.* **1993**, *115*, 118.
- (274) Durham, B.; Dressick, W. J.; Meyer, T. J. *J. Chem. Soc., Chem. Commun.* **1979**, 381.
- (275) DeLaive, P. J.; Sullivan, B. P.; Meyer, T. J.; Whitten, D. G. *J. Am. Chem. Soc.* **1979**, *101*, 4007.
- (276) Bauer, R.; Königstein, C. *Z. Naturforsch.* **1991**, *46b*, 1544.
- (277) Burstall, F. H. *J. Chem. Soc.* **1936**, 173.
- (278) Liu, C. F.; Liu, N. C.; Bailar, J. C., Jr. *Inorg. Chem.* **1964**, *3*, 1085.
- (279) Gafney, H. D.; Adamson, A. W. *J. Am. Chem. Soc.* **1972**, *94*, 8238.
- (280) Young, R. C.; Meyer, T. J.; Whitten, D. G. *J. Am. Chem. Soc.* **1975**, *97*, 4781.
- (281) Meyer, T. J. *Acc. Chem. Res.* **1978**, *11*, 94.
- (282) Valenty, S. J.; Gaines, G. L. *J. Am. Chem. Soc.* **1977**, *99*, 1285.
- (283) Harriman, A. *J. Chem. Soc., Chem. Commun.* **1977**, 777.
- (284) Seefeld, K. P.; Möbius, D.; Kuhn, H. *Helv. Chim. Acta* **1977**, *60*, 2608.
- (285) Yellowlees, L. J.; Dickinson, R. G.; Halliday, C. S.; Bonham, J. S.; Lyons, L. E. *Aust. J. Chem.* **1978**, *31*, 431.
- (286) Moradpour, A.; Amouyal, E.; Keller, P.; Kagan, H. *Nouv. J. Chem.* **1979**, *2*, 547.
- (287) Kalyanasundaram, K.; Kiwi, J.; Grätzel, M. *Helv. Chim. Acta* **1978**, *61*, 2720.
- (288) Miller, D.; McLendon, G. *Inorg. Chem.* **1981**, *20*, 950.
- (289) Keller, P.; Moradpour, A. *J. Am. Chem. Soc.* **1980**, *102*, 7193.
- (290) Ebbesen, T. W. *J. Phys. Chem.* **1984**, *88*, 4131.
- (291) Bauer, R.; Werner, H. A. F. *J. Mol. Catal.* **1992**, *72*, 67.
- (292) Königstein, C. *J. Photochem. Photobiol. A* **1995**, *90*, 141.
- (293) Amouyal, E.; Zidler, B.; Keller, P.; Moradpour, A. *Chem. Phys. Lett.* **1980**, *74*, 314.
- (294) Launikonis, A.; Loder, J. W.; Mau, A. W.-H.; Sasse, W. H. F.; Wells, D. *Isr. J. Chem.* **1982**, *22*, 158.
- (295) Amouyal, E.; Zidler, B. *Isr. J. Chem.* **1982**, *22*, 117.
- (296) Lehn, J. M.; Sauvage, J. P. *Nouv. J. Chem.* **1977**, *1*, 449.
- (297) Kirch, M.; Lehn, J. M.; Sauvage, J. P. *Helv. Chim. Acta* **1979**, *62*, 1345.
- (298) Brown, G. M.; Chan, S.-F.; Creutz, C.; Schwarz, H. A.; Sutin, N. *J. Am. Chem. Soc.* **1979**, *101*, 7638.
- (299) Chan, S.-F.; Chou, M.; Creutz, C.; Matsubara, T.; Sutin, N. *J. Am. Chem. Soc.* **1981**, *103*, 369.
- (300) Krishnan, C. V.; Sutin, N. *J. Am. Chem. Soc.* **1981**, *103*, 2141.
- (301) Krishnan, C. V.; Brunshwig, B. S.; Creutz, C.; Sutin, N. *J. Am. Chem. Soc.* **1985**, *107*, 2005.
- (302) Tait, A. M.; Hoffman, M. Z.; Hayon, E. *J. Am. Chem. Soc.* **1976**, *98*, 86.
- (303) Rillema, D. P.; Endicott, J. F. *Inorg. Chem.* **1976**, *15*, 1459.
- (304) Krishnan, C. V.; Creutz, C.; Mahajan, D.; Schwarz, H. A.; Sutin, N. *Isr. J. Chem.* **1982**, *22*, 98.
- (305) Goldsmith, J. I.; Hudson, W. R.; Lowry, M. S.; Anderson, T. H.; Bernhard, S. *J. Am. Chem. Soc.* **2005**, *127*, 7502.
- (306) Lowry, M. S.; Goldsmith, J. I.; Slinker, J. D.; Rohl, R.; Pascal, R. A., Jr.; Malliaras, G. G.; Bernhard, S. *Chem. Mater.* **2005**, *17*, 5712.
- (307) See Thematic Issue on Organic Electronics and Optoelectronics: *Chem. Rev.* **2007**, *104*, 923.
- (308) Du, P.; Schneider, J.; Jarosz, P.; Eisenberg, R. *J. Am. Chem. Soc.* **2006**, *128*, 7726.
- (309) Du, P.; Schneider, J.; Jarosz, P.; Zhang, J.; Brennessel, W. W.; Eisenberg, R. *J. Phys. Chem. B* **2007**, *111*, 6887.
- (310) Ozawa, H.; Haga, M.-A.; Sakai, K. *J. Am. Chem. Soc.* **2006**, *128*, 4926.
- (311) Ozawa, H.; Yokoyama, Y.; Haga, M.-A.; Sakai, K. *Dalton Trans.* **2007**, 1197.
- (312) Rau, S.; Schäfer, B.; Gleich, D.; Anders, E.; Rudolph, M.; Friedrich, M.; Görls, H.; Henry, W.; Vos, J. G. *Angew. Chem., Int. Ed.* **2006**, *45*, 6215.
- (313) Zhang, J.; Du, P.; Schneider, J.; Jarosz, P.; Eisenberg, R. *J. Am. Chem. Soc.* **2007**, *129*, 7726.
- (314) Engel, G. S.; Calhoun, T. R.; Read, E. L.; Ahn, T.-K.; Mancal, T.; Cheng, Y.-C.; Blankenship, R. E.; Fleming, G. R. *Nature* **2007**, *446*, 782.
- (315) For a general introduction to this topic, see: Darwent, J.; Douglas, P.; Harriman, A.; Porter, G.; Richoux, M.-C. *Coord. Chem. Rev.* **1982**, *44*, 83.
- (316) McLendon, G.; Miller, D. S. *J. Chem. Soc., Chem. Commun.* **1980**, 533.
- (317) Kalyanasundaram, K.; Grätzel, M. *Helv. Chim. Acta* **1980**, *63*, 478.
- (318) Harriman, A.; Richoux, M.-C. *J. Photochem.* **1981**, *15*, 335.
- (319) Darwent, J.; Douglas, P.; Harriman, A.; Porter, G.; Richoux, M.-C. *Coord. Chem. Rev.* **1982**, *44*, 83.
- (320) Kalyanasundaram, K. *J. Chem. Soc., Faraday Trans. II* **1983**, *79*, 1365.
- (321) Okura, I.; Shin, K. *Inorg. Chim. Acta* **1981**, *54*, L249.
- (322) Persaud, L.; Bard, A. J.; Campion, A.; Fox, M. A.; Mallouk, T. E.; Webber, S. E.; White, J. M. *J. Am. Chem. Soc.* **1987**, *109*, 7309.
- (323) Wang, S.; Tabata, I.; Hisada, K.; Hori, T. *Dyes Pigm.* **2002**, *55*, 27.
- (324) Wang, S.; Tabata, I.; Hisada, K.; Hori, T. *J. Porphyrins Phthalocyanines* **2003**, *7*, 199.
- (325) Amao, Y.; Kamachi, T.; Okura, I. *J. Porphyrins Phthalocyanines* **1998**, *2*, 201.
- (326) Szulbinski, W.; Strojek, J. W. *Inorg. Chim. Acta* **1986**, *118*, 91.
- (327) Hosono, H. *Chem. Lett.* **1997**, 523.
- (328) Hosono, H.; Tani, T.; Uemura, I. *Chem. Commun.* **1996**, 1893.
- (329) Hosono, H.; Kaneko, M. *J. Chem. Soc., Faraday Trans.* **1997**, *93*, 1313.
- (330) Hosono, H. *J. Photochem. Photobiol. A* **1999**, *126*, 91.
- (331) Ciamician, G.; Silber, P. *Ber. Dtsch. Chem. Ges.* **1900**, *33*, 2911.
- (332) Ciamician, G.; Silber, P. *Ber. Dtsch. Chem. Ges.* **1901**, *34*, 2040.
- (333) Grätzel, C. K.; Grätzel, M. *J. Chem. Soc., Chem. Commun.* **1979**, 7741.
- (334) Nguyen, K.-T.; Okura, I. *J. Photochem.* **1980**, *13*, 257.
- (335) Jones, G. H.; Edwards, D. W.; Parr, D. *J. Chem. Soc., Chem. Commun.* **1976**, 969.
- (336) Johansen, O.; Mau, W.-H.; Sasse, W. H. F. *Chem. Phys. Lett.* **1983**, *94*, 107.
- (337) Johansen, O.; Mau, W.-H.; Sasse, W. H. F. *Chem. Phys. Lett.* **1983**, *94*, 113.
- (338) Edel, A.; Marnot, P. R.; Sauvage, J. P. *Nouv. J. Chem.* **1984**, *8*, 495.
- (339) Krasna, A. I. *Photochem. Photobiol.* **1979**, *29*, 267.
- (340) Bellin, J. S.; Alexander, R.; Mahoney, R. D. *Photochem. Photobiol.* **1973**, *17*, 17.
- (341) Krasna, A. I. *Photochem. Photobiol.* **1979**, *31*, 75.
- (342) Yamase, T. *Photochem. Photobiol.* **1981**, *34*, 111.
- (343) Kotani, H.; Ohkubo, K.; Fukuzumi, S. *J. Phys. Chem. B* **2006**, *110*, 24047.
- (344) Kotani, H.; Ono, T.; Ohkubo, K.; Fukuzumi, S. *Phys. Chem. Chem. Phys.* **2007**, *9*, 1487.
- (345) Grant, J. L.; Goswami, K.; Spreer, L. O.; Otvos, J. W.; Calvin, M. *J. Chem. Soc., Dalton Trans.* **1987**, 2105.
- (346) Craig, C. A.; Spreer, L. O.; Otvos, J. W.; Calvin, M. *J. Phys. Chem.* **1990**, *94*, 7957.
- (347) Ziessel, R.; Hawecker, J.; Lehn, J.-M. *Helv. Chim. Acta* **1986**, *69*, 1065.
- (348) Keene, R. F.; Cruetz, C.; Sutin, N. *Coord. Chem. Rev.* **1985**, *64*, 247.
- (349) Beley, M.; Collin, J.-P.; Ruppert, R.; Sauvage, J.-P. *J. Chem. Soc., Chem. Commun.* **1984**, 1315.

- (350) Sutin, N.; Creutz, C.; Fujita, E. *Comments Inorg. Chem.* **1997**, *19*, 67.
- (351) Matsuoka, S.; Yamamoto, K.; Ogata, T.; Kusaba, M.; Nakashima, N.; Fujita, E.; Yanagida, S. *J. Am. Chem. Soc.* **1993**, *115*, 601.
- (352) Ogata, T.; Yanagida, S.; Brunschwig, B. S.; Fujita, E. *J. Am. Chem. Soc.* **1995**, *117*, 6708.
- (353) Kimura, E.; Bu, X.; Shionoya, M.; Wada, S.; Maruyama, S. *Inorg. Chem.* **1992**, *31*, 4542.
- (354) Kimura, E.; Wada, S.; Shionoya, M.; Okazaki, Y. *Inorg. Chem.* **1994**, *33*, 770.
- (355) Willner, I.; Maiden, R.; Mandler, D.; Dürr, H.; Dörr, G.; Zengerle, K. *J. Am. Chem. Soc.* **1987**, *109*, 6080.
- (356) For authoritative treatments on these topics, the interested reader is directed toward the other articles in this special issue.
- (357) Yagi, T. *J. Biochem.* **1970**, *68*, 649.
- (358) Okura, I.; Nakamura, S.; Kim-Thuan, N.; Nakamura, K.-I. *J. Mol. Catal.* **1979**, *6*, 261.
- (359) Okura, I.; Nakamura, K.-I.; Nakamura, S. *J. Inorg. Biochem.* **1981**, *14*, 155.
- (360) Okura, I.; Aono, S.; Kita, T. *Chem. Lett.* **1984**, 55.
- (361) Okura, I.; Kim-Thuan, N. *J. Mol. Catal.* **1979**, *6*, 227.
- (362) Okura, I.; Takeuchi, M.; Kim-Thuan, N. *Chem. Lett.* **1980**, 765.
- (363) Okura, I.; Takeuchi, M.; Kim-Thuan, N. *Photochem. Photobiol.* **1981**, *33*, 413.
- (364) Okura, I.; Kusunoki, S.; Aono, S. *Inorg. Chem.* **1983**, *22*, 3828.
- (365) Okura, I.; Aono, S.; Yamada, M.; Kita, T.; Kusunoki, S. *Inorg. Chim. Acta* **1983**, *76*, L91.
- (366) Asakura, N.; Miyaji, A.; Kamachi, T.; Okura, I. *J. Porphyrins Phthalocyanines* **2002**, *6*, 26.
- (367) Okura, I. *Coord. Chem. Rev.* **1985**, *68*, 53.
- (368) Brugger, P. A.; Infelta, P. P.; Braun, A. M.; Grätzel, M. *J. Am. Chem. Soc.* **1981**, *103*, 320.
- (369) Grätzel, C. K.; Grätzel, M. *J. Phys. Chem.* **1982**, *86*, 2710.
- (370) Okura, I.; Kita, T.; Aono, S.; Kaji, N. *J. Mol. Catal.* **1985**, *32*, 361.
- (371) Okura, I.; Kita, T.; Aono, S.; Kaji, N. *J. Mol. Catal.* **1985**, *33*, 341.
- (372) Amao, Y.; Tomonou, Y.; Ishikawa, Y.; Okura, I. *Int. J. Hydrogen Energy* **2002**, *27*, 621.
- (373) Amao, Y.; Tomonou, Y.; Okura, I. *Sol. Energy Mater. Sol. Cells* **2003**, *79*, 103.
- (374) Qian, D.-J.; Wenk, S.-O.; Nakamura, C.; Wakayama, T.; Zorin, N.; Miyake, J. *Int. J. Hydrogen Energy* **2002**, *27*, 1481.
- (375) Okura, I.; Kaji, N.; Aono, S. *J. Chem. Soc., Chem. Commun.* **1986**, 170.
- (376) Kaji, N.; Aono, S.; Okura, I. *J. Mol. Catal.* **1986**, *36*, 201.
- (377) Okura, I.; Kaji, N.; Aono, S.; Nishisaka, T. *Bull. Chem. Soc. Jpn.* **1987**, *60*, 1243.
- (378) Aono, S.; Kaji, N.; Okura, I. *J. Mol. Catal.* **1988**, *45*, 175.
- (379) Kinumi, Y.; Okura, I. *J. Mol. Catal.* **1989**, *52*, L33.
- (380) Okura, I.; Kinumi, Y.; Nishisaka, T. *Inorg. Chim. Acta* **1989**, *156*, 169.
- (381) Okura, I.; Kinumi, Y. *Bull. Chem. Soc. Jpn.* **1990**, *63*, 2922.
- (382) Amao, Y.; Kamachi, T.; Okura, I. *J. Mol. Catal. A* **1997**, *120*, L5.
- (383) Amao, Y.; Kamachi, T.; Okura, I. *J. Porphyrins Phthalocyanines* **1998**, *2*, 201.
- (384) Amao, Y.; Okura, I. *J. Mol. Catal. A* **1999**, *145*, 51.
- (385) Amao, Y.; Okura, I. *J. Mol. Catal. B* **2002**, *17*, 9.
- (386) Asakura, N.; Miyaji, A.; Kamachi, T.; Okura, I. *J. Porphyrins Phthalocyanines* **2002**, *6*, 26.
- (387) Ott, S.; Kritikos, M.; Åkermark, B.; Sun, L. *Angew. Chem., Int. Ed.* **2003**, *42*, 3285.
- (388) Ott, S.; Kritikos, M.; Åkermark, B.; Sun, L.; Lomoth, R. *Angew. Chem., Int. Ed.* **2004**, *43*, 1006.
- (389) Ott, S.; Borgström, M.; Kritikos, M.; Lomoth, R.; Bergquist, J.; Åkermark, B.; Hammarström, L.; Sun, L. *Inorg. Chem.* **2004**, *43*, 4683.
- (390) Sun, L.; Åkermark, B.; Ott, S. *Coord. Chem. Rev.* **2005**, *249*, 1653.
- (391) Ekström, J.; Abrahamsson, M.; Olson, C.; Bergquist, J.; Kaynak, F. B.; Eriksson, L.; Sun, L.; Becker, H.-C.; Åkermark, B.; Hammarström, L.; Ott, S. *Dalton Trans.* **2006**, *38*, 4599.
- (392) Na, Y.; Pan, J.; Wang, M.; Sun, L. *Inorg. Chem.* **2007**, *46*, 3813.
- (393) Song, L.-C.; Tang, M.-Y.; Mei, S.-Z.; Huang, J.-H.; Hu, Q.-M. *Organometallics* **2007**, *26*, 1575.
- (394) Song, L.-C.; Tang, M.-Y.; Su, F.-H.; Hu, Q.-M. *Angew. Chem., Int. Ed.* **2006**, *45*, 1130.
- (395) Okura, I.; Kobayashi, M. *J. Mol. Catal.* **1985**, *30*, 301.
- (396) Okura, I.; Takeuchi, M.; Kusunoki, S.; Aono, S. *Inorg. Chim. Acta* **1982**, *63*, 157.
- (397) Millsaps, J. F.; Bruce, B. D.; Lee, J. W.; Greenbaum, E. *Photochem. Photobiol.* **2001**, *73*, 630.
- (398) Greenbaum, E. *J. Phys. Chem.* **1988**, *92*, 4571.
- (399) O'Neill, H.; Greenbaum, E. *Chem. Mater.* **2005**, *17*, 2654.
- (400) Evans, B. R.; O'Neill, H. M.; Hutchens, S. A.; Bruce, B. D.; Greenbaum, E. *Nano Lett.* **2004**, *4*, 1815.
- (401) McTavish, H. *J. Biochem.* **1998**, *123*, 644.
- (402) Ihara, M.; Nishihara, H.; Yoon, K.-S.; Lenz, O.; Friedrich, B.; Nakamoto, H.; Kojima, K.; Honma, D.; Kamachi, T.; Okura, I. *Photochem. Photobiol.* **2006**, *82*, 676.
- (403) Komatsu, T.; Wang, R.-M.; Zunsain, P. A.; Curry, S.; Tsuchida, E. *J. Am. Chem. Soc.* **2006**, *128*, 16297.
- (404) Saiki, Y.; Ishikawa, Y.; Amao, Y. *Chem. Lett.* **2002**, 218.
- (405) Saiki, Y.; Amao, Y. *Biotechnol. Bioeng.* **2003**, *82*, 710.
- (406) LaVan, D. A.; Cha, J. N. *Proc. Natl. Acad. Sci. U.S.A.* **2006**, *103*, 5251.
- (407) Milstein, D.; Calabrese, J. C.; Williams, I. D. *J. Am. Chem. Soc.* **1986**, *108*, 6387.
- (408) Dorta, R.; Rozenberg, H.; Shimon, L. J. W.; Milstein, D. *J. Am. Chem. Soc.* **2002**, *124*, 188.
- (409) Burn, M. J.; Fickes, M. G.; Hartwig, J. F.; Hollander, F. J.; Bergman, R. G. *J. Am. Chem. Soc.* **1993**, *115*, 5875.
- (410) Tani, K.; Iseki, A.; Yamagata, T. *Angew. Chem., Int. Ed.* **1998**, *37*, 3381.
- (411) Dorta, R.; Togni, A. *Organometallics* **1998**, *17*, 3423.
- (412) Morales-Morales, D.; Lee, D. W.; Wang, Z.; Jensen, C. M. *Organometallics* **2001**, *20*, 1144.
- (413) Schrock, R. R.; Seidel, S. W.; Mosch-Zanetti, N. C.; Shih, K.-Y.; O'Donoghue, M. B.; Davis, W. M.; Reiff, W. M. *J. Am. Chem. Soc.* **1997**, *119*, 11876.
- (414) Lin, W.; Frei, H. *J. Am. Chem. Soc.* **2005**, *127*, 1610.
- (415) Fujita, E.; Brunschwig, B. S. In *Catalysis of Electron Transfer, Heterogeneous and Gas-phase Systems*; Balzani, V., Ed.; Electron Transfer in Chemistry; Wiley-VCH: Weinheim, Germany, 2001; Vol. 4, p 88.
- (416) Simón-Manso, E.; Kubiak, C. P. *Organometallics* **2005**, *24*, 96.
- (417) Hammouche, M.; Lexa, D.; Momenteau, M.; Savéant, J.-M. *J. Am. Chem. Soc.* **1991**, *113*, 8455.
- (418) Beley, M.; Collin, J.-P.; Ruppert, R.; Sauvage, J.-P. *J. Am. Chem. Soc.* **1986**, *108*, 7461.
- (419) Laitar, D. S.; Müller, P.; Sadighi, J. P. *J. Am. Chem. Soc.* **2005**, *127*, 17196.

CR050193E